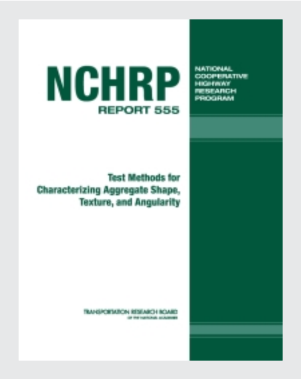

Test Methods for Characterizing Aggregate Shape, Texture, and Angularity

DETAILS

84 pages | | PAPERBACK
ISBN 978-0-309-09882-3 | DOI 10.17226/14017

AUTHORS

Taleb Al-Rousan; Eyad A Masad; Dallas N Little; Joe W Button; Erol Tutumluer; Transportation Research Board

NATIONAL COOPERATIVE HIGHWAY RESEARCH PROGRAM

NCHRP REPORT 555

Test Methods for Characterizing Aggregate Shape, Texture, and Angularity

E. Masad, T. Al-Rousan, J. Button, and D. Little
TEXAS TRANSPORTATION INSTITUTE
College Station,TX

AND

E. Tutumluer
UNIVERSITY OF ILLINOIS AT URBANA-CHAMPAIGN
Urbana, IL

Subject Areas
Pavement Design, Management, and Performance • Materials and Construction

Research sponsored by the American Association of State Highway and Transportation Officials
in cooperation with the Federal Highway Administration

TRANSPORTATION RESEARCH BOARD

WASHINGTON, D.C.
2007
www.TRB.org

NATIONAL COOPERATIVE HIGHWAY RESEARCH PROGRAM

Systematic, well-designed research provides the most effective approach to the solution of many problems facing highway administrators and engineers. Often, highway problems are of local interest and can best be studied by highway departments individually or in cooperation with their state universities and others. However, the accelerating growth of highway transportation develops increasingly complex problems of wide interest to highway authorities. These problems are best studied through a coordinated program of cooperative research.

In recognition of these needs, the highway administrators of the American Association of State Highway and Transportation Officials initiated in 1962 an objective national highway research program employing modern scientific techniques. This program is supported on a continuing basis by funds from participating member states of the Association and it receives the full cooperation and support of the Federal Highway Administration, United States Department of Transportation.

The Transportation Research Board of the National Academies was requested by the Association to administer the research program because of the Board's recognized objectivity and understanding of modern research practices. The Board is uniquely suited for this purpose as it maintains an extensive committee structure from which authorities on any highway transportation subject may be drawn; it possesses avenues of communications and cooperation with federal, state and local governmental agencies, universities, and industry; its relationship to the National Research Council is an insurance of objectivity; it maintains a full-time research correlation staff of specialists in highway transportation matters to bring the findings of research directly to those who are in a position to use them.

The program is developed on the basis of research needs identified by chief administrators of the highway and transportation departments and by committees of AASHTO. Each year, specific areas of research needs to be included in the program are proposed to the National Research Council and the Board by the American Association of State Highway and Transportation Officials. Research projects to fulfill these needs are defined by the Board, and qualified research agencies are selected from those that have submitted proposals. Administration and surveillance of research contracts are the responsibilities of the National Research Council and the Transportation Research Board.

The needs for highway research are many, and the National Cooperative Highway Research Program can make significant contributions to the solution of highway transportation problems of mutual concern to many responsible groups. The program, however, is intended to complement rather than to substitute for or duplicate other highway research programs.

NCHRP REPORT 555

Project 4-30A
ISSN 0077-5614
ISBN: 978-0-309-09882-3
Library of Congress Control Number 2007926566

NOTICE

The project that is the subject of this report was a part of the National Cooperative Highway Research Program conducted by the Transportation Research Board with the approval of the Governing Board of the National Research Council. Such approval reflects the Governing Board's judgment that the program concerned is of national importance and appropriate with respect to both the purposes and resources of the National Research Council.

The members of the technical committee selected to monitor this project and to review this report were chosen for recognized scholarly competence and with due consideration for the balance of disciplines appropriate to the project. The opinions and conclusions expressed or implied are those of the research agency that performed the research, and, while they have been accepted as appropriate by the technical committee, they are not necessarily those of the Transportation Research Board, the National Research Council, the American Association of State Highway and Transportation Officials, or the Federal Highway Administration, U.S. Department of Transportation.

Each report is reviewed and accepted for publication by the technical committee according to procedures established and monitored by the Transportation Research Board Executive Committee and the Governing Board of the National Research Council.

The Transportation Research Board of the National Academies, the National Research Council, the Federal Highway Administration, the American Association of State Highway and Transportation Officials, and the individual states participating in the National Cooperative Highway Research Program do not endorse products or manufacturers. Trade or manufacturers' names appear herein solely because they are considered essential to the object of this report.

Published reports of the

NATIONAL COOPERATIVE HIGHWAY RESEARCH PROGRAM

are available from:

Transportation Research Board
Business Office
500 Fifth Street, NW
Washington, DC 20001

and can be ordered through the Internet at:

http://www.national-academies.org/trb/bookstore

Printed in the United States of America

THE NATIONAL ACADEMIES

Advisers to the Nation on Science, Engineering, and Medicine

The **National Academy of Sciences** is a private, nonprofit, self-perpetuating society of distinguished scholars engaged in scientific and engineering research, dedicated to the furtherance of science and technology and to their use for the general welfare. On the authority of the charter granted to it by the Congress in 1863, the Academy has a mandate that requires it to advise the federal government on scientific and technical matters. Dr. Ralph J. Cicerone is president of the National Academy of Sciences.

The **National Academy of Engineering** was established in 1964, under the charter of the National Academy of Sciences, as a parallel organization of outstanding engineers. It is autonomous in its administration and in the selection of its members, sharing with the National Academy of Sciences the responsibility for advising the federal government. The National Academy of Engineering also sponsors engineering programs aimed at meeting national needs, encourages education and research, and recognizes the superior achievements of engineers. Dr. William A. Wulf is president of the National Academy of Engineering.

The **Institute of Medicine** was established in 1970 by the National Academy of Sciences to secure the services of eminent members of appropriate professions in the examination of policy matters pertaining to the health of the public. The Institute acts under the responsibility given to the National Academy of Sciences by its congressional charter to be an adviser to the federal government and, on its own initiative, to identify issues of medical care, research, and education. Dr. Harvey V. Fineberg is president of the Institute of Medicine.

The **National Research Council** was organized by the National Academy of Sciences in 1916 to associate the broad community of science and technology with the Academy's purposes of furthering knowledge and advising the federal government. Functioning in accordance with general policies determined by the Academy, the Council has become the principal operating agency of both the National Academy of Sciences and the National Academy of Engineering in providing services to the government, the public, and the scientific and engineering communities. The Council is administered jointly by both the Academies and the Institute of Medicine. Dr. Ralph J. Cicerone and Dr. William A. Wulf are chair and vice chair, respectively, of the National Research Council.

The **Transportation Research Board** is a division of the National Research Council, which serves the National Academy of Sciences and the National Academy of Engineering. The Board's mission is to promote innovation and progress in transportation through research. In an objective and interdisciplinary setting, the Board facilitates the sharing of information on transportation practice and policy by researchers and practitioners; stimulates research and offers research management services that promote technical excellence; provides expert advice on transportation policy and programs; and disseminates research results broadly and encourages their implementation. The Board's varied activities annually engage more than 5,000 engineers, scientists, and other transportation researchers and practitioners from the public and private sectors and academia, all of whom contribute their expertise in the public interest. The program is supported by state transportation departments, federal agencies including the component administrations of the U.S. Department of Transportation, and other organizations and individuals interested in the development of transportation. **www.TRB.org**

www.national-academies.org

AUTHOR ACKNOWLEDGMENTS

The research reported herein was performed under NCHRP Project 4-30A by the Texas Transportation Institute, Texas A&M University; and the Department of Civil and Environmental Engineering, University of Illinois at Urbana-Champaign. Texas A&M University is the contractor of this study. The University of Illinois served as a subcontractor.

Eyad Masad, Assistant Professor of Civil Engineering, Texas A&M University, was the principal investigator; the work was done under his general supervision. Other authors of this report are Taleb Al-Rousan, Research Assistant at Texas Transportation Institute (currently an Assistant Professor at the Hashemite University in Jordan); Joe Button, Head of the Materials and Pavement Division, Texas Transportation Institute; Dallas Little, Professor, Texas Transportation Institute; and Erol Tutumluer, Associate Professor, University of Illinois.

The researchers would like to extend their gratitude to all the individuals who provided direction and guidance in this project and also to thank all individuals and agencies that gave permission to include their test methods in this study.

FOREWORD

By Amir N. Hanna
Staff Officer
Transportation Research Board

This report presents a methodology for classifying aggregates based on the distribution of shape, texture, and angularity characteristics and recommends a test method for measuring these characteristics to help improve specifications for aggregates used in highway pavements. The test method measures shape, texture, and angularity characteristics of aggregates used in hot-mix asphalt, hydraulic cement concrete, and unbound base and subbase layers of highway pavements, and it is appropriate for use in central and field laboratories. This report will be of particular interest to materials engineers, researchers, and others concerned with the design and construction of flexible and rigid pavements.

The properties of coarse and fine aggregates used in hot-mix asphalt (HMA) and hydraulic cement concrete and unbound base and subbase layers are very important to the performance of the pavement system in which they are used. Particle shape, texture, and angularity are among the aggregate properties that have significant effects on performance. These properties vary widely with the type and source of aggregates and processing variables. However, current aggregate specifications do not address, in a direct manner, the measurement of these properties, thus leading to inconsistent interpretation and use of test results. Also, a thorough evaluation of available methods for measuring aggregate shape, texture, and angularity characteristics has not been performed to identify appropriate methods. Without this information, a rational recommendation for incorporating such test methods in aggregate specifications can not be made. Thus, research was needed to evaluate potential test methods and identify or develop suitable test methods for measuring relevant properties in central and field laboratories, and to develop recommendations to help improve specifications for aggregates used in highway pavements.

Under NCHRP Project 4-30A, "Test Methods for Characterizing Aggregate Shape, Texture, and Angularity," Texas A&M University of College Station was assigned the objective of identifying or developing—for use in central and field laboratories—suitable test methods for measuring shape, texture, and angularity characteristics of aggregates used in HMA, hydraulic cement concrete, and unbound base and subbase layers of highway pavements. The research focused on the characteristics of coarse aggregates with limited consideration given to the characteristics of fine aggregates. To accomplish this objective, the researchers performed the following tasks:

1. Reviewed and synthesized information relevant to available test methods for measuring aggregate characteristics.
2. Conducted tests using 13 different coarse aggregates and 5 different fine aggregates to evaluate test methods' accuracy, repeatability, reproducibility, ease of use, and ease of interpretation

of results, and considered other factors, such as cost, readiness for implementation, portability, and applicability for the different aggregate sizes and types. Based on this information, 13 potential test methods were selected for further evaluation and ranking.

3. Used an Analytical Hierarchy Process for evaluating and ranking potential test methods; the highest ranked method—the Aggregate Imaging System (AIMS)—was recommended for implementation.
4. Developed a methodology to classify aggregates based on the distribution of characteristics—not average values—for use in materials selection and specifications.
5. Prepared a draft protocol for a proposed "Standard Method of Test for Shape, Angularity, and Texture of Aggregate Particles Using the Aggregate Imaging System (AIMS)" for consideration by AASHTO.

In the methodology described in this report, aggregate characteristics are represented by cumulative distribution functions and not by average values to better represent the effects of blending and crushing of aggregates. This approach helps better explore the influence of different crushing and blending processes, facilitate quality control, identify possible effects on performance, and improve specifications. The proposed method of test, recommended for implementation, can be used to measure aggregate shape, texture, and angularity characteristics that relate to performance and thus it provides a means for evaluating and selecting aggregates used in paving materials. The test procedure will be particularly useful to highway agencies and is recommended for consideration and adoption by AASHTO as a standard test method.

Appendixes B through E contained in the research agency's final report are not published herein. These appendixes are accessible on the web as *NCHRP Web-Only Document 80* at http://trb.org/news/blurb_detail.asp?id=7276. These appendixes are titled as follows:

Appendix B: Review of Aggregate Characteristics Affecting Pavement Performance
Appendix C: Image Analysis Methods for Characterizing Aggregate Shape Properties
Appendix D: Test Methods for Measuring Aggregate Characteristics
Appendix E: Photographs of Aggregate Samples

CONTENTS

SUMMARY

Test Methods for Characterizing Aggregate Shape, Texture, and Angularity

The literature review conducted in this project revealed that the characteristics of coarse and fine aggregates used in hot-mix asphalt and hydraulic cement concrete mixtures, and unbound base and subbase layers influence the performance of the pavement system in which they are used. Aggregate characteristics can be identified by three independent components: shape (or form), angularity, and texture. Methods currently used for measuring these characteristics have several limitations: they are laborious, subjective, lack direct relation with performance parameters, and have a limited ability to separate the influence of angularity from that of texture. A number of research studies have shown that aggregates, especially coarse aggregates that exhibit high texture, do not necessarily have high angularity. Consequently, it is important to develop methods that are capable of quantifying each of the aggregate characteristics rather than a manifestation of their interactions.

This study evaluated available test methods for measuring aggregate characteristics. The evaluation was conducted based on accuracy, repeatability, reproducibility, cost, ease of use, ease of interpretation of the results, readiness of the test for implementation, portability, and applicability for the different aggregate sizes and types. Thirteen different coarse aggregate types and five different fine aggregate types were used in this evaluation.

The evaluation of imaging-based test methods considered both the characteristics of the image acquisition procedure and the accuracy of the image analysis methods. Evaluation of the accuracy of the image analysis methods was conducted in two steps. In the first step, all the analysis methods were used to quantify the characteristics of particle projections that geologists have used for visual evaluation of particles. This step helped to identify analysis methods that are capable of distinguishing between particles of distinct characteristics. These methods were further evaluated in step 2 through the analysis of images of the aggregates used in this study. This step identified the analysis methods that are able to accurately rank aggregates based on their characteristics. The analysis results revealed that some of the available analysis methods do not distinguish between angularity and shape and some analysis methods do not distinguish between texture and angularity.

Accuracy of the test methods was assessed through statistical analysis of the correlations between the results from these methods with measurements of shape using a digital caliper and visual rankings of surface irregularity and texture by experienced individuals.

Analyses of repeatability and reproducibility results were conducted following the guidelines of the American Society of Testing and Materials (ASTM) standards E 177, C 802, and C 670. The Analytical Hierarchy Process (AHP)—a process of developing a numerical score to rank test methods based on how each of these methods meets certain criteria of desirable characteristics—was used to rank the test methods. The desirable characteristics of repeatability, reproducibility, accuracy, operational characteristics, and applicability for different sources of aggregates were considered in the evaluation.

The Aggregate Imaging System (AIMS) was recommended for measuring the characteristics of both coarse and fine aggregates. The system employs methods based on sound scientific concepts for the analysis of shape, angularity, and texture and provides the distribution of each of the characteristics in an aggregate sample. It has very good control of lighting and provides repeatable and reproducible results. The University of Illinois Aggregate Image Analyzer (UIAIA) can also be used for measuring the shape, angularity, and texture of coarse aggregates. For measuring the coarse aggregate shape only, the Multiple Ratio Shape analysis method (MRA) was the most appropriate and is much cheaper than all the other test methods. Similar to the imaging systems, the MRA provides the distribution of shape in an aggregate sample, but it cannot be used for measuring angularity or texture. All these test methods can be used for routine analysis of aggregate characteristics as they require minimal training and provide an easy to use summary of the results. Proposed procedures for conducting these tests are provided in Appendix A.

The ability of X-ray computed tomography (CT)—a nondestructive technique to capture the three dimensions of materials—to provide detailed measurements of aggregate characteristics was assessed. The X-ray CT proved to be a powerful tool, but is premature for use in the routine measurements of aggregate characteristics. The image processing techniques used in separating the particles in X-ray CT require substantial manual manipulation of images, which could influence the measurements of angularity and texture.

A methodology for classification of aggregates based on their characteristics was developed in this project. The methodology unifies the methods used to measure the characteristics of fine and coarse aggregates, and describes these characteristics by cumulative distribution functions rather than average values, thus better defining the effects of blending and crushing on aggregate characteristics. This methodology can be used to (1) explore the influence of different processes such as crushing and blending on aggregate shape, (2) conduct quality control by detecting changes in the distribution of any of the characteristics, (3) relate the distribution of different characteristics to performance, and (4) develop specifications based on the distribution of aggregate characteristics rather than average indices.

CHAPTER 1

Introduction and Research Approach

This section of the report presents the project background, objectives, and descriptions of the tasks performed in the research project.

Project Background

The properties of coarse and fine aggregates used in hot-mix asphalt (HMA) and hydraulic cement concrete mixtures, and unbound base and subbase layers influence the performance of the pavement system in which they are used. Particle shape, texture, and angularity are among the aggregate properties that have significant effect on performance. These properties vary widely with the type and source of aggregates and processing techniques. However the current aggregate specifications do not address in a direct manner the measurements of these properties, thus leading to inconsistent interpretation and use of test results.

Several methods for measuring aggregate shape, texture, and angularity characteristics were developed in recent years, and others are being developed as part of ongoing research efforts. However an evaluation of these methods with respect to their practicality, labor requirements, ease of use, cost, versatility, field applicability, use in multiple-ratio shape analysis, and other factors has not been performed. Without this information, a rational recommendation for incorporating such test methods in aggregate specifications cannot be made. Research was needed to evaluate potential test methods and identify or develop suitable test methods for measuring relevant properties in central and field laboratories, and to develop recommendations to help improve specifications for aggregates used in highway pavements. This need was addressed in this NCHRP project.

Research Objective

The objective of this research was to identify or develop, for use in central and field laboratories, suitable test methods for measuring shape, texture, and angularity characteristics of aggregates used in HMA and hydraulic cement concrete mixtures, and unbound base and subbase layers of highway pavements. The research focused on the characteristics of coarse aggregates, but also considered the characteristics of fine aggregates.

Scope of Study

This study included collecting and reviewing information relative to the effects of shape, texture, and angularity characteristics of aggregate on the performance of HMA and hydraulic cement concrete mixtures, and unbound materials used in highway pavements. This information was obtained from domestic and foreign literature, contacts with public and private agencies and industry organizations, and other sources. The collected information was used to (1) identify aggregate particle characteristics that are likely to influence performance and (2) to identify test procedures currently used in the United States and other countries for measuring these characteristics. The merits and deficiencies of the test methods were evaluated based on the published information with consideration to relevance, practicality, labor requirements, cost, duration of test, repeatability, versatility, field applicability, use in multiple ratio shape analysis, and other pertinent factors.

The evaluation of all available test methods was followed with the execution of an experimental plan to evaluate and validate the most promising test methods, and if necessary, to develop new methods for measuring shape, texture, and angularity characteristics of aggregates. The test methods recommended as a result of the experimental evaluations are presented in Appendix A. Note: Appendixes B through E are not published herein. These appendixes are accessible as *Web-Only Document 80* at http://trb.org/news/blurb_detail.asp?id=7276.

Research Approach

A comprehensive literature review was conducted during this study. The literature search focused on aggregate particle characteristics that are likely to influence pavement performance (summarized in Appendix B). The literature search also covered image analysis methods for characterizing aggregate shape properties (summarized in Appendix C), and test procedures currently used in the United States and other countries and those proposed as part of recent research for measuring these characteristics (summarized in Appendix D). The research also included critical evaluation of all available test methods based on the published literature, identification of test methods for experimental evaluation, conduct of statistically designed experiments to evaluate test methods, rank and recommendation of test methods for measuring aggregate characteristics, and development of a methodology for classification of aggregates based on shape.

Evaluation of Test Methods

Information gathered from the literature was used (1) to conduct a comparative analysis of the available test methods and (2) to select test methods that will be subjected to intensive experimental evaluation in this study. The advantages and disadvantages of all test methods were summarized. Three steps were used to select test methods (Figure 1). In the first step, methods were categorized into direct and indirect. Direct methods were defined as those wherein particle characteristics (shape, texture, and angularity) are measured, described qualitatively, and possibly quantified through direct measurement of individual particles. In indirect methods, particle characteristics are lumped together as geometric irregularities and determined based on measurements of bulk properties. In the second step, methods that share the same analysis concept were grouped together to ensure that the selected candidate methods represent different analysis concepts. In the third step, tests were selected from each group based on practicality, labor requirements, cost, repeatability, versatility, and field applicability for further evaluation. Some of the currently used test methods were included in the intensive evaluation for comparison.

The following test methods were considered for further experimental evaluation: Uncompacted Void Content of Fine Aggregates (AASHTO T 304), Uncompacted Void Content of Coarse Aggregates (AASHTO TP56), Compacted Aggregate Resistance (CAR), Percentage of Fractured Particles in Coarse Aggregate (ASTM D 5821), Flat and Elongated Coarse Aggregates (ASTM D 4791), Multiple Ratio Shape Analysis (MRA), VDG-40 Videograder, Buffalo Wire Works PSSDA, Camsizer, WipShape, Aggregate Imaging System (AIMS), University of Illinois Aggregate Image Analyzer (UIAIA), and Laser-Based Scanning Analysis System (LASS).

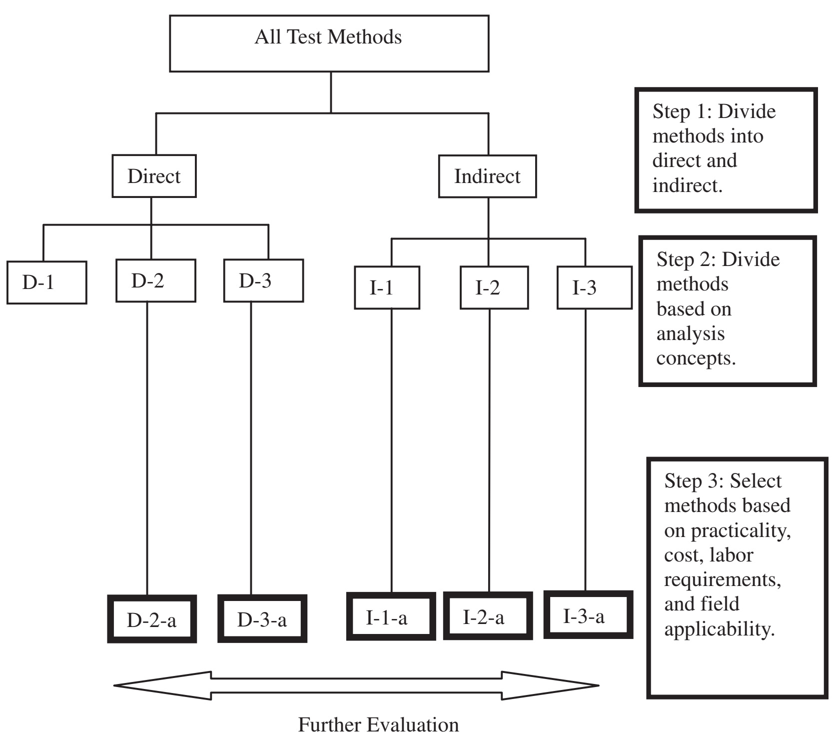

Figure 1. Approach for preliminary evaluation, screening, and prioritization of test methods.

Table 1. Recommended test methods for measuring aggregate characteristics.

Recommended Test Method	Coarse Aggregates		Fine Aggregates
	Shape, Angularity and Texture	Shape Only	Angularity
Aggregate Imaging System (AIMS)	Recommended		Recommended
University of Illinois Aggregate Image Analyzer (UIAIA)	Recommended		
Multiple Ratio Shape Analysis		Recommended	

Experimental Design and Statistical Analysis

Aggregates were selected to cover a wide spectrum of origin, rock type, and characteristics. Three sizes of 13 coarse aggregate types and three sizes of five fine aggregate types were used in this study. Experienced individuals from the industry and highway agencies assisted in selecting and providing these aggregates (photographs of representative samples of these aggregates are provided in Appendix E).

Statistically-designed experiments were conducted to evaluate repeatability, reproducibility, and accuracy of the selected methods. Information about cost and operational characteristics was gathered from vendors, researchers, and operators who are familiar with these systems. The operational characteristics of ease of use, portability, ability of interpreting data, readiness for implementation in central laboratories as well as field laboratories, and applicability of test method to measure different aggregate types and sizes were considered.

Ranking and Recommendation of Test Methods

The Analytical Hierarchy Process (AHP) was implemented in a program and used to provide a ranking, or a priority list of all the methods included in the evaluation. Criteria for the preferred characteristics of test methods were developed and used in the rankings. The AHP program provides flexibility in defining the objectives, ranking criteria, and relative importance or priorities of the different criteria elements. Test methods recommended based on the AHP rankings are listed in Table 1.

A statistical-based methodology was developed to (1) summarize the analysis results, (2) facilitate the comparison between the characteristics of different aggregate sources, and (3) classify aggregates based on the distribution of their characteristics. The methodology was presented in the form of macro-driven Microsoft Excel®, a Visual Basic application.

CHAPTER 2

Findings

Evaluation of Merits and Deficiencies of Test Methods

Information gathered from the literature (summarized in Appendix D) was used to compare 21 available test methods and identify test methods for further experimental evaluation in this study. The advantages and disadvantages of the test methods are summarized in Table 2.

The test methods were divided into 11 groups based on analysis concept, as shown in Table 3. The four indirect methods in the first group rely on packing of aggregates that flow through a specific-sized orifice. Uncompacted void content of fine aggregates (also known as Fine Aggregate Angularity [FAA] test) and uncompacted void content of coarse aggregates were selected for further evaluation because they are widely used and cheaper and easier to use than other tests in the same group. Janoo and Korhonen (*1*) concluded that the FAA test was the easiest to use when it compared to time index, rugosity, and particle index. Time index was not selected because it is a time consuming test (*1*) and was classified as having fair performance, predictability, precision, and accuracy (*2*).

In the second group of tests, a compacted specimen is exposed to pressure or shear forces. Of these methods, the CAR test is a relatively new test and has not received enough evaluation. Chowdhury and Button (*3*) concluded that the CAR test method offers much more sensitivity than either the FAA test or the direct shear test. This method also has more advantages than the Florida bearing ratio and direct shear tests; it was selected for evaluation.

The percentage of fractured particles in coarse aggregate method (ASTM D 5821) was selected because it is currently included in the Superpave system. Rao and Tutumluer (*4*) described this method as being time consuming, labor intensive, and subjective. Also, it was classified in another study as having low prediction and precision, with medium practicality (*5*).

Both the ASTM D 4791 test method for measuring flat and elongated coarse aggregates and the multiple ratio shape analysis test method were selected. The multiple ratio shape analysis provides more detailed measurements in terms of the distribution of the dimensional ratio. ASTM D 4791 was selected because it is included in the Superpave system although it was described as tedious, labor extensive, and time consuming (*16, 17*) and it does not identify spherical or rounded particles and measure one particle at a time (*4, 7*).

The next group of tests uses one camera to image and evaluate particles. It includes the VDG-40 Videograder, Computer Particle Analyzer, Micromeritics OptiSizer PSDA, Video Imaging System (VIS), and Buffalo Wire Works PSSDA. Of these methods only the VDG-40 Videograder and Buffalo Wire Works PSSDA were selected for evaluation. The VDG-40 Videograder was selected because it is capable of analyzing every particle in the sample and it showed good correlation with manual measurements of flat and elongated particles (*8, 9*). The PSSDA method was selected because of its ability to analyze particles with a wide range of sizes (from passing sieve #200 to 1.5 in.).

The Camsizer system uses two cameras to capture images at different resolutions; it evaluates a large number of particles in the sample as they fall in front of a backlight. Using two cameras improves the accuracy of measuring the characteristics of both coarse and fine aggregates. The system has the capability of automatically producing the distribution of particles' size, shape, angularity, and texture.

The WipShape system uses two cameras to capture images of aggregates passing on a mini-conveyor or on a rotating circular lighting table. This system was selected because it can analyze large quantities of particles in a short time and has the potential to measure and report various shape factors including sphericity, roundness, and angularity (*10, 11*).

UIAIA uses three cameras to capture images from three orthogonal directions and build a 3-D shape of each particle; it automatically determines flat and elongated particles, coarse aggregate angularity, coarse aggregate texture, and gradation. The use of three images for each particle allows an accurate

Table 2. Advantages and disadvantages of the testing methods used to measure aggregate characteristics.

Test Method	Estimated Equipment Cost ($)	Measured Aggregate Characteristics	Advantages	Disadvantages
AASHTO T 304 (ASTM C 1252) Uncompacted Void Content of Fine Aggregate	250	• A combination of angularity, texture, and shape.	• Simple. • Inexpensive. • Saeed et al. (2001) selected it to measure the properties of aggregates in unbound layers. • Meininger (1998) selected it to measure the properties of aggregates in PCC pavements. • Janoo and Korhonen (1999) recommended it over time index, rugosity, and particle index. • Used in the current Superpave system.	• Lee et al. (1999a) and Chowdhury and Button (2001) reported that the test does not consistently identify angular and cubical aggregates. Also, some fine aggregate with good field performance history did not meet the Superpave criteria. • The results are influenced by shape, angularity, texture, and bulk specific gravity.
AASHTO TP56 Uncompacted Void Content of Coarse Aggregate	500	• A combination of angularity, texture, and shape.	• Simple. • Inexpensive. • Kandhal and Parker (1998) selected it to measure the properties of aggregates in asphalt pavements. • Meininger (1998) selected it to measure the properties of aggregates in PCC pavements.	• The results are influenced by shape, angularity, texture, and bulk specific gravity.
ASTM D 3398 Standard Test Method for Index of Aggregate Particle Shape and Texture	400	• A combination of angularity, texture, and shape.	• Simple. • Inexpensive.	• Saeed et al. (2001) classified this test as having fair performance, predictability, precision, and accuracy. • Meininger (1998) reported that the results have high correlation with the FAA test, which is more practical and easier to use. • Fowler et al. (1996) reported that the method does not provide good correlation with concrete performance. • Results influenced by bulk properties, shape, angularity, and texture.
Compacted Aggregate Resistance (CAR) Test	500	• A combination of angularity, texture, and shape.	• Simple. • Inexpensive. • Chowdhury and Button (2001) reported that the CAR test method is more sensitive to changes in aggregate characteristics than FAA and direct shear test methods.	• The results are influenced by shape, angularity, texture, and bulk properties.
Florida Bearing Value of Fine Aggregate	1,000	• A combination of angularity, texture, and shape.	• Simple.	• The results are influenced by shape, angularity, texture, and bulk properties. • Less practical and involves more steps than the FAA test. • Operates based on the same concept as the CAR test but requires more equipment and time. • Lee et al. (1999b) stated that FAA test has better correlation with HMA performance than this test.
Rugosity	500	• A combination of angularity, texture, and shape.	• Simple. • Inexpensive.	• The results are influenced by shape, angularity, texture, and bulk properties. • It is based on the same concept as the FAA test and the uncompacted voids in coarse aggregates test. However, it requires more time and is less practical than these tests.
Time Index	500	• A combination of angularity, texture, and shape.	• Simple. • Inexpensive.	• The results are influenced by shape, angularity, texture, and bulk properties. • It is based on the same concept as the FAA test and the uncompacted voids in coarse aggregates test. However, it requires more time and is less practical than these tests.
AASHTO T 236 (ASTM D 3080) Direct Shear Test	10,000	• A combination of angularity, texture, and shape.	• Simple. • Chowdhury and Button (2001) reported that the test method has good correlation with HMA performance.	• Expensive. • The results are influenced by shape, angularity, texture, mineralogy, and particle size distribution. • Nonuniform stress distribution causes discrepancies in the measured internal friction.

(continued on next page)

Table 2. (Continued).

Test Method	Estimated Equipment Cost ($)	Measured Aggregate Characteristics	Advantages	Disadvantages
ASTM D 5821 Determining the Percentages of Fractured Particles in Coarse Aggregate	0	• Angularity.	• Simple. • Inexpensive. • Used in the current Superpave system.	• Labor intensive and time consuming. • Depends on the operator's judgment. • Meininger (1998) classified this method as having low prediction, precision, and medium practicality.
Flat and Elongated Coarse Aggregates ASTM D 4791	250	• Shape.	• Used in current Superpave system. • Able to identify large portions of flat and elongated particles. • Gives accurate measurements of particle dimension ratio. • Found to be related to performance of unbound pavement layers (Saeed et al. 2001).	• Tedious, labor extensive, time consuming to be used on a daily basis (Yeggoni et al. 1996, Rao and Tutumluer 2000). • Limited to test only one particle at a time. • Unable to identify spherical, rounded, or smooth particles. • Doesn't directly predict performance (Meininger 1998, Fowler et al. 1996).
Multiple Ratio Shape Analysis	1,500	• Shape.	• Simple. • Inexpensive. • Provides the distribution of dimensional ratio in aggregate sample.	• Does not address angularity or texture.
VDG-40 Videograder	45,000	• Shape.	• Measures the shape of large aggregate quantity. • Weingart and Prowel (1999) and Tutumluer et al. (2000) reported good correlation with manual measurements of flat-elongated particles.	• Expensive. • Does not address angularity or texture. • Assumes idealized particle shape (ellipsoid). • Uses one camera magnification to capture images of all sizes.
Computer Particle Analyzer CPA	25,000	• Shape.	• Measures the shape of large aggregate quantity.	• Expensive. • Does not address angularity or texture. • Assumes idealized particle shape (ellipsoid). • Uses one camera magnification to capture images of all sizes.
Micromeritics OptiSizer PSDA	50,000	• Shape.	• Measures the shape of large aggregate quantity.	• Expensive. • Does not address angularity or texture. • Assumes idealized particle shape (ellipsoid). • Uses one camera magnification to capture images of all sizes.
Video Imaging System (VIS)	60,000	• Shape.	• Measures the shape of large aggregate quantity.	• Expensive. • Does not address angularity or texture. • Assumes idealized particle shape (ellipsoid). • Uses one camera magnification to capture images of all sizes.
Camsizer	45,000	• Shape. • Angularity.	• Measures the shape of large aggregate quantity. • Uses two cameras to capture images at different magnifcations based on aggregate size.	• Expensive. • Assumes idealized particle shape (ellipsoid).
WipShape	35,000	• Shape. • Angularity.	• Measures the shape of large aggregate quantity. • Measures the three dimensions of aggregates.	• Expensive. • Does not address texture. • Uses same camera magnification to capture images of all sizes.
University of Illinois Aggregate Image Analyzer (UIAIA)	35,000	• Shape. • Angularity. • Texture.	• Measures the shape of large aggregate quantity. • Measures the three dimensions of aggregates.	• Expensive. • Uses same camera magnification to capture images of all sizes.
Aggregate Imaging System (AIMS)	35,000	• Shape. • Angularity. • Texture.	• Measures the three dimensions of aggregates. • Uses a mechanism for capturing images at different resolutions based on particle size. • Gives detailed analysis of texture.	• Expensive.
Laser-Based Aggregate Analysis System	25,000	• Shape. • Angularity. • Texture.	• Measures the three dimensions of aggregates.	• Expensive. • Use the same scan to analyze aggregates with different sizes.

Note: Prices listed are estimates based on information from users and vendors.

Table 3. Features and consideration of test methods for experimental evaluation.

Test Method	Direct (D) or Indirect (I) Method	Features of Analysis Concept	Consideration for Further Experimental Evaluation
Uncompacted Void Content of Fine Aggregates AASHTO T304	I	Packing of aggregate that flows through a given sized orifice	Yes
Uncompacted Void Content of Coarse Aggregates AASHTO TP56	I		Yes
Rugosity	I		No
Time Index	I		No
Index for Particle Shape and Texture ASTM D3398	I	Packing of aggregate in a mold using two levels of compactions	No
Compacted Aggregate Resistance CAR	I	Exposing a compacted specimen to pressure or shear forces	Yes
Florida Bearing Ratio	I		No
Angle of Internal Friction from Direct Shear Test	I		No
Percentage of Fractured Particles in Coarse Aggregate ASTM D5821	D	Visual inspection of particles	Yes
Flat and Elongated Coarse Aggregates ASTM D4791	D	Measuring particle dimension using caliper	Yes
Multiple Ratio Shape Analysis	D		Yes
VDG-40 Videograder	D	Using one camera to image and evaluate particles in the sample as they fall in front of a backlight	Yes
Computer Particle Analyzer	D		No
Micromeritics OptiSizer PSDA	D		No
Video Imaging System (VIS)	D		No
Buffalo Wire Works PSSDA	D		Yes
Camsizer	D	Uses two cameras to image and evaluate particles in the sample as they fall in front of a back light	Yes
WipShape	D	Uses two cameras to capture image of aggregates passing on a mini conveyor system	Yes
University of Illinois Aggregate Image Analyzer (UIAIA)	D	Uses three cameras to capture three projections of a particle moving on a conveyor belt	Yes
Aggregate Imaging System (AIMS)	D	Uses one camera and autofocus microscope to measure the characteristics of coarse and fine aggregates	Yes
Laser-Based Aggregate Analysis System	D	Uses a laser scan	Yes

computation of the volume of each aggregate particle and provides information about the actual 3-D characteristics of the aggregate.

AIMS uses one video camera and a microscope to capture different types of images based on the type of aggregate and the property to be measured. The system measures the three dimensions of the aggregate particles. Images can be captured using different resolutions based on the particle size detected by the system. The system is reported to analyze the characteristics of fine and coarse aggregates and provide a detailed analysis of texture for coarse aggregates.

LASS uses a laser scan to determine particles' shape and angularity; although this system was selected initially for evaluation, it was not available to this study during the experimental evaluation period.

Aggregate Selection

This section includes a description of the aggregates that were selected and used to evaluate the testing methods presented in Table 3. Aggregates were selected to cover a range of origin, rock type, and characteristics. The thirteen coarse aggregates and five fine aggregates described in Table 4 were used in this study. Three coarse sizes and three fine sizes were used to perform the evaluation (see Table 4). Experienced individuals from the industry and highway agencies assisted in selecting and

Table 4. Aggregate sources and sizes.

Label	Source	Aggregate Description	Aggregate Sizes					
			25.4 - 19.0 mm (1-3/4")	12.5 - 9.5 mm (1/2-3/8")	9.5 - 4.75 mm (3/8"-#4)	4.75 - 2.36 mm (#4 - #8)	2.36 - 1.18 mm (#8 - #16)	0.6 - 0.3 mm (#30 - #60)
1	Montgomery AL	Uncrushed River Gravel and Sand	X	X	X	X	X	X
2	Montgomery AL	Crushed River Gravel and Sand	X	X	X	X	X	X
3	Childersburg AL	Limestone	X	X	X			
4	Auburn AL	Dolomite	X	X	X			
5	Birmingham AL	Slag	X	X	X	X	X	X
6	Brownwood TX	Limestone	X	X	X	X	X	X
7	Fairfield OH	Crushed Glacial Gravel	X	X	X			
8	Fairfield OH	Uncrushed Glacial Gravel	X	X	X			
9	Forsyth GA	Granite	X	X	X			
10	Ruby GA	Granite	X	X	X	X	X	X
11	Knippa TX	Traprock	X	X	X			
12	San Antonio TX	Limestone	X	X	X			
13	Augusta GA	Granite	X	X	X			

providing these aggregates (pictures of representative samples are provided in Appendix E).

Mineralogical content of the thirteen aggregates was determined using X-ray diffraction (XRD)—a technique that uses X-rays of a single wavelength for establishing the structures of crystalline solids. The sample analyzed was in a powder form, consisting of fine grains of single crystalline material. Aggregates of the size 9.5 to 4.75 mm (3/8″ to sieve #4) were ground to a powder form (smaller than 0.075 mm and passes sieve #200). A few grams of the powder sample was placed in a holder, and then the sample was illuminated with X-rays of a fixed wave length in the diffractometer. The intensity of the reflected radiation was recorded. These data were then analyzed for the reflection angle to calculate the interatomic spacing (d-value in angstrom units of 10^{-7} cm). The intensity was measured to discriminate the various d-spacing, and the results were compared to specific tables to identify possible matches with mineral phases. The mineralogical content of the aggregates used in this study is presented in Table 5.

The ASTM C 702 test procedure was followed to obtain representative aggregate samples. Randomization was employed in dividing the aggregate into smaller representative samples to reduce bias due to unforeseen factors that would affect measurements. Aggregates selected for evaluation were sieved, reduced to smaller samples, and washed according to ASTM and AASHTO standard procedures.

The same sample used in the nondestructive tests was used by all operators and for all test replicates. Each sample of a coarse aggregate size was 1 kg, while each sample of a fine aggregate was 0.5 kg. In conducting the tests, the operators were asked to return the aggregates to the sample after running each test, and mix the sample before running the following test using the same method or a different method.

Table 5. Mineralogical content of aggregates.

Aggregate	Aggregate Description	Minerals Present
1	Uncrushed River Gravel and Sand	Quartz, Dolomite (trace)
2	Crushed River Gravel and Sand	Quartz
3	Limestone	Calcite, Dolomite, Quartz
4	Dolomite	Dolomite
5	Slag	Akermanite, Calcite, Quartz
6	Limestone	Calcite, Quartz, Dolomite
7	Crushed Glacial Gravel	Dolomite, Calcite, Quartz
8	Uncrushed Glacial Gravel	Dolomite, Calcite, Quartz
9	Granite	Quartz, Biotite, Albite, Labradorite
10	Granite	Quartz, Chlorite, Albite, Amesite, Anorthite, Phlogophite (Mica), Muscovite
11	Traprock	Tephrite, Diopside, Augite, Anorthite
12	Limestone	Calcite
13	Granite	Quartz, Albite, Calcite, Anorthite, Microcline, Kaolinite

Experimental Design and Statistical Analysis

This section documents the experimental evaluation of the test methods. The evaluation covered the repeatability, reproducibility, accuracy, cost, and operational characteristics. The first three characteristics were evaluated through statistical analysis of the characteristics of a wide range of aggregates from different sources with various characteristics. The accuracy analysis was conducted for the parameters employed in the test methods, and for the test methods themselves including the hardware components. The information that pertains to cost and operational characteristics was collected from vendors, researchers, and operators who have dealt with these systems.

As indicated earlier, some of the selected methods have been in practice for years and they are usually performed using standard procedures. However, for the methods that have been developed recently, the manufacturer's or the developer's instructions were followed to perform the testing. It was necessary in some cases to perform the standard tests with minor modifications in order to conduct the tests on the selected aggregate sizes. A summary of aggregate sizes and parameters obtained from each of the selected test methods is shown in Table 6. Descriptions of the testing procedures and modifications, if any, and aggregate properties are provided in Appendix D.

Evaluation of Repeatability and Reproducibility

Repeatability and reproducibility of test methods were evaluated through measuring the characteristics of aggregate samples several times by single and multiple operators. The operators were uniformly trained on the application of the test methods and were provided with the same set of instructional guidelines.

One coarse aggregate size (12.5 – 9.5 mm [1/2 – 3/8″]), and one fine aggregate size (2.36 – 1.18 mm [sieve #8 – #16]) were used for the repeatability analysis. Each of the operators measured the properties of these aggregate sizes three times. Reproducibility was assessed by measuring the shape characteristics (as applicable to the test method, see Table 6) for aggregate sizes listed in Table 4 by each of the three operators. All operators conducted measurements using the same samples.

Standard deviation and coefficient of variation were used to quantify repeatability and reproducibility. Analysis of variance (ANOVA) was used in the statistical analysis according to the ASTM procedures (ASTM E 177, ASTM C 802, and ASTM C 670). The repeatability and reproducibility statistical parameters were calculated for each test method as follows:

- Repeatability calculations: For each material and operator, the average of replicates is given by Equation 1, and the variation in measurements is calculated by Equation 2.

$$\bar{x}_i = \frac{\sum_{j=1}^{n} x_{ij}}{n} \quad (1)$$

$$S_i^2 = \frac{\left(\sum_{j=1}^{n} x_{if}^2 - n\bar{x}_i\right)^2}{(n-1)} \quad (2)$$

Where n is the number of measurements by an operator for one material and $\bar{x}_i$ is the average of the measurements of operator i, and S_i^2 is the variance for operator i. Table 7 shows the arrangement of variation data within and between operators for one single material using one test method. The repeatability of a test method is evaluated for each aggregate material and all operators by Equation 3:

$$S_m^2(pooled) = \frac{\sum_{i=1}^{p} s_i^2}{p} \quad (3)$$

where p = 3 is the number of operators.

- Reproducibility Calculations: The average of measurements made by all operators for a singe material is given by Equation 4 and the variation between operators is given by Equation 5.

$$\bar{x}_m = \frac{\sum \bar{x}_i}{p} \quad (4)$$

$$s_{\bar{x}_m}^2 = \frac{\sum \bar{x}_i^2 - p(\bar{x}_m)^2}{(p-1)} \quad (5)$$

Variations between operators are calculated by:

$$S_{L_m}^2 = S_{\bar{x}_m}^2 - \left[S_m^2(pooled)/n\right] \quad (6)$$

Then, reproducibility of a test method is given by:

$$S_R^2 = S_{L_m}^2 + S_m^2(pooled) \quad (7)$$

Repeatability and reproducibility of the test method on all aggregates were estimated by pooling standard deviations and coefficients of variations over all materials according to the guidelines of ASTM C 802. Because each of the selected test methods measures aggregate characteristics using different

Table 6. Aggregate size and characteristics measured using the test methods.

Test	Aggregate Size						Characteristics		
	C 1	C 2	C 3	F 1	F 2	F 3	Shape (Abbreviation)	Angularity (Abbreviation)	Texture (Abbreviation)
Uncompacted Void Content of Fine Aggregates AASHTO T 304					X	X		% Loose Uncompacted Void Content (UCVCF)	
Uncompacted Void Content of Coarse Aggregates AASHTO TP 56		X	X					% Loose Uncompacted Void Content (UCVCC)	
Compacted Aggregate Resistance CAR				X	X	X		Max Shear Resistance (CAR)	
Percentage of Fractured Particles in Coarse Aggregate ASTM D 5821	X	X	X					% of Fractured Faces (PFF)	
Flat and Elongated Coarse Aggregates ASTM D 4791	X	X	X				Flat Elongated Ratio (FER)		
Multiple Ratio Shape Analysis	X	X	X				Dimensional Ratio (MRA)		
VDG-40 Videograder	X	X	X	X			Flat Ratio (VDG-40 FLAT) & Slenderness ratio (VDG-40 SLEND)		
Buffalo Wire Works PSSDA-Large	X	X	X				Roundness (PSSDA-Large ROUND)	Roundness (PSSDA-Large ROUND)	
Buffalo Wire Works PSSDA-Small				X	X	X	Roundness (PSSDA-Small ROUND)	Roundness (PSSDA-Small ROUND)	
Camsizer		X	X	X	X	X	Sphericity (CAMSPHT), Symmetry (CAMSYMM), Ratio of Length to Breadth (CAML/B)	Convexity (CAMCONV)	
WipShape	X	X	X				Dimensional Ratio (WSFER)	Minimum Average Curve Radius (WSMACR)	
University of Illinois Aggregate Image Analyzer (UIAIA)	X	X	X	X			Flat Elongated Ratio (UIFER)	Angularity Index (UIAI)	Surface Texture Index (UISTI)
Aggregate Imaging System (AIMS)	X	X	X	X	X	X	Sphericity (AIMSSPH) & Form 2-D Index (AIMSFORM)	Gradient Angularity Index (AIMSGRAD), Radius Angularity Index (AIMSRAD)	Texture Index (Wavelet) (AIMSTXTR)

Aggregate sizes:
C1 = 25.4 – 19.0 mm (1 – 3/4"); C2 = 12.5 – 9.5 mm (1/2 – 3/8"); C3 = 9.5 – 4.75 mm (3/8" – #4); F1 = 4.75 – 2.36 mm (#4 – #8); F2 = 2.36 – 1.18 mm (#8 – #16); F3 = 0.6 – 0.3 mm (#30 – #60).

Table 7. Arrangement of variation in measurements within and between operators for one aggregate.

Operator	Data (replicates) x_{ij}			Average $\bar{x}_i$	Within Operator Variance S_i^2
1	I	II	III	$\bar{x}_1$	S_1^2
2	I	II	III	$\bar{x}_2$	S_2^2
3	I	II	III	$\bar{x}_3$	S_3^2

analysis parameters or indices with different scales, repeatability and reproducibility were assessed independently for each parameter. The final results of repeatability and reproducibility for all test methods are reported for each characteristic and for coarse and fine aggregates separately in Tables 8 and 9, respectively. The abbreviations of the parameters provided in the manuals and standards of test methods are used here.

In interpreting the results, the following factors should be taken into consideration:

(1) The methods differ significantly in the level of detail provided in the results. While the indirect methods provide only an average index, direct methods can provide the distribution of characteristics in an aggregate sample. This advantage of direct methods has not been considered because the calculations are based on average values in order to analyze all test methods using the same statistical methods.
(2) The test methods differ in the range of results. Some methods have analysis parameters with narrow ranges that make it difficult to distinguish between aggregates, while others have wide ranges.
(3) Measurements from a test method were all conducted using a single device and well-trained operators.
(4) The high sensitivity of some test methods to variations in aggregate characteristics, which is an advantage, can increase variation and reduce the repeatability and reproducibility.

Considering all these factors, it is recommended to differentiate among test methods based on the levels of variability shown in Tables 8 and 9.

The percentage of fractured faces test had very high variability compared to all other test methods as also reported by Meininger (*5*) and Saeed et al. (*2*). According to the results in Table 9, the uncompacted void content test for fine aggregate had low variability. Saeed et al. (*2*) rated this test as having a fair precision (ability to repeatedly provide correct results). The results of this test were analyzed using the same specific gravity for each aggregate. The variability of the test results is mainly due to error in measuring the specific gravity. Therefore, it is expected that the variability of the uncompacted void content test would increase significantly when the variability in specific gravity measurements is considered.

The image analysis methods had high variability when the percentage of particles with a dimensional ratio of 5:1 was considered. This was mainly due to the small percentages of particles that exhibited this characteristic, such that any slight variation in accounting for these particles was manifested as high coefficient of variation. Therefore, the variability was evaluated based on the percentage of particles with a dimensional ratio smaller or larger than 3:1.

The image analysis methods (UIAIA, AIMS, Camsizer, PSSDA, WipShape) had low to medium variability in terms of angularity and texture measurements. The AIMS angularity indices had low variability, while the texture indices had medium variability. As will be discussed later, automation of the AIMS top lighting intensity would reduce the variability.

Evaluation of Accuracy

The accuracy of the test methods can be evaluated by correlating the measurements from these tests with the measurements obtained from standards or reference tests that are considered to be accurate. The three dimensions of coarse particles can be measured using a digital caliper—an accurate, but slow method. However, because test methods that are accepted to be accurate in quantifying texture and angularity are not available, the following approach was adopted to assess the accuracy of the test methods:

- The accuracy was evaluated based on the procedure recommended by standards and/or by the developers, and for the analysis methods (mathematical functions and indices) employed in the imaging-based systems. This approach allowed evaluation of the accuracy of the analysis methods irrespective of the characteristics of the image acquisition setup.

Table 8. Classification of coarse aggregate test methods based on repeatability and reproducibility.

Characteristics	Test Method	Parameter Abbreviation	Measured Parameter as Reported by Test Method	Coefficient of Variation (CV)	
				Repeatability	Reproducibility
Angularity	Uncompacted Void Content of Coarse Aggregate	UCVCC	Percent Uncompacted Voi d Content	L	L
	Percent Fractured Faces	PFF	0 Fractured Faces	H	H
			1 Fractured Face	M	H
			2 Fractured Faces	M	H
	Camsizer	CAMCONV	Conv3	L	L
	WipShape	WSMACR	Minimal Average Curve Radius	L	L
	University of Illinois Aggregate Imaging System UIAIA	UIAI	Angularity Index	L	L
	Aggregate Imaging System AIMS	AIMSGRAD	Gradient Angularity	L	L
		AIMSRAD	Radius Angularity	L	L
	Buffalo Wire Works PSSDA-Large	PSSDA-Large ROUND	Average Roundness	L	L
Texture	University of Illinois Aggregate Imaging System UIAIA	UISTI	Mean Surface Texture Index	L	L
	Aggregate Imaging System AIMS	AIMSTXTR	Texture Index	M	M
	Camsizer	CAMCONV	Conv3	L	L
	Uncompacted Void Content of Coarse Aggregate	UCVCC	Percent Uncompacted Voi d Content	L	L
	WipShape	WSMACR	Minimal Average Curve Radius	L	L
Shape/Parameter	Camsizer	CAMSPHT	SPHT3	L	L
		CAMSYMM	Symm3	L	L
	Aggregate Imaging System AIMS	AIMSFORM	Form 2-D	L	L
		AIMSSPH	Sphericity	L	L
	Buffalo Wire Works PSSDA-Large	PSSDA-Small ROUND	Average Roundness	L	L
Shape/ Dimensional Ratio	Flat and Elongated Ratio	FER	Percent of Flat and Elongated Particles	L	H
	Multiple Ratio Analysis MRA	MRA	<Wt 2:1	L	L
			Wt 2:1– 3:1	L	L
			Wt 3:1– 4:1	H	H
			Wt 4:1– 5:1	M	H
	VDG-40 Videograder	VDG-40 SLEND	Slenderness Ratio	L	L
		VDG-40 FLAT	Flatness Factor	L	L
	Camsizer	CAML/B	l/b3	L	L
	WipShape	WSFER	<2:1	L	M
			<3:1	M	H
			<4:1	H	H
	University of Illinois Aggregate Imaging System UIAIA	UIFER	< 3:1	L	L
			3:1 – 5:1	H	H
	Aggregate Imaging System AIMS	AIMSFER	<3:1	L	L
			3:1 – 5:1	H	H

Low (L) CV<=10%, Medium (M) 10%< CV<=20%, High (H) CV>20%

- Accuracy of analysis methods in imaging-based systems was evaluated through:
  - Analysis of diagrams of particles with different characteristics. These diagrams were developed by geologists in the past to describe and quantify the two-dimensional shape and angularity of sediments. They were plotted based on actual observations of sediments and manual measurements of their shape and angularity. This task provided an initial screening test for the analysis methods by determining whether the analysis methods are capable of (1) identifying clear differences between particle projections or (2) separating the different characteristics (shape, angularity, and texture).
  - Analysis of the uniqueness of test methods. It was necessary to evaluate the correlations among the different test methods to identify analysis methods that are able

Table 9. Classification of fine aggregate test methods based on repeatability and reproducibility.

Characteristics	Test Method	Parameter Abbreviation	Measured Parameter as Reported by Test Method	Coefficient of Variation (CV) Repeatability	Coefficient of Variation (CV) Reproducibility
Angularity	Uncompacted Void Content of Fine Aggregates	UCVCF	Percent Uncompacted Void Content	L	L
	Camsizer	CAMCONV	Conv3	L	L
	Aggregate Imaging System AIMS	AIMSGRAD	Gradient Angularity	L	L
		AIMSRAD	Radius Angularity	L	L
	Buffalo Wire Works PSSDA-Small	PSSDA-Small ROUND	Average Roundness	M	M
	Compacted Aggregate Resistance CAR	CAR	Aggregate Resistance	L	L
Shape	Camsizer	CAMSPHT	SPHT3	L	L
		CAMSYMM	Symm3	L	L
		CAML/B	l/b3	L	L
	Aggregate Imaging System AIMS	AIMSFORM	Form 2-D	L	L
	Buffalo Wire Works PSSDA-Small	PSSDA-Small ROUND	Average Roundness	M	M

Low (L) CV<=10%, Medium (M) 10%<CV<=20%

to capture the same characteristics. Consequently, the method that is easier to implement and interpret was to be recommended.

- Accuracy of test methods is evaluated through:
  - Comparison between the shape measurements using the test methods and the measurements of particles' dimensions using a digital caliper.
  - Comparison between the texture and angularity visual rankings of aggregates by experienced individuals and results of test methods. This comparison identified test methods that are not capable of ranking aggregates with extreme differences in angularity and texture characteristics (e.g., uncrushed river gravel vs. crushed gravel, uncrushed river gravel vs. crushed granite).

Accuracy of Analysis Methods

Comparison with geological projections. The two dimensional image analysis methods listed in Table 10 were used to analyze the particle projections shown in Figure 2 (a detailed description of these analysis techniques is presented in Appendix C). These particle projections were developed by geologists in the past to describe and quantify the 2-D shape and angularity of sediments. These shapes were plotted based on actual

Table 10. Methods used in analyzing aggregate images.

Analysis Method	Description
Texture Index Using Wavelet	Used by AIMS analysis Software (AIMSTXTR)
Gradiant Angularity Index	Used by AIMS analysis Software (AIMSGRAD)
Radius Angularity Index	Used by AIMS analysis Software (AIMSRAD)
2-D Form Index	Used by AIMS analysis Software (AIMSFORM)
Sphericity	Used by AIMS analysis Software (AIMSSPH)
Texture Index (Fourier)	(FRTXTR)
Angularity Index (Fourier)	(FRANG)
Form Index (Fourier)	(FRFORM)
Flat & Elongated Ratio	Used By University of Illinois System (UIFER)
Angularity Using Outline Slope	Used By University of Illinois System (UIAI)
Surface Texture Using Erosion-Dilation Technique	Used By University of Illinois System (UISTI)
Aspect Ratio	Used in Image Pro Software (ASPTPRO)
Fractal Dimension	Used in Image Pro Software (FRCTLPRO)
Roundness	Used in Image Pro Software (ROUNDPRO)

Note: Analysis methods are described in Appendix D.

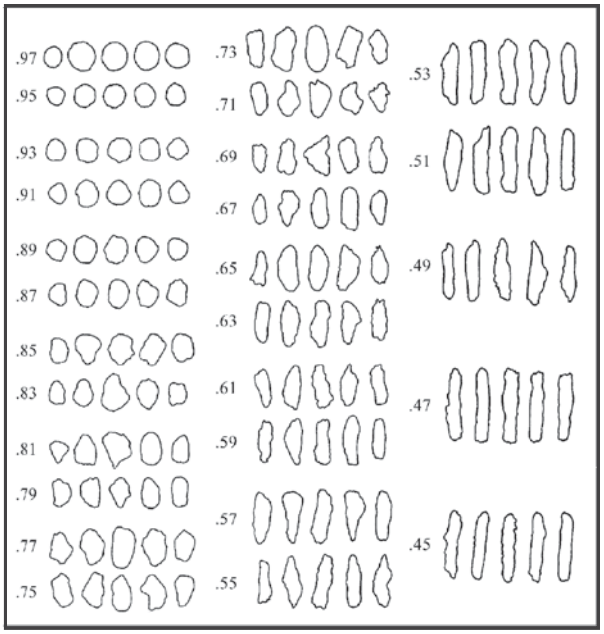

(**a**) Rittenhouse (1943)

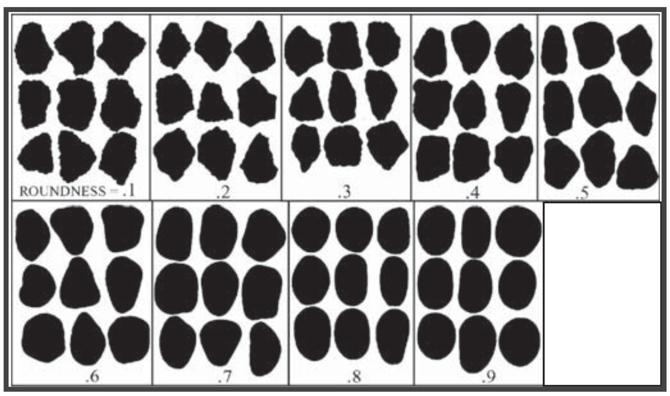

(**b**) Krumbein (1941)

Figure 2. Charts used by geologists in the past for visual evaluation of granular materials.

observations of sediments and manual measurements of their shape and angularity. Figure 2(a) was developed by Rittenhouse (*13*) based on an earlier version developed by Wadell (*14, 15*) to measure 2-D shape; it is considered a standard and accurate method for evaluating shape (*16, 17*). Figure 2(b) was developed by Krumbein (*18*) to evaluate angularity.

Correlations between analysis method parameters and visual numbers by Rittenhouse and Krumbein (Figure 2) were analyzed using the Pearson and Spearman coefficients. The Pearson coefficient (r) is defined as in Equation 8:

$$r = \frac{\sum_{i=1}^{n}(x_i - \bar{x})(y_i - \bar{y})}{\sqrt{\sum_{i=1}^{n}(x_i - \bar{x})^2 \sum_{i=1}^{n}(y_i - \bar{y})^2}} \quad (8)$$

Table 11. Pearson and Spearman correlation coefficients of Rittenhouse sphericity.

Analysis Method Parameter	Pearson Correlation Coefficient	Spearman Correlation Coefficient	Applicability
AIMSGRAD	0.458	-0.54	N
AIMSRAD	-0.868	-0.894	Y*
AIMSFORM	-0.98	-0.991	Y*
FRFORM	-0.918	-0.993	Y
FRANG	-0.814	-0.99	Y*
FRTXTR	-0.858	-0.999	Y*
UIFER	-0.938	-0.993	Y
UIAI	-0.388	-0.368	N
UISTI	0.273	0.425	N
ASPTPRO	-0.938	-0.995	Y
FRCTLPRO	0.256	-0.322	N
ROUNDPRO	-0.941	-0.996	Y*

* Method correlates with two characteristics.

where x and y represent two p-dimensional observations (items) $x = [x_1, x_2, \ldots, x_p]$ and $y = [y_1, y_2, \ldots, y_p]$. x represents the values measured by the image analysis methods on the projections, and y represents the visual numbers assigned to the projections in Figures 2a and 2b. The Spearman coefficient is defined exactly as the Pearson coefficient in Equation 8, but x and y represent the ranking of the image analysis results and visual numbers, respectively, instead of the actual values. The correlation results are shown in Tables 11 and 12. Examples of the correlations of image analysis methods with angularity visual numbers are shown in Figure 3.

Rittenhouse (*13*) and Krumbein (*18*) projections can be used to identify analysis methods capable of capturing changes in shape and angularity, respectively. The correlation results shown in Tables 11 and 12 suggest that:

- The following methods can be used only to describe shape without being affected by angularity of a particle: (a) Flat Elongated Ratio used by University of Illinois test method (UIFER), (b) Form Index measured using Fourier Series

Table 12. Pearson and Spearman correlation coefficients of Krumbein roundness.

Analysis Method Parameter	Pearson Correlation Coefficient	Spearman Correlation Coefficient	Applicability
AIMSGRAD	-0.886	-0.983	Y
AIMSRAD	-0.964	-0.967	Y*
AIMSFORM	-0.958	-0.967	Y*
FRFORM	-0.016	-0.033	N
FRANG	-0.908	-0.883	Y*
FRTXTR	-0.942	-0.967	Y*
UIFER	0.486	-0.317	N
UIAI	-0.959	-0.983	Y
UISTI	-0.957	-0.983	Y
ASPTPRO	-0.414	0.317	N
FRCTLPRO	-0.869	-0.867	Y
ROUNDPRO	-0.959	-0.967	Y*

* Method correlates with two characteristics.

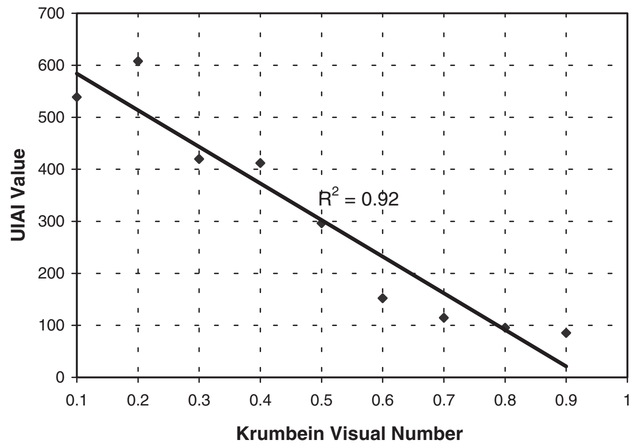

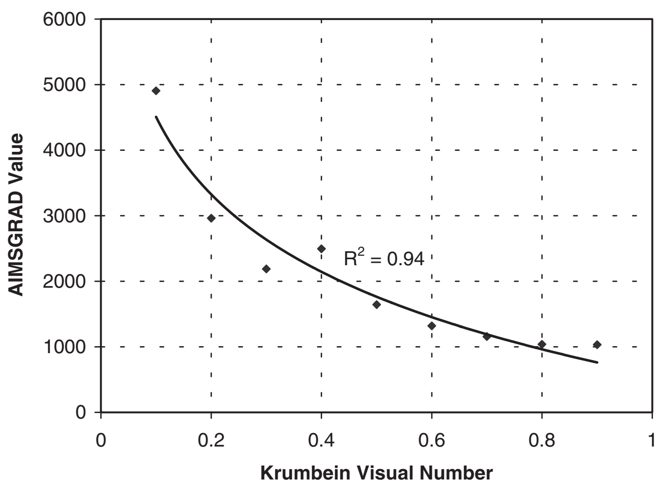

Figure 3. Examples of the correlations of image analysis methods with visual numbers of angularity.

(FRFORM), and (c) Aspect Ratio measured using Image Pro software (ASPTPRO).

- The following methods can be used to describe angularity without being affected by shape: (a) Gradient Angularity used in the Aggregate Imaging System AIMS (AIMSGRAD), (b) Angularity Index used by the University of Illinois test method (UIAI), (c) Fractal technique used in Image Pro software (FRCTLPRO).
- Roundness measured using Image Pro (ROUNDPRO), and Texture Index using Fourier (FRTXTR), Angularity Index using Fourier (FRANG), Form Index Using AIMS (AIMSFORM), and Radius Angularity using AIMS (AIMSRAD) have good correlation with Rittenhouse sphericity numbers and Krumbein roundness numbers. This indicates that these methods are not as unique as the other methods in distinguishing between angularity and shape of particles. The Angularity Index (UIAI) and Texture Index (UISTI) have high correlations with each other. This could be attributed to the nature of the projections in Figure 2b as they might have been created to have the same levels of surface irregularities at the angularity and texture scales. In other words, there was no distinction between angularity and texture in the projections in Figure 2b.

Uniqueness of test methods. This task was performed to examine the uniqueness of the analysis methods in capturing aggregate characteristics. A simple setup of a camera and a microscope was used to capture images of 50 randomly selected coarse particles (12.5 – 9.5 mm; 1/2 – 3/8 in.), and 50 fine particles (2.36 – 1.18 mm; sieve #8–#16) of each aggregate type at specific resolution. The setup was equipped with top lighting to capture gray images for texture analysis and a backlighting to capture black and white images for angularity analysis. The resulting images were analyzed using standard image analysis techniques, some of which are employed in the imaging-based tests evaluated in this study.

Using the capabilities of SPSS software, the analysis results from the 50 images of the coarse aggregate size of each aggregate type were used to cluster the analysis methods. The analysis methods were clustered on the basis of similarities or distances using Ward's Linkage method.

Two types of similarities were used. The Pearson correlation coefficient, given by Equation 8, was used as a measure of proximity when variables (analysis methods) were grouped, and the Euclidean distance, given by Equation 9, was used to cluster aggregates.

$$d(x,y)=\sqrt{\sum_{i=1}^{p}(x_i-y_i)^2} \qquad (9)$$

where x and y represent two p-dimensional observations (items) $x = [x_1, x_2, \ldots, x_p]$ and $y = [y_1, y_2, \ldots, y_p]$.

Ward's Linkage method was applied with Pearson correlation proximity measure to the analysis results to identify clusters of analysis methods. The results of the cluster analysis are shown in Table 13. For each aggregate type, the test methods that have the same number (1, 2, 3, or 4) are more correlated with each other than with other test methods and are considered clustered. For example, the data from AIMSTXTR analysis of CA-1 is statistically different than the data from all the other test methods, indicating that this analysis method captures an aggregate characteristic different than what is captured by all the other methods. The percentage of aggregates that a test method is clustered with other test methods is shown in Table 14. For example, the AIMSTXTR method is clustered alone in 54 percent of aggregates, clustered with another method in 31 percent of aggregates, and with two other methods in 9 percent of aggregates. The increase in percentage in the cells toward the left of the table indicates an increase in the uniqueness of the characteristic measured using this method. Based on the results in Tables 15 and 16, AIMSTXTR is the most unique among the texture parameters, AIMSGRAD and

Table 13. Clustering of analysis methods (4 clusters) based on Pearson correlation.

Analysis Method	Coarse Aggregate												
	1	2	3	4	5	6	7	8	9	10	11	12	13
AIMSTXTR	1	1	1	1	1	1	1	1	1	1	1	1	1
AIMSGRAD	2	2	2	2	2	2	2	2	2	2	1	2	2
AIMSRAD	2	2	3	2	2	3	2	1	2	3	2	3	3
AIMSFORM	2	2	2	2	2	3	2	1	2	3	2	3	3
AIMSSPH	3	3	3	3	3	1	3	3	3	1	3	1	4
UIFER	4	4	4	4	4	4	4	3	4	4	4	4	1
UIAI	4	4	4	4	4	4	4	2	4	4	4	4	2
UISTI	4	4	4	4	4	4	4	2	4	4	4	4	1
FRFORM	2	2	2	2	2	3	2	1	2	3	2	3	3
FRANG	2	2	2	2	2	3	2	1	2	3	2	3	3
FRTXTR	2	2	2	2	2	3	2	4	2	3	2	3	3
ASPCTPRO	2	2	2	2	2	3	2	1	2	3	2	3	3
FRCTLPRO	2	2	3	2	2	3	3	1	2	3	2	3	3
ROUNDPRO	2	2	2	2	2	3	2	1	2	3	2	3	3

UIAI are the most unique among the angularity parameters, and AIMSSPH is the most unique among the shape parameters. The UIAI and UISTI methods are clustered together for 12 of the 13 aggregates.

Clustering of aggregates based on the results of analysis methods. Ward's Linkage method was used to cluster aggregates based on the angularity and texture measured using each of the analysis methods; results are shown in Tables 15 and 16.

As shown in Table 15, both the FRTXTR and FRACTLPRO texture parameters place aggregates CA-1 (uncrushed gravel) and aggregates CA-9 and CA-10 (both are granite) in the same cluster, indicating the inability of methods to detect significant differences between these aggregates. Similarly, UISTI places both aggregates CA-2 (crushed gravel) and CA-10 (granite) in the same texture cluster.

The results in Table 16 show that AIMSRAD, FRANG, and ROUNDPRO methods cluster the uncrushed (CA-1) and crushed gravel (CA-2) in the same group, indicating the inability of these methods to distinguish the difference in angularity. Table 17 summarizes the characteristics of the analysis methods.

Accuracy of Test Methods

A digital caliper was used to measure the three dimensions of 100 particles selected randomly from each of the aggregates

Table 14. Percentage of clustered aggregates for each analysis method.

Analysis Method	Number of Methods to Cluster With					
	0	1	2	6	7	8
AIMSTXTR	54%	31%	8%	8%	8%	
AIMSGRAD	23%	15%	8%	8%	8%	38%
AIMSRAD			8%		54%	38%
AIMSFORM				8%	54%	38%
AIMSSPH	54%	38%	8%			
UIFER		8%	92%			
UIAI		8%	92%			
UISTI			100%			
FRFORM				8%	54%	38%
FRANG				8%	54%	38%
FRTXTR	8%			8%	46%	38%
ASPCTPRO				8%	54%	38%
FRCTLPRO		8%	8%		46%	38%
ROUNDPRO				8%	54%	38%

Table 15. Coarse aggregates in texture classes estimated using Ward's Linkage.

Method	Class 1	Class 2	Class 3	Class 4
AIMSTXTR	1, 2, 12	3, 5, 10, 11, 13	4, 6, 7, 8	9
UISTI	1, 8	2, 3, 7, 10, 11, 13	4, 6, 9, 12	5
FRTXTR	1, 7, 9, 10, 12	2, 4	3, 5, 6, 11, 13	8
FRACTLPRO	1, 4, 9, 10, 12	2, 3, 6, 11, 13	5, 7	8

Table 16. Coarse aggregates in angularity classes estimated using Ward's Linkage.

Method	Class 1	Class 2	Class 3	Class 4
AIMSGRAD	1, 8	2, 4, 6, 7, 12	5, 9, 10	3, 11, 13
AIMSRAD	1, 2, 9	3, 4, 11, 13	5, 6, 7, 10, 12	8
UIAI	1	2, 6, 9	3, 4, 5, 7, 10, 11, 12, 13	8
FRANG	1, 2, 3, 6, 9, 11, 12	4, 5, 7, 10	8	13
FRACTLPRO	1, 4, 9, 10, 12	2, 3, 6, 11, 13	5, 7	8
ROUNDPRO	1, 2, 6, 12	3, 4, 5, 7, 9, 10, 11	8	13

with sizes passing a 12.5 mm (½ in.) sieve and retained on a 9.5 mm (⅜ in.) sieve. The percentage of particles with a longest to shortest ratio dimension of 3:1 or more sphericity was calculated; the results are shown in Table 18. The correlations between the caliper measurements and results of test methods were estimated in terms of the coefficient of multiple determinations (R^2). R^2 is a statistic that measures how successful the fit is in explaining the variation of the data. It is defined as the ratio of the sum of squares of the regression (SSR) and the total sum of squares (also known as sum of squares about the mean [SST]) and is expressed as

$$R^2 = \frac{SSR}{SST} = \frac{\sum_{i=1}^{n}(\hat{y}_i - \bar{y})^2}{\sum_{i=1}^{n}(y_i - \bar{y})^2} \qquad (10)$$

The MRA method had the highest correlation with the digital caliper. The UIFER test method was not able to measure all

Table 17. Features of methods used in analyzing aggregate images.

Analysis Method	Features
AIMSTXTR	• Capable of separating aggregates with different texture characteristics. • Most unique among the texture parameters.
AIMSGRAD	• Capable of separating aggregates with different angularity characteristics. • Capable of separating angularity from shape.
AIMSRAD	• Captures angularity but it is not capable of separating 2-D shape from angularity.
AIMSFORM	• Captures 2-D shape but it is not capable of separating shape from angularity.
AIMSSPH	• Capable of separating aggregates with different characteristics. • Captures unique characteristics of aggregates.
FRTXTR	• Does not separate angularity from shape. • Clusters aggregates with distinct characteristics. This can be improved if different image resolutions are used.
FRANG	• Does not separate angularity from shape. • Clusters aggregates with distinct characteristics. This can be improved if different image resolutions are used.
FRFORM	• Capable of separating shape from angularity. • Clusters aggregates with distinct characteristics. This can be improved if different image resolutions are used.
Used by University of Illinois System (UIFER)	• Capable of separating aggregates with different characteristics. • Capable of separating shape from angularity.
UISTI	• Capable of separating aggregates with different aggregate characteristics. • Clusters aggregates similar to UIAI. This can be improved if different image resolutions are used.
ASPTPRO	• Separates angularity from shape.
FRCTLPRO	• Separates angularity from shape. • Clusters aggregates with distinct characteristics in the same group. This can be improved if different image resolutions are used.
ROUNDPRO	• Separates angularity from shape. • Clusters aggregates with distinct characteristics in the same group. This can be improved if different image resolutions are used.

Table 18. Aggregate sphericity from longest to shortest dimensions from digital caliper results.

Coarse Aggregate	Average Sphericity	3:1 & Higher (%)
CA 1	0.717	8
CA 2	0.740	2
CA 3	0.675	18
CA 4	0.662	30
CA 5	0.731	2
CA 6	0.711	6
CA 7	0.624	42
CA 8	0.706	6
CA 9	0.643	38
CA 10	0.697	18
CA 11	0.659	22
CA 12	0.666	18
CA 13	0.638	38

aggregates used in this study due to their dark color. Both AIMS and PSSDA-Large provide a sphericity value. The sphericity measured using the digital caliper had very good agreement with AIMS and PSSDA-Large measurements. Figure 4 shows a comparison between AIMS measurements and digital caliper measurements for sphericity.

Measurements of angularity and texture of coarse aggregates were compared with visual rankings of aggregates made by five evaluators with backgrounds in asphalt pavements, concrete pavements, geology, and petrographic analysis. These evaluators were provided with a form to fill with the rankings. R^2 values between the evaluators for texture and angularity rankings are shown in Table 19.

The rankings made by the evaluators were more correlated for texture than for angularity. The evaluators suggested that the main difficulty was in visually separating angularity from texture. Therefore, aggregates were ranked based on surface irregularity that combines both angularity and texture. Therefore, it was decided for this study to establish a visual ranking of surface irregularity; the correlation between rankings is shown in Table 19.

The experimental measurements were compared to the visual rankings of surface irregularity and texture. The comparison with surface irregularity is useful since the evaluated tests themselves do not use the same methods to analyze angularity and texture. In fact, the definition of angularity in a certain test method can be similar to the definition of texture in another test method. Very good correlation was found between the evaluators ranking aggregates based on surface irregularity; average rankings are shown in Table 20. Similarly, the evaluators ranked fine aggregate angularity by examining their shape under a microscope; visual rankings are shown in Table 21.

The correlations between the measurements and the corresponding visual ranking were used to rank the test methods, as described later.

Cost and Operational Characteristics of Test Methods

Information about cost and operational characteristics was collected from vendors, researchers, and operators who have familiarity with these systems for use in ranking the test methods. The information included cost, ease of use, portability, ability of interpreting data, readiness for implementation

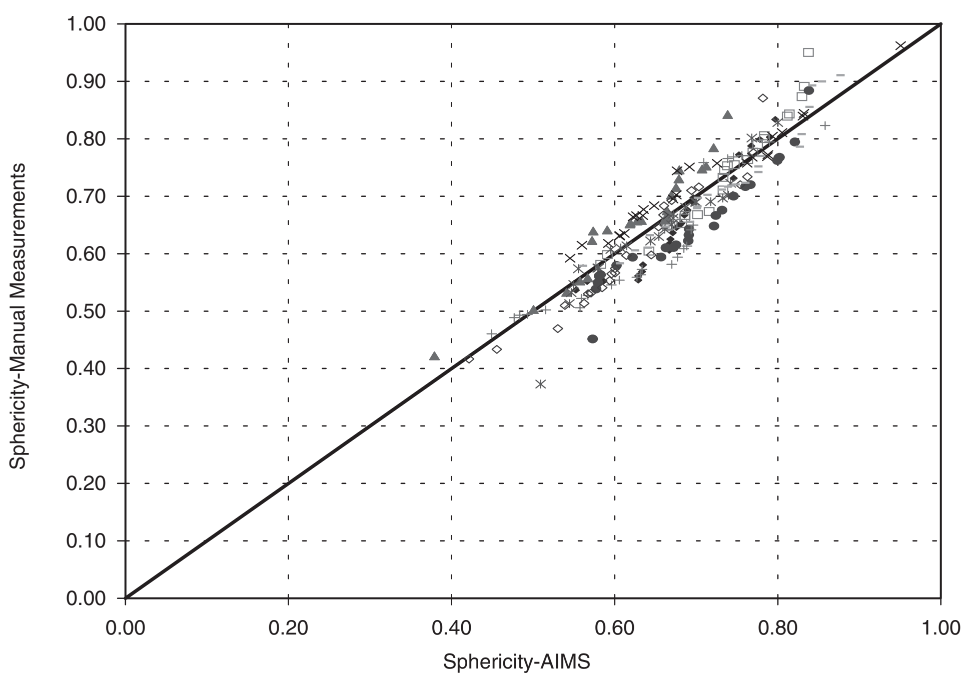

Figure 4. Comparison between sphericity measurements of AIMS and the digital caliper.

Table 19. Coefficients of multiple determinations (R^2) between the rankings of evaluators.

	Evaluator	I	II	III	IV	V
Angularity	I	1	0.57	0.58	0.37	0.3
	II		1	0.9	0.41	0.57
	III			1	0.41	0.46
	IV				1	0.41
	V					1
Texture	Evaluator	I	II	III	IV	V
	I	1	0.91	0.92	0.89	0.82
	II		1	0.95	0.79	0.84
	III			1	0.84	0.82
	IV				1	0.74
	V					1
Surface Irregularity	Evaluator	I	II	III	IV	V
	I	1	0.77	0.80	0.76	0.59
	II		1	0.95	0.69	0.79
	III			1	0.70	0.72
	IV				1	0.71
	V					1

in central laboratories and field laboratories, and applicability of test method to measure different aggregate types and sizes. Table 22 lists this information.

Ranking of Test Methods Using the Analytical Hierarchy Process

The Analytical Hierarchy Process (AHP) has been adapted to rank the test methods according to their repeatability, reproducibility, accuracy, cost, and operational characteristics. The process is presented as computational software to expedite conducting the calculations and provides the user with flexibility in specifying the objectives, ranking criteria, and relative importance or priorities of the different criteria elements.

Table 20. Average visual rankings of coarse aggregates by evaluators.

Aggregate	Texture	Surface Irregularity
CA-1	1.6	1.8
CA-2	4.4	4.2
CA-3	6.8	8.6
CA-4	7.4	8.1
CA-5	12.8	9.8
CA-6	5.2	5.8
CA-7	5.8	6.0
CA-8	1.4	1.2
CA-9	11.4	9.9
CA-10	11.6	10.4
CA-11	9.0	10.3
CA-12	3.6	4.2
CA-13	10.0	10.7

Notes: 1- CA= coarse aggregate; 2- Higher rank is associated with higher angularity and/or texture.

Background on the Process

AHP is a decision making process that transforms complex decision making into a series of one-on-one comparisons and then combines the results to help arrive at the best, most justified decision. The process incorporates both subjective and objective evaluation measures such that the bias in decision making is reduced and has been used in several applications dealing with the selection of alternatives, investment distribution, and energy allocation (*21*).

The AHP method is based on decomposing the goal into its component parts, moving from the general to the specific (i.e., proceeding from the goal to objectives and criteria subobjectives down to the alternative courses of action). After structuring the hierarchy of all criteria, the next step is to assign a relative weight to each criterion. Weights are assigned

Table 21. Visual ranking of fine aggregate angularity by evaluators.

Aggregate	Visual Ranking
FA-1	2
FA-2	4
FA-5	5
FA-6	1
FA-9	3

Notes: 1- FA= fine aggregate; 2- Higher rank is associated with higher angularity.

Table 22. Rating of test methods' operational characteristics.

Test Method	Estimated Price ($)	Readiness for Implementation[(a)]	Ability to Interpret Data[(b)]	Ease of Use by Technician[(b)]	Portability[(c)]	Applicability to Aggregate Type and Size[(d)]	
						Coarse	Fine
Uncompacted Void Content of Fine Aggregates AASHTO T 304	250	1	1	1	1	N/A	1
Uncompacted Void Content of Coarse Aggregates AASHTO T P56	500	1	1	1	1	1	N/A
Compacted Aggregate Resistance (CAR)	500	1	1	1	1	N/A	1
Percentage of Fractured Particles in Coarse Aggregate ASTM D 5821	0	1	1	1	1 (N/A)	1	N/A
Flat and Elongated Coarse Aggregates ASTM D 4791	250	1	1	1	1	1	N/A
Multiple Ratio Shape Analysis	1,500	2	2	2	1	1	N/A
VDG-40 Videograder	40,000 - 50,000	2	3	2	2	1	1
Buffalo Wire Works PSSDA -Large	30,000 - 40,000	3	3	3	2	1	N/A
Buffalo Wire Works PSSDA -Small	30,000 - 40,000	2	3	2	2	N/A	1
Camsizer	40,000 - 50,000	2	3	2	2	2	1
WipShape	30,000 - 40,000	2	3	3	2	1	N/A
University of Illinois Aggregate Image Analyzer (UIAIA)	30,000 - 40,000	3	3	3	2	3	N/A
Aggregate Imaging System (AIMS)	30,000 - 40,000	2	3	3	2	1	1

Notes: [(a)] 1: Available commercially. Wide use in laboratories. 2: Available commercially. Limited use in laboratories. 3: Not available commercially. Limited use in research laboratories. Can be made available commercially.
[(b)] 1: Very Easy, 2: Easy, 3: Intermediate, 4: Difficult.
[(c)] 1: Can be used in central and field laboratories. Requires less than 1 hr to move it. 2: Can be used in central and field laboratories. Requires less than 4 hrs to move it. 3: Not portable. Cannot be used in central and field laboratories.
[(d)] 1: Measure all aggregate sizes and types, 2: Measure all aggregate types but not all sizes, 3: Measure all sizes but not very dark colored aggregates, N/A: Not Applicable.

by the user based on a pairwise comparison judgment scale of 1 to 9 (also known as standard preference table). Then the user calculates priorities, using a simple mathematical procedure, to arrive at overall priorities for the alternatives. The sum of all the criteria beneath a given parent criterion in each level of the model must equal one. Each priority list shows its relative importance within the overall structure. From the overall priority list, the decision maker can choose among alternatives by selecting the highest priority alternative. The mathematical functions involved in AHP can be found in Saaty (*21*).

Program Description

Computational software was developed to make the calculation process easier and faster. The program provides the user flexibility in changing objectives or selection criteria weights before making the final selection from available alternatives. The software was created using VC++ programming language that can be run on any computer irrespective of the operating system.

The program uses the crude estimate, specified by Saaty (*21*), to calculate the priority vector through the process of averaging over normalized columns technique. The elements of each column are divided by the sum of that column, and then the elements in each resulting row are added and divided by the sum of the numbers in that row.

The program uses a graphical interface environment; the process is summarized in the following steps (for illustration, fine aggregate angularity is used to describe the operation steps of the new program): (1) The user enters the number of testing methods being compared and the characteristics determining the performance of the test method (Figure 5a). (2) Generic text boxes are generated and the user inputs the names of each of the characteristics and testing methods (Figure 5b). (3) The user enters the weights assigned to test methods when pairwise comparison is conducted with respect to each characteristic (Figure 6a). Note that because the lower triangle of these matrices is the reciprocal of the upper triangle with ones along the diagonal, the user inputs the upper half of the matrix and the other values are updated automatically. (4) The user is prompted to enter the weights comparing the various characteristics with respect to overall satisfaction with a method in a new interface (Figure 6b). (5) The program calculates the priority vectors for each of the matrices and displays them in a new interface window (Figure 7a). (6) The program also

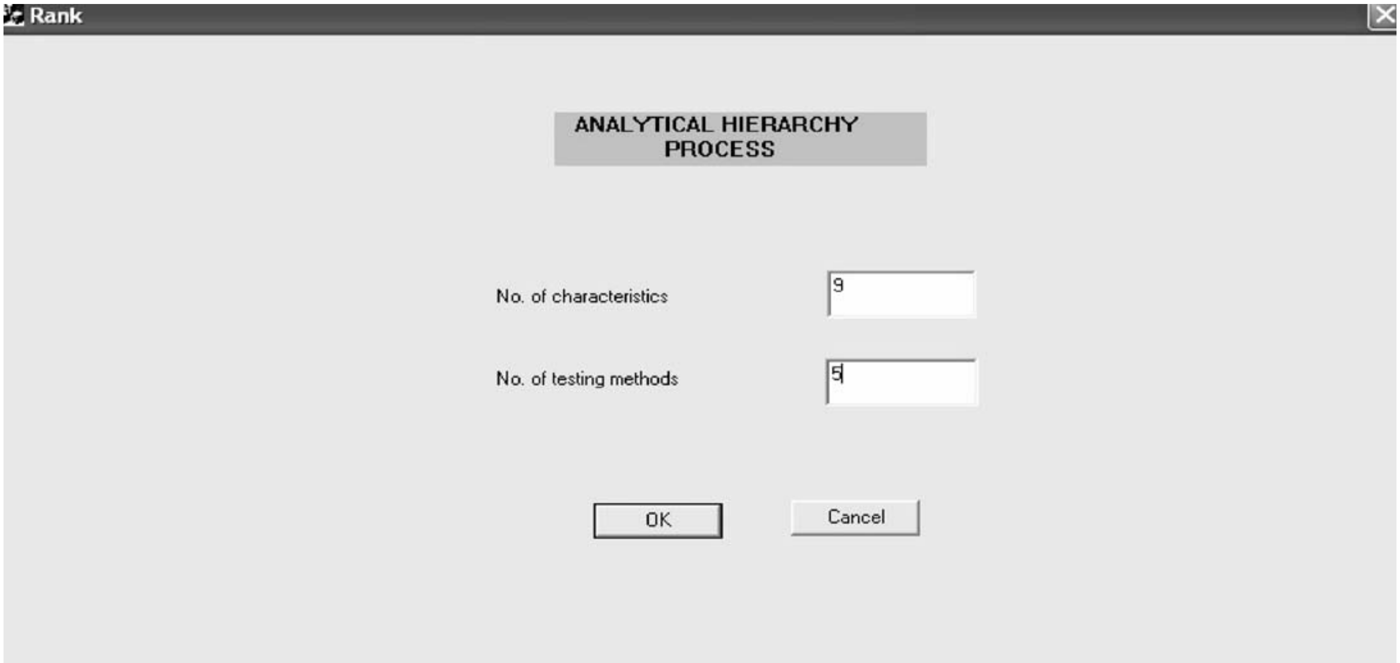

(a) Number of Characteristics and Test Methods

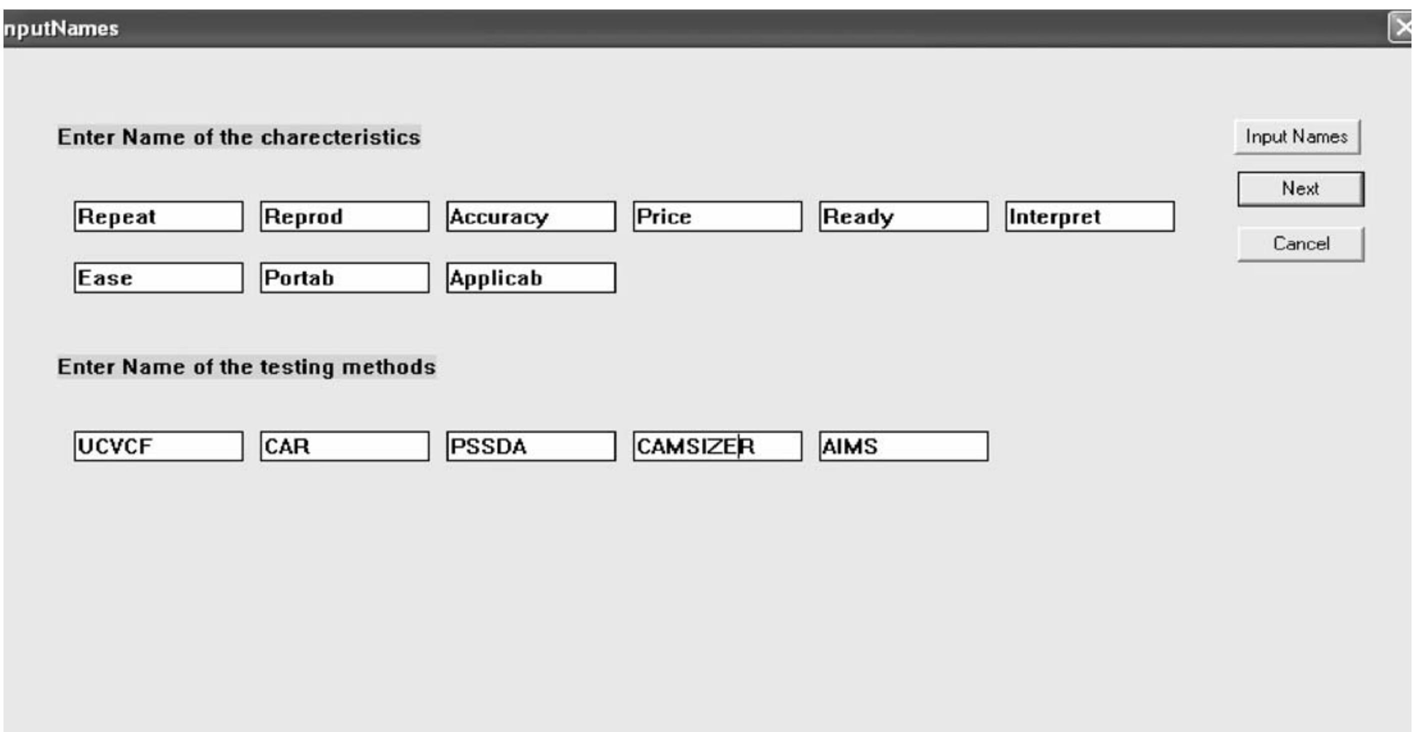

(b) Names of Characteristics and Test Methods

Figure 5. Screens of interface to enter numbers and names of characteristics and test methods.

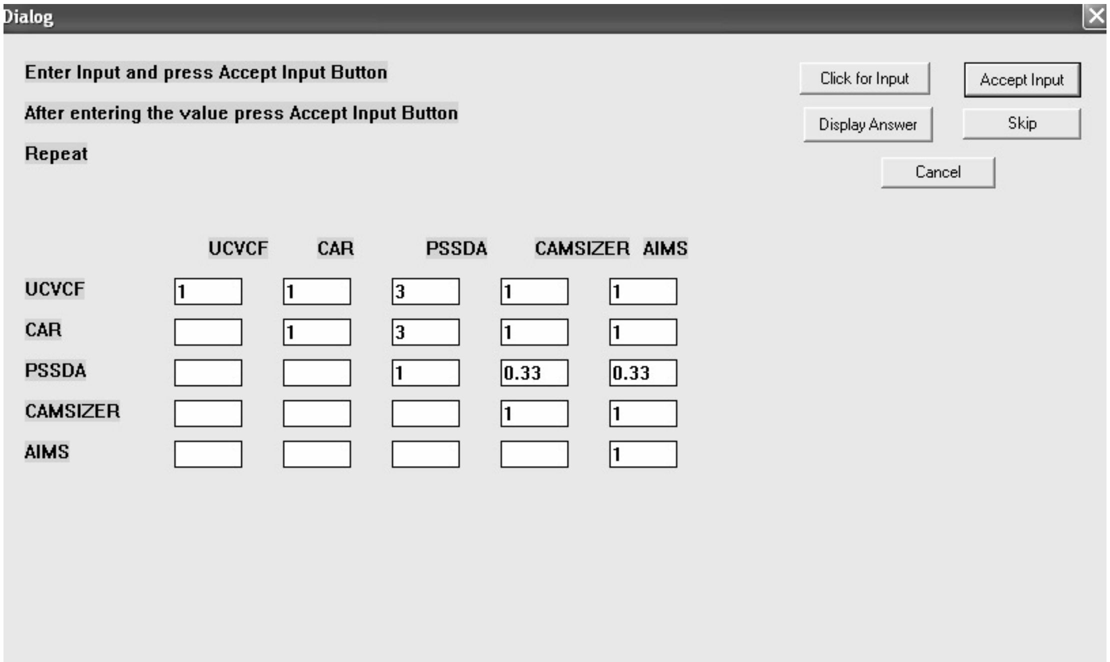

(a) Weights Comparing Test Methods to Characteristics

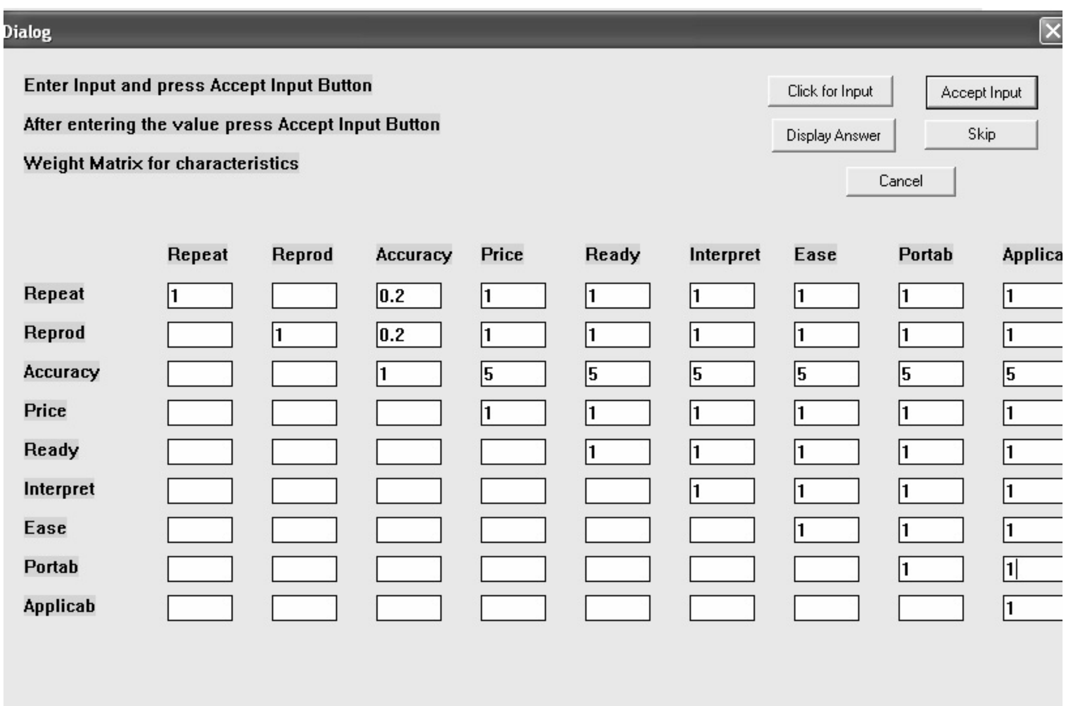

(b) Weights Comparing Characteristics

Figure 6. Screens of interface to enter weights comparing test methods to characteristics, and characteristics with respect to overall satisfaction with method.

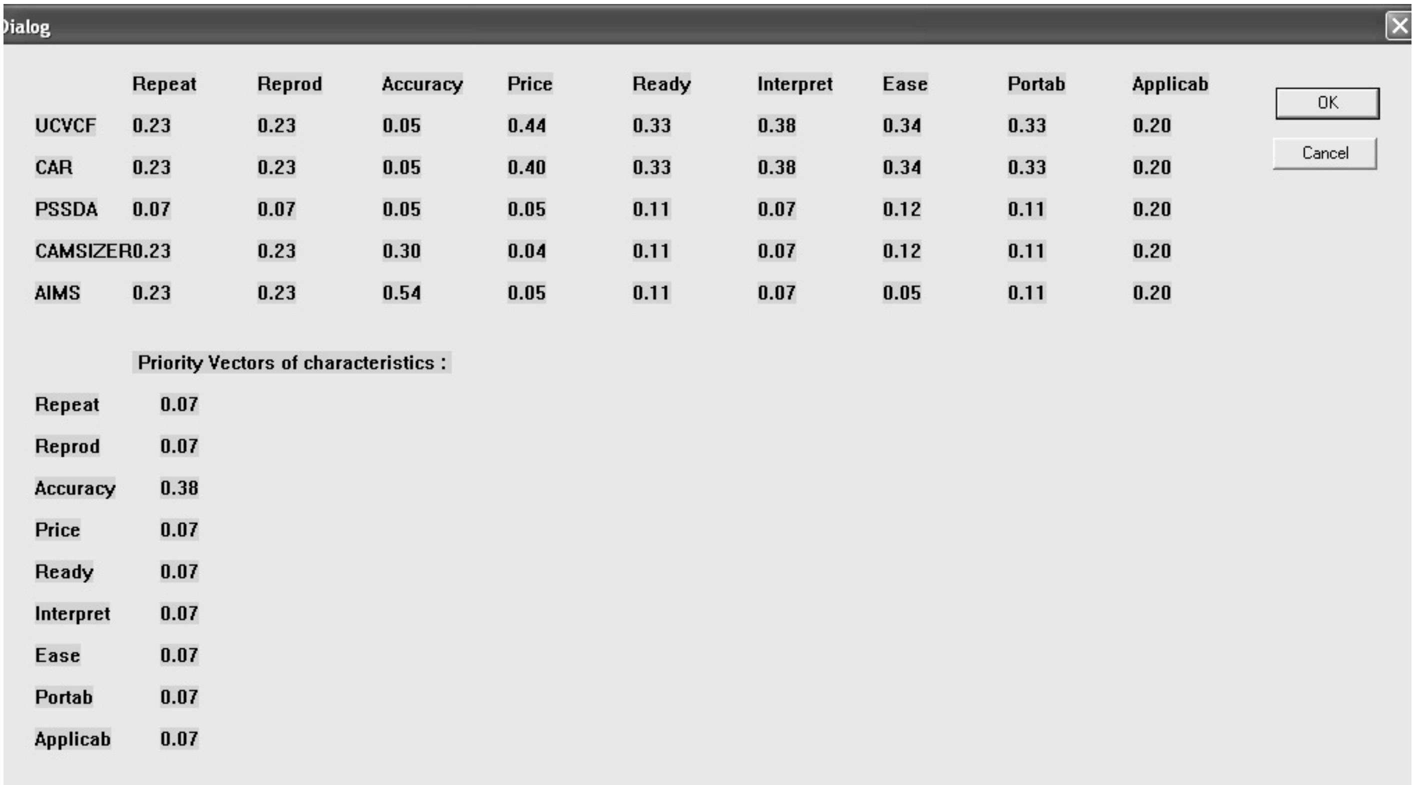

Dialog

	Repeat	Reprod	Accuracy	Price	Ready	Interpret	Ease	Portab	Applicab
UCVCF	0.23	0.23	0.05	0.44	0.33	0.38	0.34	0.33	0.20
CAR	0.23	0.23	0.05	0.40	0.33	0.38	0.34	0.33	0.20
PSSDA	0.07	0.07	0.05	0.05	0.11	0.07	0.12	0.11	0.20
CAMSIZER	0.23	0.23	0.30	0.04	0.11	0.07	0.12	0.11	0.20
AIMS	0.23	0.23	0.54	0.05	0.11	0.07	0.05	0.11	0.20

OK

Cancel

Priority Vectors of characteristics :

Repeat	0.07
Reprod	0.07
Accuracy	0.38
Price	0.07
Ready	0.07
Interpret	0.07
Ease	0.07
Portab	0.07
Applicab	0.07

(a) Priority Vectors

Dialog

Final Priority Vector:

UCVCF	0.21
CAR	0.20
PSSDA	0.08
CAMSIZER	0.20
AIMS	0.29

OK

Cancel

(b) Overall Ranking

Figure 7. Screens of priority vectors and overall ranking of test methods.

calculates the overall ranking of the test methods by multiplying the priority matrix of the methods by the priority vector of the characteristics and displays it in a separate interface window (Figure 7b).

The program also has features that enable the user to: (1) extract the priority vectors and the overall ranking from a text file and (2) examine the influence of changes in the weights or importance of one or more of the characteristics without changing the remaining ones (i.e., the software has to be executed several times with just one matrix change) without a need to re-enter the unchanged matrices.

AHP Ranking of Test Methods

The ranking of test methods depends on the desired outcomes from the test. This section provides an example of how the AHP can be used to determine the ranking of test methods measuring fine aggregate angularity, and texture and shape of coarse aggregates.

The first level in AHP is the overall goal, which is the satisfaction with test methods. The second level consists of the criteria elements by which this satisfaction is measured. These characteristics are repeatability, reproducibility, accuracy, price, readiness for implementation, ability to interpret data and results, ease of use by technician, portability, and applicability to measure different aggregate types and sizes. The third level consists of the test methods that are under evaluation. Figure 8 illustrates a basic hierarchy for the ranking process.

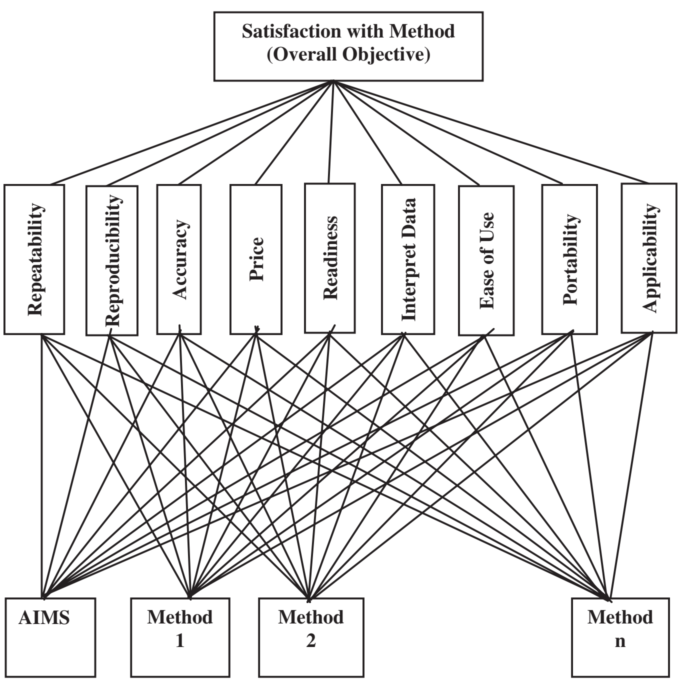

Figure 8. An example of basic analytical hierarchy process (AHP).

The ranking is determined using pairwise comparisons of the characteristics (level 2) and the test methods (level 3). The first pairwise comparison is conducted among the characteristics in the second level using the comparison scale given in Table 23 and results are listed in Table 24. The number in each cell of the table is a weight that reflects the relative importance of the characteristic in the horizontal list compared with the one in the vertical list. If this number is higher than one, it means that the characteristic listed in the row is more important than the characteristic listed in the column. For example, accuracy is considered three times as important as repeatability and reproducibility and five times as important as all the other characteristics. All other characteristics are considered to be equal in their importance.

Weights that compare test methods based on each of the characteristics are based on the measurements and data presented in Chapter 2; these are listed in Table 25. The comparison scale values shown in Table 28 were selected based on the importance of each of the desired characteristics as follows:

- Repeatability/Reproducibility: Repeatability and reproducibility are categorized into three main categories as Levels 1, 2, and 3. Levels 1 and 2 can be considered as acceptable scales and some of the test methods can move from Level 2 to 1 with some minor improvements. However, Level 3 is unacceptable because it covers high ranges of coefficient of variations. Therefore, the difference between Levels 3 and 2 is less desirable than the difference between Levels 1 and 2.
- Accuracy: Accuracy of test methods was assessed based on the correlation between the test method and a reference method. The scale for accuracy was established by dividing the R^2 values into four categories as shown in Table 26. The ratio between the numbers assigned to each accuracy group is then used to assign the accuracy scale.
- Price: The price scale is assigned taking into consideration that the lowest price of a test method is about $250, while the highest price is about $45,000 ($250 is taken as the basis for the cost ratio).

Table 23. Rating scale.

Verbal Judgment of Preference	Numerical Rating
Equally Important or Preferred	1
Weakly More Important	3
Moderately More Important	5
Strongly More Important	7
Absolutely More Important	9
Weakly Less Important	1/3
Moderately Less Important	1/5
Strongly Less Important	1/7
Absolutely Less Important	1/9

Table 24. Example of the relative importance of the test methods characteristics.

Characteristics of Test Methods	Repeatability	Reproducibility	Accuracy	Price	Readiness	Interpret Data	Ease of Use	Portability	Applicability
Repeatability	1	1	0.33	1	1	1	1	1	1
Reproducibility	1	1	0.33	1	1	1	1	1	1
Accuracy	3	3	1	5	5	5	5	5	5
Cost	1	1	0.2	1	1	1	1	1	1
Readiness	1	1	0.2	1	1	1	1	1	1
Interpret Data	1	1	0.2	1	1	1	1	1	1
Ease of Use	1	1	0.2	1	1	1	1	1	1
Portability	1	1	0.2	1	1	1	1	1	1
Applicability	1	1	0.2	1	1	1	1	1	1

- Readiness/Portability: The scale for readiness reflects the preference for a test method that has been used by research and testing laboratories and thus methods that are not available commercially are considered slightly less desirable than those that are available. However, this point is not highly emphasized in the scale (the maximum possible ratio is only 5) because any of the methods can be made available commercially in the future. The same applies for portability, as the portability of those methods that are given a scale of "3 Not portable" can be improved with some design changes.
- Interpretation of Data and Ease of Use: The values assigned in Table 22 are based on current knowledge of the test methods regarding their use in routine analysis of aggregates. Except for the methods labeled (4:difficult), technical training can improve the assigned value from (3:intermediate) to (2:easy) or even (1:very easy) indicating that the change from 3 to 4 is less desirable than the change from 1 to 3.
- Applicability to Measure Different Aggregate Types and Sizes: Test methods are expected to measure all aggregate types and sizes. If the method fails to measure some sizes or some aggregate types, or both, its applicability rating should be reduced. The values assigned for the applicability of test method to measure different aggregate types and sizes listed in Table 22 are based on current knowledge and experience with the test methods. The assigned values assume that it is weakly more important (assigned a value of 3) to have a method that can measure all aggregate types and sizes than a method that can measure all aggregate types but not all aggregate sizes or to have a method that can measure some aggregate sizes for all aggregate types than a method that can measure all sizes for some aggregate types. It is considered moderately more important (assigned a value of 5) to have a method that can measure all aggregate types and sizes than a method that can measure all aggregate sizes but not all aggregate types. A few examples are provided to highlight the process for ranking the test methods.

Fine Aggregate Angularity

AHP was used to rank the test methods that measure fine aggregate angularity: uncompacted void content of fine aggregate (UCVCF), compacted aggregate resistance (CAR), Camsizer, Buffalo Wire Works (PSSDA-Small), and AIMS. In this example, the same weights (1) were assigned for all the characteristics in the second level (i.e., characteristics were considered equally important). This means that all cells in Table 27 will have a value of 1.

A pairwise comparison of all test methods according to one characteristic was then conducted using numerical ratings selected from Table 23. These ratings are used in Table 28 in order to compare a test method from the horizontal list to that of the vertical list based on the characteristics under consideration.

Once the values in Tables 27 and 28 are assigned, the next step consists of the computation of priority lists of test methods for each of the desirable characteristics. In mathematical terms, the principal eigen vector is computed for each matrix which gives the vector of priority ordering. Saaty (*21*) proposed some crude estimates that can be easily followed to calculate these vectors. One good estimate method is to divide the elements of each column in the matrix by the sum of that column (i.e., normalize the column). Then elements in each resulting row are added then divided by the number of elements in the row. This is a process of averaging over the normalized column.

The resulting priority vectors from each matrix in Table 29 are then combined to create a matrix that represents priority of test method by each characteristic. In order to obtain the overall ranking of the test methods, the priority matrix of the methods by each characteristic will be multiplied by the

Table 25. Weights that compare test methods based on each of the characteristics.

Characteristic	Criterion	Comparison Scale				
		1	3	5	7	9
Repeatability/ Reproducibility	2:1		X			
	3:2			X		
	3:1					X
Accuracy Coarse-Shape (Ratio of R^2 groups)	2:1		X			
	3:1			X		
	3:2		X			
	4:1					X
	4:2				X	
	4:3		X			
Accuracy Coarse-Irregularity (Ratio of R^2 groups)	2:1		X			
	3:1			X		
	3:2		X			
	4:1					X
	4:2				X	
	4:3		X			
Accuracy Coarse-Texture (Ratio of R^2 groups) (Rankings)	2:1		X			
	3:1			X		
	3:2		X			
	4:1					X
	4:2				X	
	4:3		X			
Accuracy Fine-Angularity (Ratio of R^2 groups)	2:1		X			
	3:1			X		
	3:2		X			
	4:1					X
	4:2				X	
	4:3		X			
Price (Ratio of Cost)	<6	X				
	>6 <20		X			
	>20 <50			X		
	>50 <80				X	
	>80					X
Readiness	2:1		X			
	3:2		X			
	3:1			X		
Portability	2:1		X			
	3:2		X			
	3:1			X		
Data Interpretation	2:1		X			
	3:2		X			
	3:1			X		
	4:3				X	
	4:2					X
Ease of Use	2:1		X			
	3:2		X			
	3:1			X		
	4:3				X	
	4:2					X
Applicability	2:1		X			
	3:2		X			
	3:1			X		

Table 26. Accuracy categories based on R^2 values.

R^2	Category
> 0.70	1
0.6 – 0.7	2
0.5 – 0.6	3
< 0.5	4

priority vector of the characteristics resulting from Table 27. In other words, the overall ranking of a method can be obtained by multiplying the weight indicating the rank of a test method with respect to the characteristic by the weight of that characteristic then add them up for all characteristics. The resulting priority vectors and the overall ranking of test methods used to measure fine aggregate angularity are presented in Table 29.

Table 27. Comparison of the characteristics based on overall satisfaction with methods.

Characteristics of Test Methods	Repeatability	Reproducibility	Accuracy	Price	Readiness	Interpret Data	Ease of Use	Portability	Applicability
Repeatability	**1**	1	1	1	1	1	1	1	1
Reproducibility	1	**1**	1	1	1	1	1	1	1
Accuracy	1	1	**1**	1	1	1	1	1	1
Cost	1	1	1	**1**	1	1	1	1	1
Readiness	1	1	1	1	**1**	1	1	1	1
Interpret Data	1	1	1	1	1	**1**	1	1	1
Ease of Use	1	1	1	1	1	1	**1**	1	1
Portability	1	1	1	1	1	1	1	**1**	1
Applicability	1	1	1	1	1	1	1	1	**1**

The results of this example show that when all characteristics were assumed to be equally important, the uncompacted void content of fine aggregate (UCVCF) method was at the top of the priority list, mainly due to the low cost of this test. However, this priority order will change if the weights assigned to the characteristics or to the methods are changed.

In another example, the accuracy of the test method was considered more important than the other characteristics, and was thus assigned a value of 5 (based on the scale provided in Table 23). The new matrix together with the calculated priority vector are presented in Table 30. Multiplying the new characteristic's priority vector by the matrix of priority vectors (resulting from comparing method with respect to the characteristics presented in Table 28) will result in the overall ranking of test methods presented in Table 31 for different accuracy levels of preference.

It is apparent from Table 31 that when only accuracy is considered moderately or absolutely more important than the other characteristics, the ranking of test methods has changed; AIMS ranked first in the priority ordering list (with more significant difference in the latter case).

The results from the two examples clearly indicate that the selected weights can have a significant influence on the overall ranking of test methods. Therefore, it is very important that the weights should be selected based on expert opinion and judgment of the process.

Coarse Aggregate Texture

AHP was used in this example to rank the test methods that are used to measure coarse aggregate texture (UCVCC, Camsizer, WipShape, UIAIA, and AIMS). In this example, accuracy was considered moderately more important than applicability of a test method to measure all aggregate sizes and types (assigned a value of 5) and absolutely more important than all other remaining characteristics (assigned a value of 9). Also, applicability to different aggregate types and sizes was considered moderately more important than other methods (assigned a value of 5). The priority list for all the characteristics based on this consideration and the resulting priority vector are presented in Table 32.

Using the weights provided in Table 25, the process described for fine aggregate angularity was followed; the resulting priority vectors presented in Table 33 for testing methods with respect to characteristics were obtained.

The overall ranking of test methods used to measure coarse aggregate texture, presented in Table 34, clearly shows that AIMS has the highest rank among all methods. As discussed in the previous section, the wavelet method that AIMS uses in analyzing coarse aggregate texture was found to be unique and most accurate; it contributed significantly to this ranking although some imaging methods have comparable characteristics.

Because imaging methods will become more practical and easy to use with some reasonable training, only repeatability, reproducibility, accuracy, and applicability should be considered in comparing test methods. When this criterion was applied, the overall ranking of test methods measuring coarse aggregate texture shown in Table 34 was obtained, placing AIMS on the top of the priority list and thus it would be the user's first choice for measuring coarse aggregate texture. The overall rankings of test methods presented in Table 34 show that UCVCC method has high priority when all characteristics are considered, but it becomes less favorable when price becomes of less concern.

Coarse Aggregate Shape

AHP was used in this example to rank test methods that measure coarse aggregate shape parameters and dimensional

Table 28. Comparison of test methods measuring fine aggregate angularity.

Characteristic	**Test Method**	**Test Method**				
		UCVCF	CAR	PSSDA-Small	Camsizer	AIMS
Repeatability	UCVCF	**1**	1	3	1	1
	CAR	1	**1**	3	1	1
	PSSDA-Small	0.33	0.33	**1**	0.33	0.33
	Camsizer	1	1	3	**1**	1
	AIMS	1	1	3	1	**1**
Reproducibility	UCVCF	**1**	1	3	1	1
	CAR	1	**1**	3	1	1
	PSSDA-Small	0.33	0.33	**1**	0.33	0.33
	Camsizer	1	1	3	**1**	1
	AIMS	1	1	3	1	**1**
Accuracy	UCVCF	**1**	1	1	0.143	0.11
	CAR	1	**1**	1	0.143	0.11
	PSSDA-Small	1	1	**1**	0.143	0.11
	Camsizer	7	7	7	**1**	0.33
	AIMS	9	9	9	3	**1**
Price	UCVCF	**1**	1	9	9	9
	CAR	1	**1**	7	9	7
	PSSDA-Small	0.11	0.14	**1**	1	1
	Camsizer	0.11	0.11	1	**1**	1
	AIMS	0.11	0.14	1	1	**1**
Readiness	UCVCF	**1**	1	3	3	3
	CAR	1	**1**	3	3	3
	PSSDA-Small	0.33	0.33	**1**	1	1
	Camsizer	0.33	0.33		**1**	1
	AIMS	0.33	0.33	1	1	**1**
Interpretation of Data	UCVCF	**1**	1	5	5	5
	CAR	1	**1**	5	5	5
	PSSDA-Small	0.20	0.20	**1**	1	1
	Camsizer	0.20	0.20	1	**1**	1
	AIMS	0.20	0.20	1	1	**1**
Ease of Use	UCVCF	**1**	1	3	3	5
	CAR	1	**1**	3	3	5
	PSSDA-Small	0.33	0.33	**1**	1	3
	Camsizer	0.33	0.33	1	**1**	3
	AIMS	0.20	0.20	0.33	0.33	**1**
Portability	UCVCF	**1**	1	3	3	3
	CAR	1	**1**	3	3	3
	PSSDA-Small	0.33	0.33	**1**	1	1
	Camsizer	0.33	0.33	1	**1**	1
	AIMS	0.33	0.33	1	1	**1**
Applicability	UCVCF	**1**	1	1	1	1
	CAR	1	**1**	1	1	1
	PSSDA-Small	1	1	**1**	1	1
	Camsizer	1	1	1	**1**	1
	AIMS	1	1	1	1	**1**

Table 29. Resulting priority vectors and overall ranking of test methods measuring fine aggregate angularity (assuming characteristics are equally important).

Priority Vectors for Test Methods with Respect to Characteristics

	Repeatability	Reproducibility	Accuracy	Price	Readiness	Interpret Data	Ease of Use	Portability	Applicability
UCVCF	0.231	0.231	0.051	0.444	0.333	0.385	0.342	0.333	0.20
CAR	0.231	0.231	0.051	0.402	0.333	0.385	0.342	0.333	0.20
PSSDA-Small	0.077	0.077	0.051	0.052	0.111	0.077	0.130	0.111	0.20
Camsizer	0.231	0.231	0.306	0.049	0.111	0.077	0.130	0.111	0.20
AIMS	0.231	0.231	0.540	0.052	0.111	0.077	0.056	0.111	0.20

×

Priority Vector of Characteristics with Respect to Overall Satisfaction with Method	
0.111	Repeatability
0.111	Reproducibility
0.111	Accuracy
0.111	Price
0.111	Readiness
0.111	Interpret Data
0.111	Ease of Use
0.111	Portability
0.111	Applicability

=

Overall Ranking	Test Method
0.283	UCVCF
0.279	CAR
0.098	PSSDA-Small
0.161	Camsizer
0.179	AIMS

Table 30. Comparison of characteristics with respect to overall satisfaction with method.

Characteristic	Repeatability	Reproducibility	Accuracy	Cost	Readiness	Interpret Data	Ease of Use	Portability	Applicability	Priority Vector
Repeatability	**1**	1	0.2	1	1	1	1	1	1	0.077
Reproducibility	1	**1**	0.2	1	1	1	1	1	1	0.077
Accuracy	5	5	**1**	5	5	5	5	5	5	0.385
Cost	1	1	0.2	**1**	1	1	1	1	1	0.077
Readiness	1	1	0.2	1	**1**	1	1	1	1	0.077
Interpret Data	1	1	0.2	1	1	**1**	1	1	1	0.077
Ease of Use	1	1	0.2	1	1	1	**1**	1	1	0.077
Portability	1	1	0.2	1	1	1	1	**1**	1	0.077
Applicability	1	1	0.2	1	1	1	1	1	**1**	0.077

Note: Accuracy is moderately more important than other characteristics.

Table 31. Overall ranking of test methods measuring fine aggregate angularity for different accuracy levels of preference.

Test Method	**Accuracy Level of Preference**		
	1 = Equally Important	**5 = Moderately Important**	**9 = Absolutely Important**
UCVCF	0.28	0.21	0.17
CAR	0.28	0.21	0.17
PSSDA-Small	0.10	0.08	0.08
Camsizer	0.16	0.21	0.23
AIMS	0.18	0.29	0.35

Table 32. Comparison of characteristics with respect to overall satisfaction with method.

Characteristic	Repeatability	Reproducibility	Accuracy	Cost	Readiness	Interpret Data	Ease of Use	Portability	Applicability	Priority Vector
Repeatability	**1**	1	0.11	1	1	1	1	1	0.2	0.046
Reproducibility	1	**1**	0.11	1	1	1	1	1	0.2	0.046
Accuracy	9	9	**1**	9	9	9	9	9	5	0.465
Cost	1	1	0.11	**1**	1	1	1	1	0.2	0.046
Readiness	1	1	0.11	1	**1**	1	1	1	0.2	0.046
Interpret Data	1	1	0.11	1	1	**1**	1	1	0.2	0.046
Ease of Use	1	1	0.11	1	1	1	**1**	1	0.2	0.046
Portability	1	1	0.11	1	1	1	1	**1**	0.2	0.046
Applicability	5	5	0.2	5	5	5	5	5	**1**	0.211

Note: Accuracy is moderately more important than applicability and absolutely more important than other characteristics.

Table 33. Priority vectors of test methods measuring coarse aggregate texture.

Test Method	**Priority Vectors for Test Methods with Respect to Characteristics**								
	Repeatability	Reproducibility	Accuracy	Cost	Readiness	Interpret Data	Ease of Use	Portability	Applicability
UCVCC	0.231	0.231	0.036	0.650	0.442	0.556	0.496	0.442	0.280
Camsizer	0.231	0.231	0.183	0.084	0.165	0.111	0.238	0.165	0.107
WipShape	0.231	0.231	0.036	0.088	0.165	0.111	0.089	0.165	0.281
UIAIA	0.231	0.231	0.372	0.088	0.063	0.111	0.089	0.165	0.051
AIMS	0.077	0.077	0.372	0.088	0.165	0.111	0.089	0.165	0.281

Table 34. Overall ranking of test methods measuring coarse aggregate texture.

Test Method	**All Characteristics Considered**	**Only Repeatability, Reproducibility, Accuracy, and Applicability Considered**
UCVCC	0.22	0.10
Camsizer	0.16	0.13
WipShape	0.13	0.10
UIAIA	0.23	0.21
AIMS	0.27	0.24

Table 35. Priority vectors of test methods measuring coarse aggregate shape with respect to characteristics.

Test Method	Priority Vectors for Test Methods with Respect to Characteristics								
	Repeatability	Reproducibility	Accuracy	Cost	Readiness	Interpret Data	Ease of Use	Portability	Applicability
FER	0.143	0.019	0.041	0.496	0.328	0.408	0.356	0.270	0.180
MRA	0.143	0.183	0.213	0.244	0.125	0.213	0.158	0.270	0.180
VDG-40	0.143	0.183	0.213	0.052	0.125	0.076	0.158	0.105	0.180
Camsizer	0.143	0.183	0.213	0.052	0.125	0.076	0.158	0.105	0.066
WipShape	0.143	0.066	0.019	0.052	0.125	0.076	0.057	0.105	0.180
UIAIA	0.143	0.183	0.088	0.052	0.046	0.076	0.057	0.105	0.034
AIMS	0.143	0.183	0.213	0.052	0.125	0.076	0.057	0.105	0.180
PSSDA-Large	0.143	0.183	0.088	0.052	0.046	0.076	0.057	0.105	0.180

ratio (FER, MRA, VDG-40 Videograder, Camsizer, WipShape, UIAIA, AIMS, and Buffalo Wire Works [PSSDA-Large]). The criterion that was used in the coarse aggregate texture example was used here. Therefore, the priority list for all the characteristics in the second level and the resulting priority vector presented in Table 35 will apply for this example.

The results presented in Table 36 show that, when all characteristics are considered, the MRA has the highest rank among all methods. The method's high accuracy, ease of use, and low cost contributes to this ranking. It is expected that the imaging methods will become more practical and easy to use after being in practice for some time and thus only repeatability, reproducibility, accuracy, and applicability should be considered in comparing test methods.

The weighting factors assigned to the accuracy categories can influence the ranking of test methods. For example, the threshold for the highest accuracy category is 0.7 (Table 26). If the analysis is conducted for an R^2 of 0.69 (instead of 0.7) for the highest accuracy level, a somewhat different ranking will result (as shown in the last column of Table 36).

X-Ray Computed Tomography of Aggregates

Traprock, limestone, and crushed river gravel aggregates were analyzed in this part of the study. Particles smaller than 12.5 mm (½ in.) but larger than 9.5 mm (3/8 in.) were placed in a plastic sample container 100 mm (4 in.) in diameter and 150 mm (6 in.) in height that was then filled with wax to eliminate any disturbance to the particle arrangement during scanning. X-ray computed tomography (CT)—a nondestructive technique to image the interior of the sample—was used to produce images (examples are shown in Figure 9) that were analyzed to quantify the characteristics of the granular materials.

The 3-D shape of particles was quantified based on measurements conducted on 3-D X-ray CT images using the Spherical Harmonic Series (SHS) presented by Garboczi (*22*).

The results of the X-ray CT images analysis are shown in Figure 10 and summarized in Table 37. These results show gravel to be the most spherical material and that traprock has the highest angularity and texture, followed by limestone and then gravel.

Table 36. Overall ranking of test methods for measuring coarse aggregate shape.

Test Method	All Characteristics Considered	Only Repeatability, Reproducibility, Accuracy, and Applicability Considered	Only Repeatability, Reproducibility, Accuracy, and Applicability Considered*
FER	0.15	0.06	0.06
MRA	0.20	0.15	0.15
VDG-40	0.18	0.15	0.15
Camsizer	0.15	0.13	0.13
WipShape	0.08	0.06	0.06
UIAIA	0.08	0.06	0.13
AIMS	0.17	0.15	0.15
PSSDA-Large	0.11	0.09	0.09

*Using different values for accuracy categories.

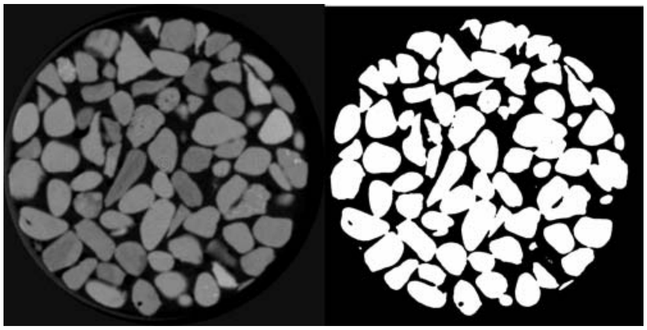

(a) Gravel

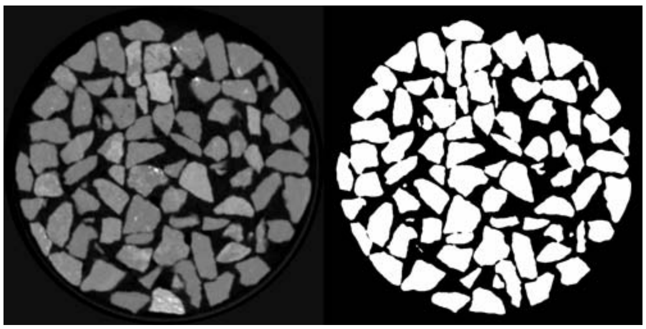

(b) Limestone

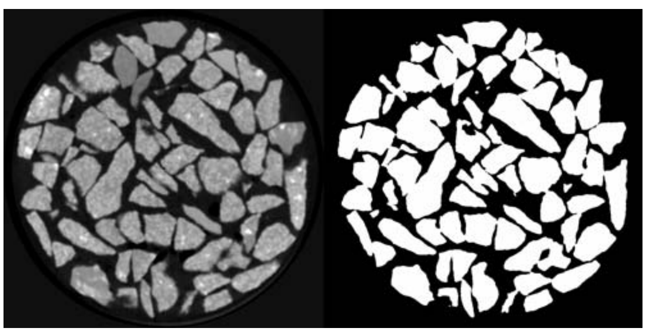

(c) Traprock

Figure 9. Examples of X-ray CT images. These 2-D images are 1024 × 1024 pixels in size, with each pixel representing a physical distance of about 0.1 mm. The slice-to-slice resolution in the out of plane direction was 0.8 mm per voxel length. The images to the left were obtained using X-ray CT; and the images to the right were thresholded to highlight aggregate particles.

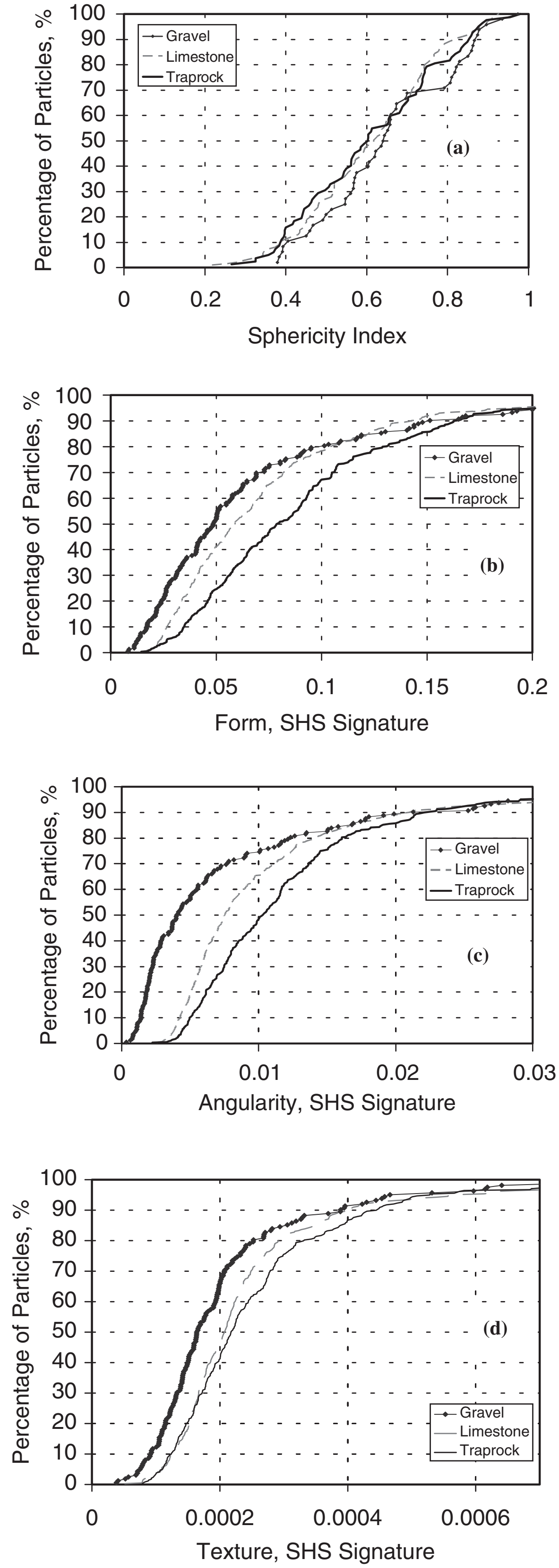

Figure 10. Results of the analysis of images obtained using X-ray CT.

The SHS based on the images supplied by 3-D imaging techniques (such as X-ray CT) can be used to reconstruct the 3-D particle profiles. These reconstructed profiles can be used in simulation programs that incorporate real 3-D particle representations (*22, 23*). Figure 11 shows 3-D reconstructed profiles of gravel, limestone, and traprock materials. These profiles show some digital layering resulting from the relatively low resolution used to capture the X-ray CT images (0.8 mm/

Table 37. Summary of the statistical analysis of X-ray CT images.

Analysis Method	Statistical Distribution Model	Mean*			St. Dev.**		
		TR.	LS.	GR.	TR.	LS.	GR.
Sphericity Index	Normal	0.61	0.61	0.65	0.16	0.17	0.16
Shape, SHS Signature	LogNormal	-1.11 (0.0773)	-1.21 (0.0610)	-1.30 (0.0496)	0.26	0.28	0.36
Angularity, SHS Signature	LogNormal	-1.98 (0.0106)	-2.06 (0.00868)	-2.33 (0.00466)	0.26	0.27	0.46
Texture, SHS Signature	LogNormal	-3.64 (2.29×10^{-4})	-3.66 (2.17×10^{-4})	-3.76 (1.76×10^{-4})	0.22	0.21	0.24

*The mean values for the LogNormal models are provided for the log scale and between brackets for the arithmetic scale.
**The standard deviation values for the LogNormal model are provided for the log scale.

slice). However, the reconstructed profiles show the smoothness of the gravel particles.

The findings of the X-ray CT of aggregate shape analysis are summarized as follows:

- SHS analysis indicated that traprock had the highest angularity and texture, followed by limestone, and then gravel.
- Analysis of X-ray CT images was capable of discriminating among the angularity and texture of the different aggregates.
- 3-D X-ray CT stores the 3-D shapes in a computer for further computer simulations.
- The image processing techniques used in separating the particles in X-ray CT require substantial manual manipulation of images. These segmentation techniques could

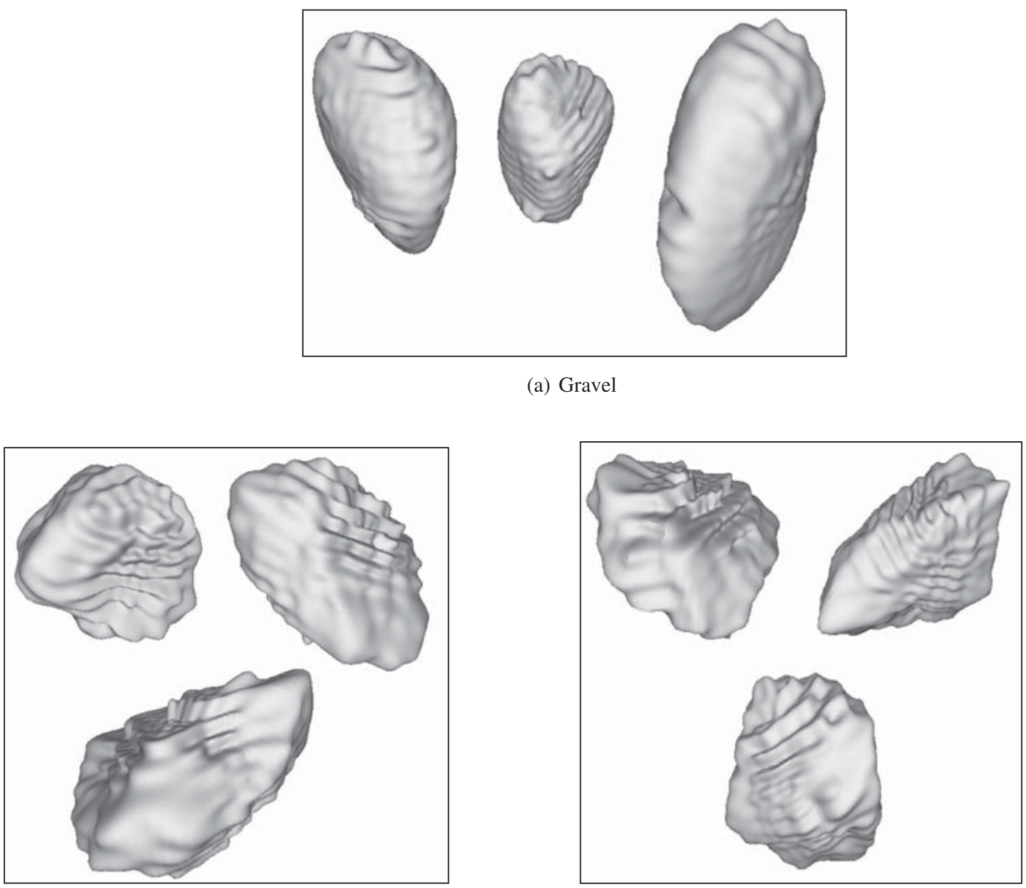

(a) Gravel

(b) Limestone

(c) Traprock

__Figure 11. Reconstruction of three-dimensional profiles of particles using spherical harmonic series.__

influence and alter the measurements of angularity and texture.
- While the X-ray CT is a powerful research tool, it is premature to use it as a practical tool for routine measurements of aggregate shape.

Statistical-Based Methodology for Classification of Aggregates

The ease of interpretation of test results is an essential part to facilitate the implementation in practice. The imaging-based tests discussed in this report provide measurements of a large number of particles. These measurements are valuable to detect differences between aggregates based on sound statistical methods. Therefore, it is essential to develop a methodology to summarize the measurements and present them to the user in a simple form that facilitates implementation.

This section contains a methodology presented in the visual basic program of an Excel workbook to summarize the aggregate characteristics and classify aggregates based on these characteristics. The program includes graphical presentations of the results, helps to compare the results from different aggregates, and combines the results of multiple analyses of the same aggregate source.

Aggregates' shape, angularity, and texture were measured using the three analysis methods that are part of the AIMS software: (1) sphericity as a 3-D measure of coarse aggregates, (2) gradient angularity for coarse and fine aggregates, and (3) texture of coarse aggregates quantified by the wavelet method. Measurements from 195 tests on coarse aggregates and 75 tests on fine aggregates were used in developing the methodology. On average, a coarse aggregate test involved 56 particles and a fine aggregate test involved about 300 particles. All these data were used in the development of the new classification system. The use of different operators and repeated measurements ensured that the classification methodology accounted for variations in measurements among operators.

Cluster analysis was used to develop groups (or clusters) of aggregates based on the distribution of their characteristics. In this study, the usual metric of Euclidean distance (Equation 9) and Ward's Linkage method were used. The clustering method was applied to all characteristics obtained from AIMS.

Three methods for grouping the analysis results were used with the objective of determining whether common group limits can be obtained for aggregates irrespective of their size. In one method, group limits were selected for each aggregate characteristic based on measurements by all operators for each size separately. In another method, the group limits were determined by averaging those obtained for the three sizes. The third method was to group the analysis results obtained for each characteristic using data from all operators and for all sizes combined. Results of clustering using the three different methods are shown in Figure 12. Figure 12a shows the groups' limits of the coarse aggregate texture for each size, the average for the limits of three sizes ("Avg. Sizes" label in Figure 12a), and for all sizes combined ("All" label in Figure 12a). The results show that the groups' limits obtained using the three were very close. The same conclusion was reached by examining the results in Figures 12b and 12d for the other characteristics.

Further analysis was also conducted to determine whether it is feasible to unify the angularity groups' limits of both the fine and coarse fractions. The groups' limits for the angularity of fine and coarse aggregates were determined, plotted in Figure 12, showing slight differences between the limits of fine and coarse fractions, with the largest difference being in the third group. This difference, however, is small compared to the actual angularity values, and thus could be unified limits. The new aggregate shape classification limits are shown in Figure 13.

Analysis and Results

The AIMS software was used to calculate the percentages of each aggregate that belong to the different groups in Figure 13; the results are shown in Figures 14 and 15. These figures show the distribution of a certain shape property in a number of aggregate samples. The variability in the characteristics within and between aggregates indicates that comparing or classifying aggregates based on percent of particles in a single group could be misleading. This is also true for the classification based on average values, especially when an aggregate sample includes a small percent of particles that have extremely high or low values. As such, the new classification methodology considers the distribution rather than an average value. The discussion provided in the following sections highlights the implications of using the developed methodology on aggregate shape classification with emphasis on examining the effects of different factors such as crushing on aggregate characteristics.

Aggregate Texture versus Angularity

The classification methodology incorporates measurements of texture and angularity for coarse aggregates, but it uses angularity measurements only for fine aggregates. A study by Masad et al. (*24*) clearly showed that a high correlation exists between angularity (measured on black and white images) and texture (measured on gray-scale images) of fine aggregates. This finding led to focusing on fine aggregates angularity measured on black and white images. This is an easier task than

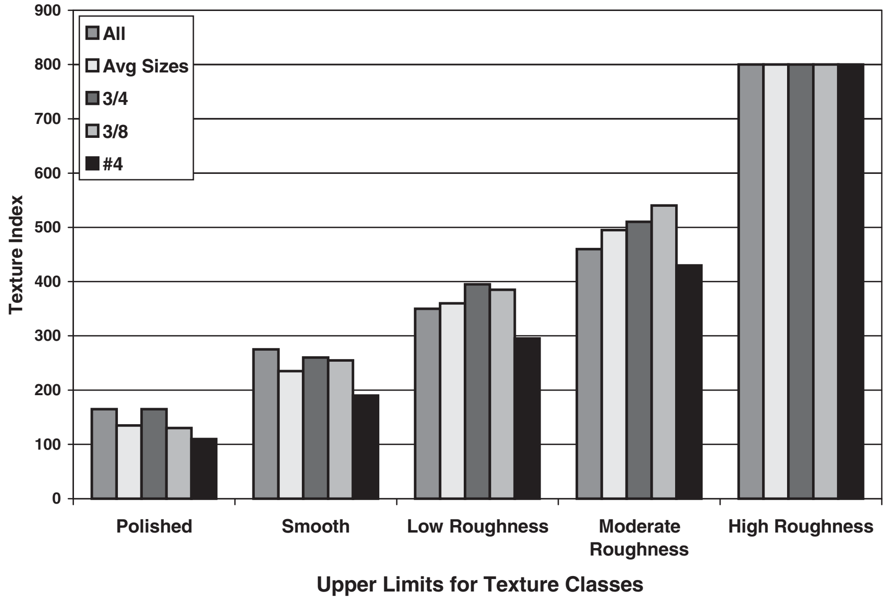

(a) Coarse Aggregates Texture

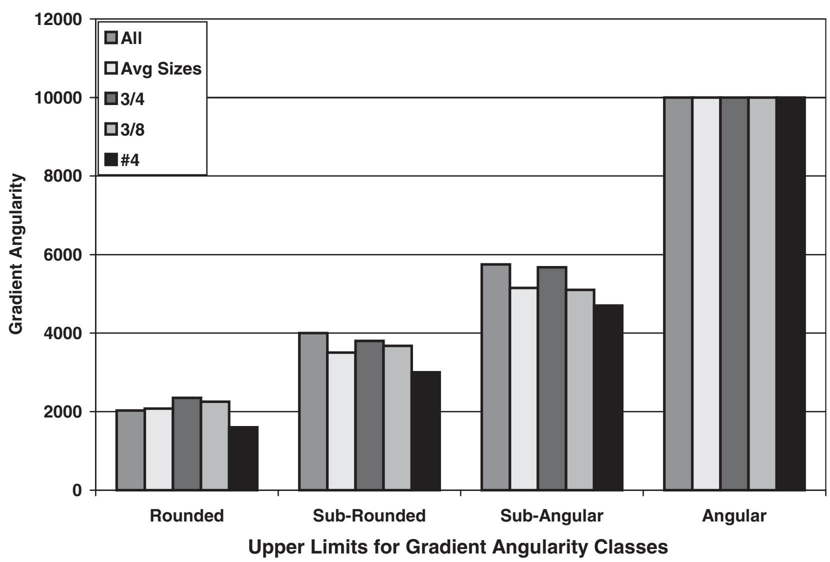

(b) Coarse Aggregates Angularity

Figure 12. Limits of groups (clusters) of individual and combined aggregates.

(continued on next page)

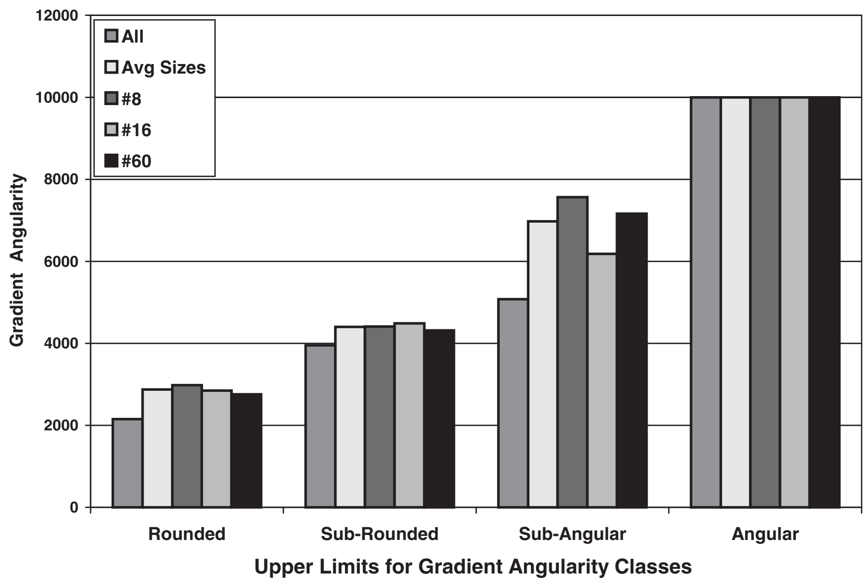

(c) Fine Aggregates Angularity

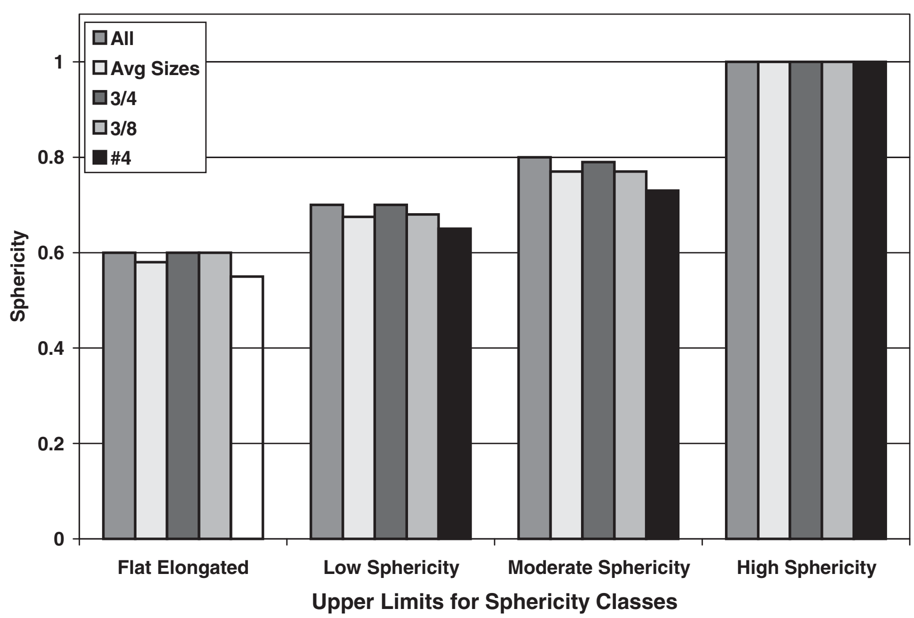

(d) Coarse Aggregates Shape (Sphericity)

Figure 12. (Continued).

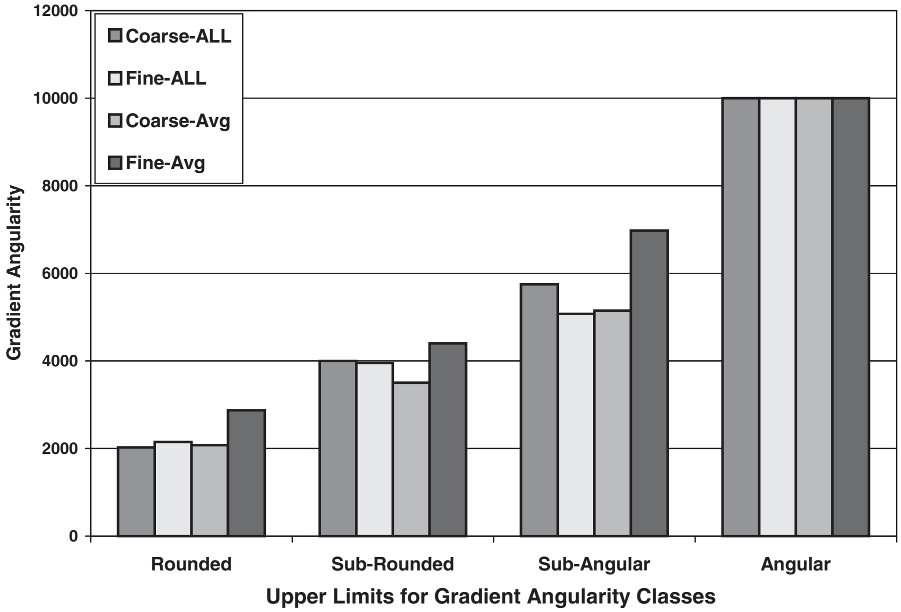

(e) Coarse and Fine Aggregates Angularity

Figure 12. (Continued).

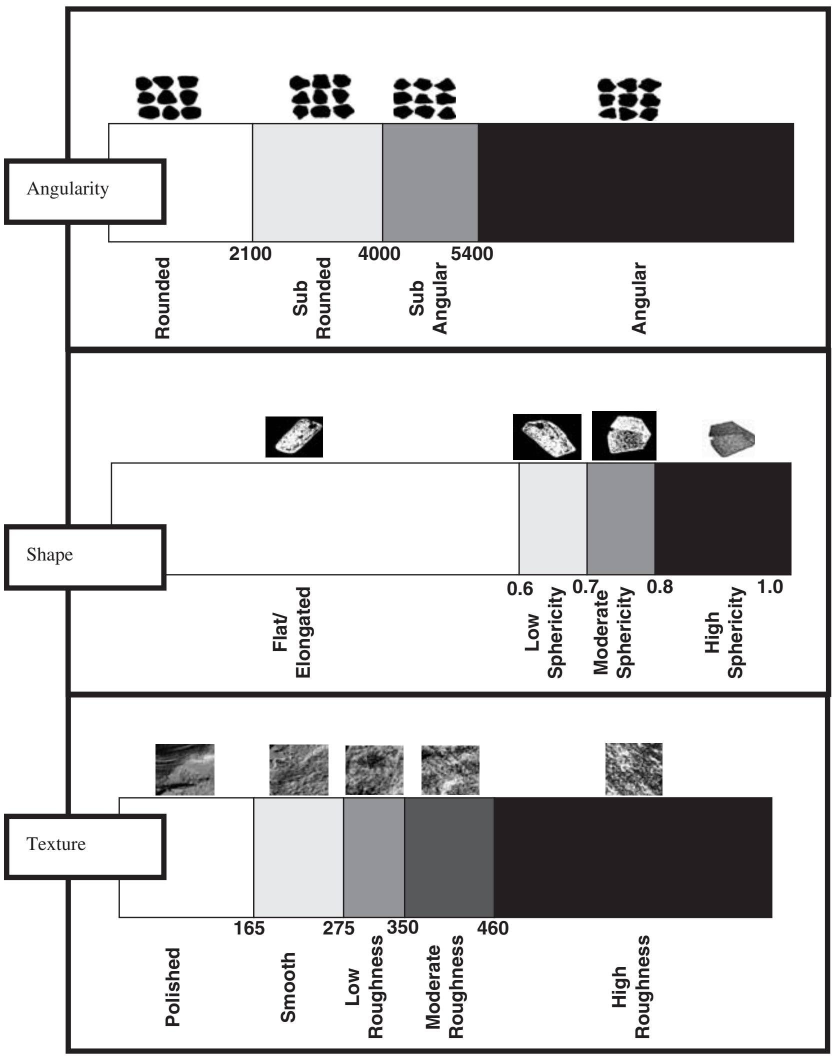

Figure 13. Aggregate characteristics classification chart.

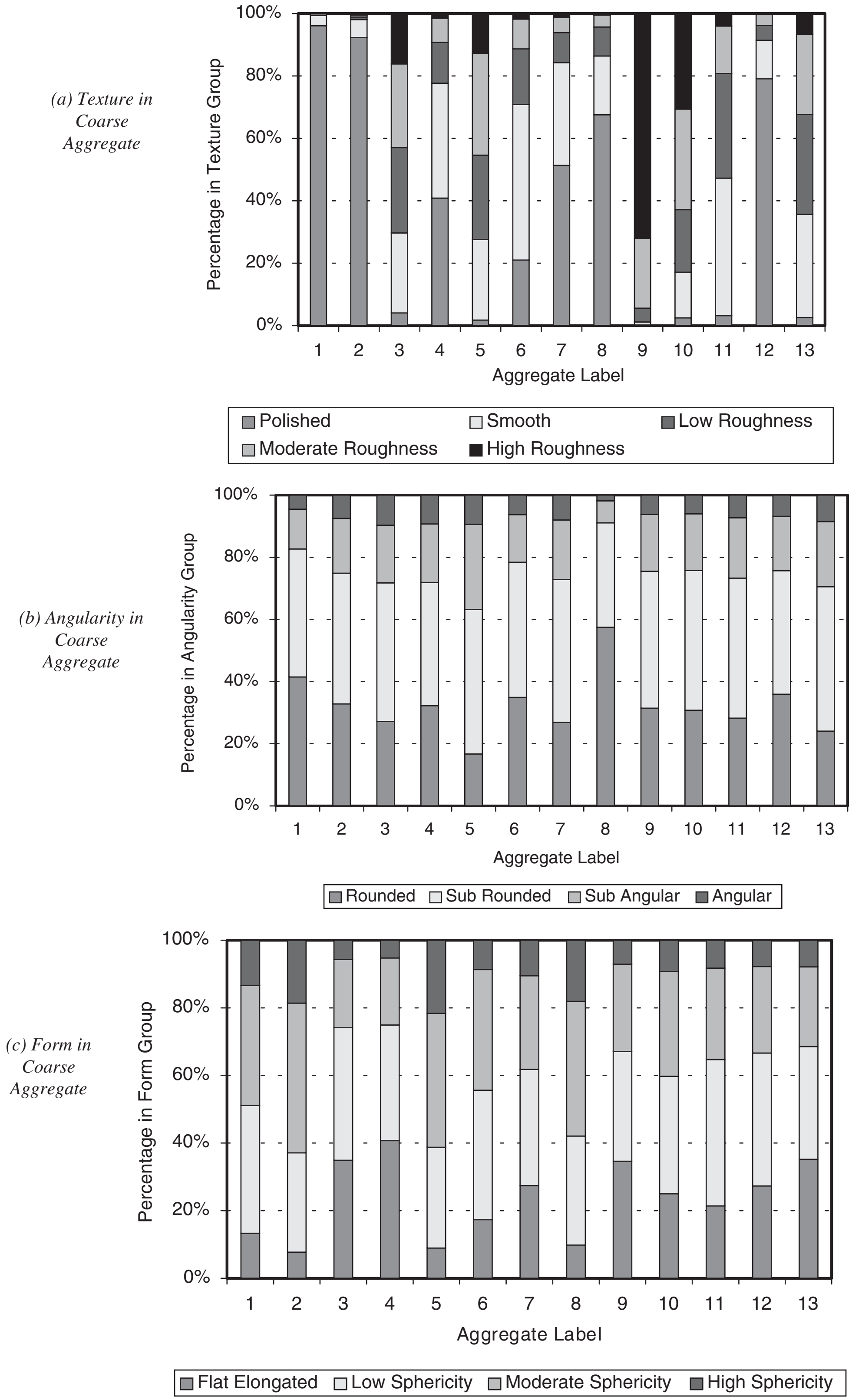

Figure 14. Distributions of coarse aggregate characteristics.

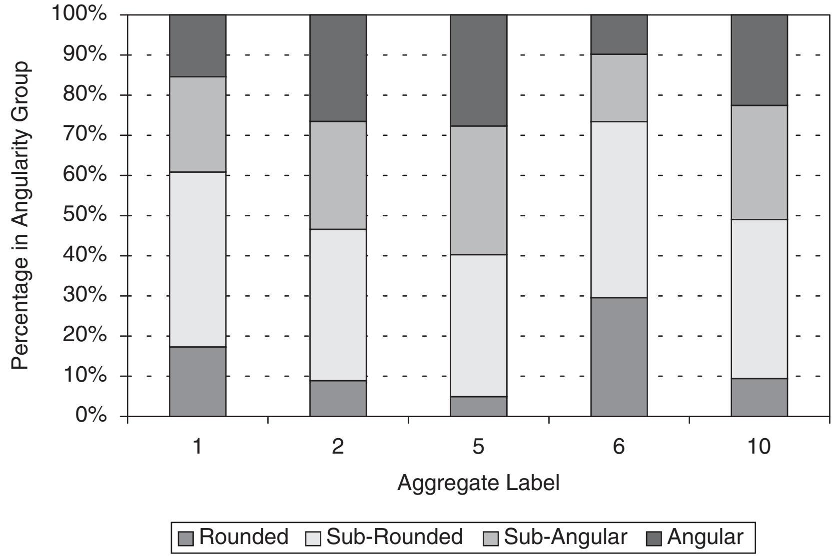

Figure 15. Distributions of fine aggregate angularity.

capturing the surface texture of fine aggregates rapidly and accurately using a computer-automated system. In the case of coarse aggregates, it was found that there is a distinct difference between angularity and texture, and these two properties have different effects on performance (*24, 25*). As can be seen from Figure 16a, which shows the average texture and corresponding angularity for each of the coarse aggregate samples, aggregates could have high angularity but low texture. This is even true for individual particles, as shown in Figure 16b. Particles from aggregates CA-2 and CA-9 (see Table 4) had comparable angularity values but there was a significant difference in texture.

The cumulative distribution of texture in the coarse aggregate samples shown in Figure 17 indicates that the texture of these aggregate samples was spread over a wide range; none of the other characteristics had such a wide range. Texture also had higher variability than angularity within an aggregate sample (see Figure 14a and Figure 14b).

Effect of Crushing and Size on Shape Properties

The developed methodology can be used to examine the influence of crushing on shape. Two types of crushed and uncrushed aggregates were used in this study: river gravel (CA-1 and CA-2) and glacial gravel (CA-7 and CA-8). CA-1 and CA-8 were uncrushed, while CA-2 and CA-7 were crushed. The results in Figures 14a and 14b show that crushing the gravel did not influence texture, but significantly increased their angularity.

Texture measurements were conducted on different sizes of the same aggregate type in order to investigate the influence of aggregate size on texture. Examples of results are shown in Figure 18. Aggregate size did not have a noticeable influence on texture. However, aggregate angularity changed with aggregate size.

The analysis methods also captured the influence of crushing on shape or proportions of particle dimensions. The effect of aggregate size on sphericity varied from one aggregate to another. For example, the sphericity of the crushed river gravel was higher than for uncrushed gravel, indicating that aggregate crushing made the particles more equi-dimensional. However, the crushed glacial gravel (CA-7) showed less sphericity than the uncrushed material (CA-8).

Crushing the natural sand FA-1 to become FA-2 increased angularity, as depicted in Figure 15. FA-1 is an example of high quality natural sand that had angularity comparable to some manufactured sands. For example, FA-1 had higher angularity than crushed limestone (FA-6).

Shown in Figure 19 is an example of the effect of size on fine aggregate angularity. Angularity increased as particle size decreased due to crushing.

Identifying Flat, Elongated, or Flat and Elongated Particles

The sphericity value gives a very good indication of the proportions of particle dimensions. However, one cannot determine whether an aggregate has flat, elongated, or flat and elongated particles using the sphericity alone. To this end, the chart shown in Figure 20 is included in the AIMS software to distinguish among flat, elongated, and flat and elongated particles. Superimposed on this chart are the 3:1 and 5:1 limits for the longest to shortest dimension ratio and the results from CA-2 and CA-4. The figure shows that both aggregates pass

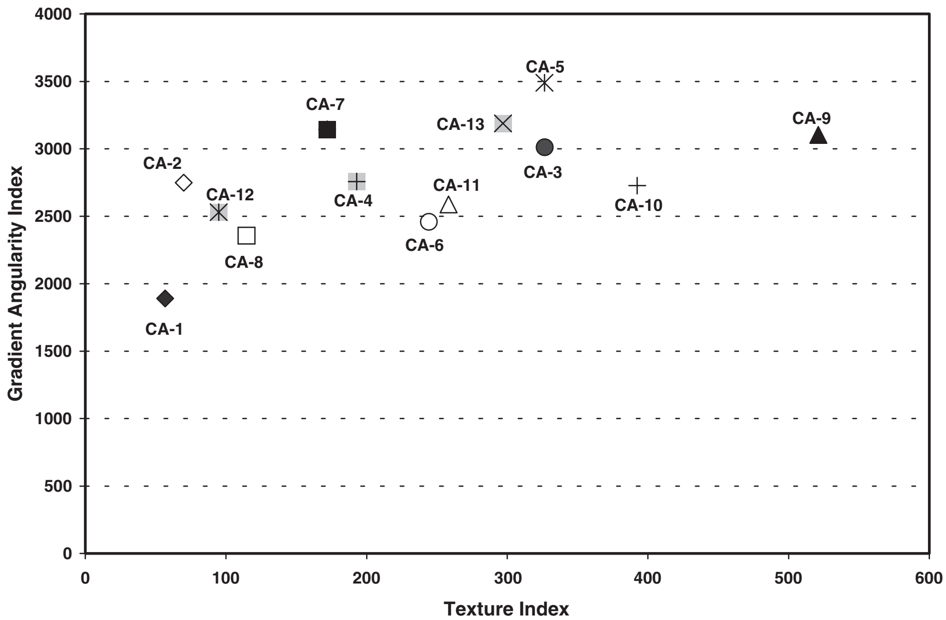

(a) Average Texture and Angularity of Coarse Aggregates

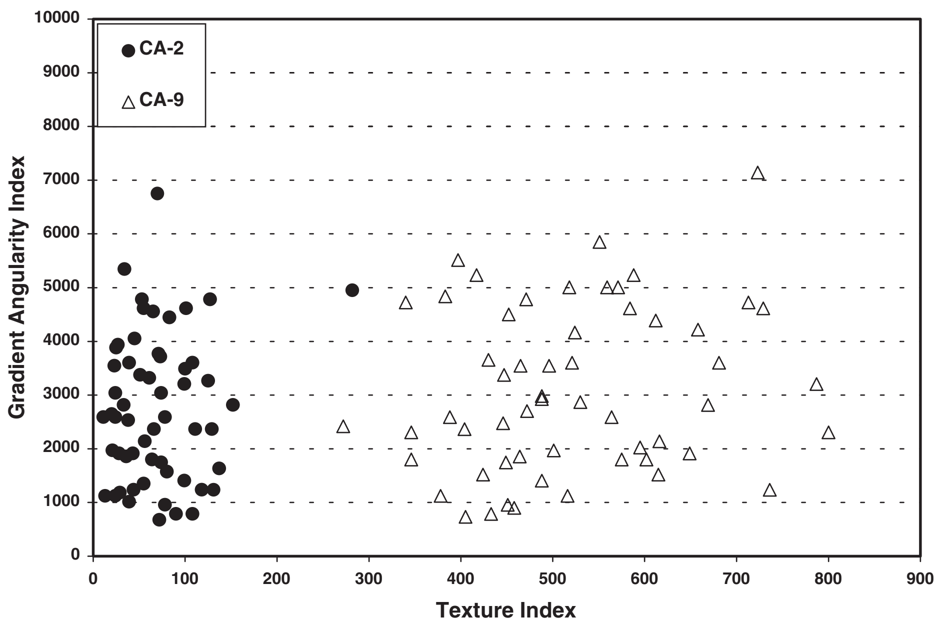

(b) Texture and Angularity of Coarse Aggregate Particles

Figure 16. Variations in texture and angularity properties in coarse aggregates.

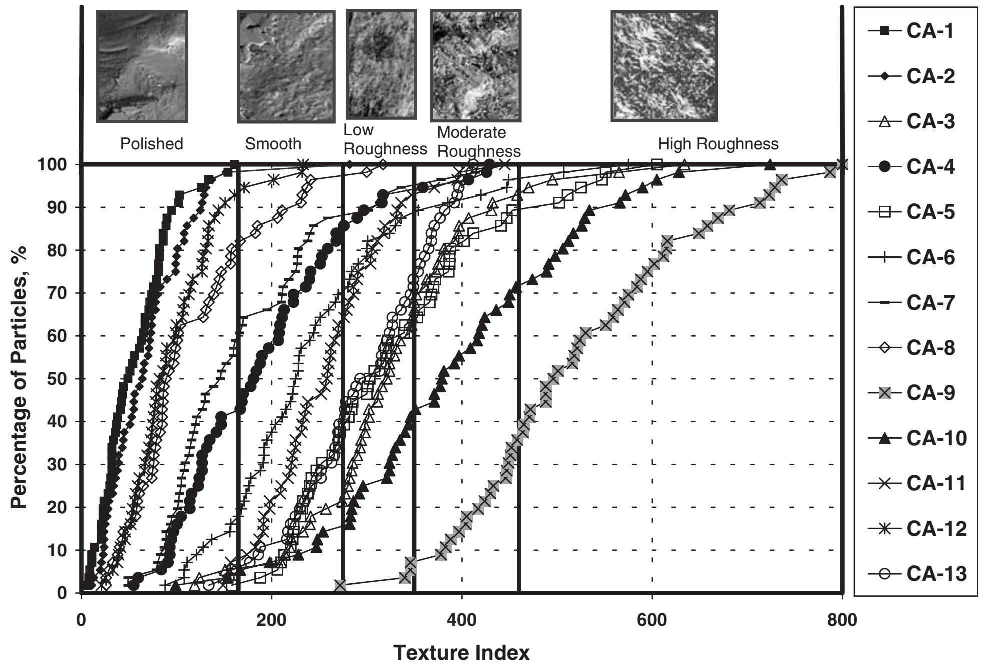

Figure 17. Texture index for different coarse aggregate types.

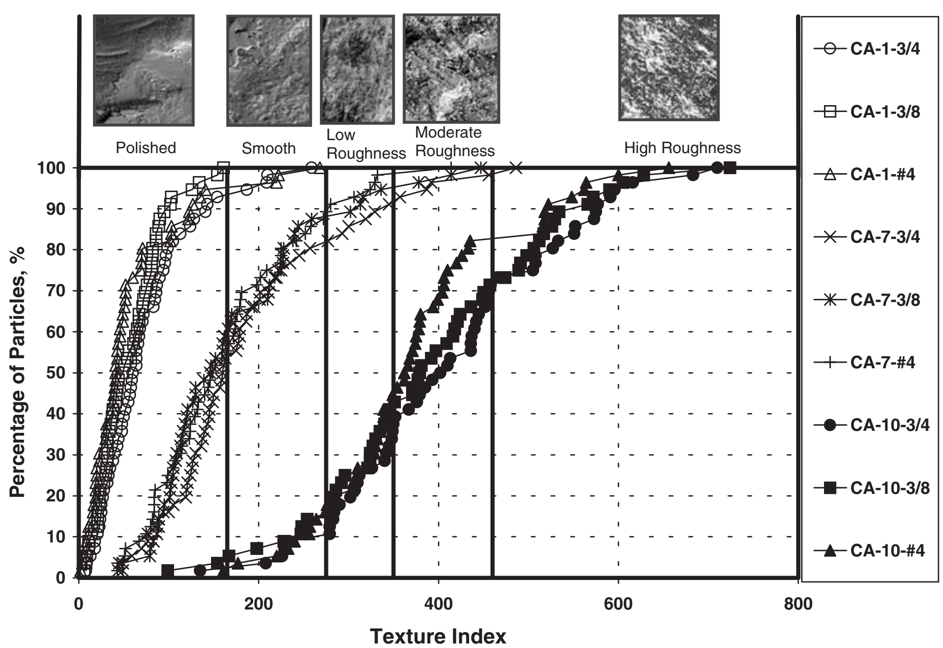

Figure 18. Examples of the effect of coarse aggregate size on texture.

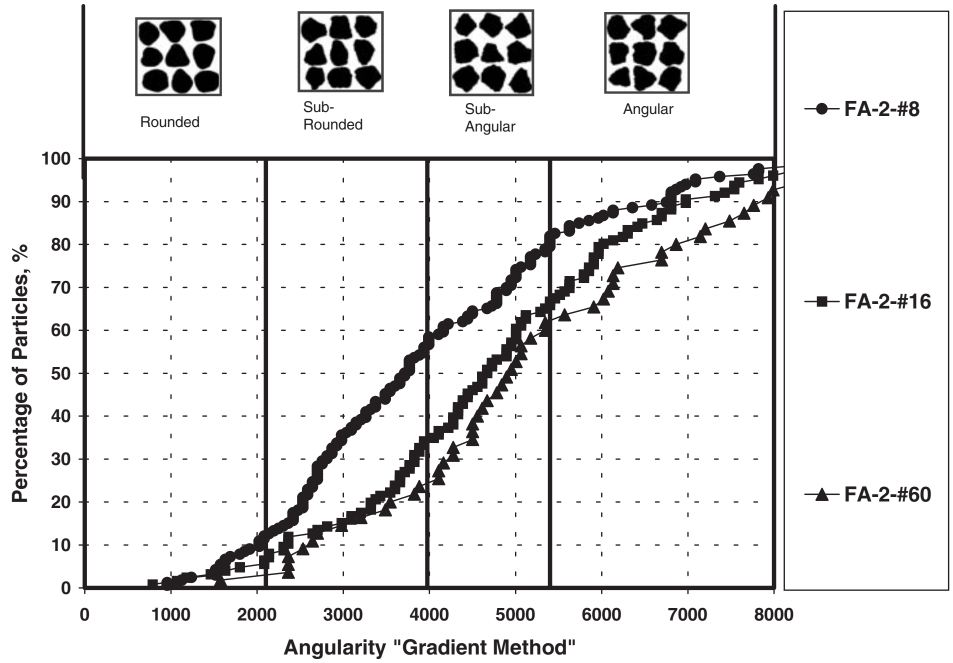

Figure 19. Example of the effect of fine aggregate size on angularity.

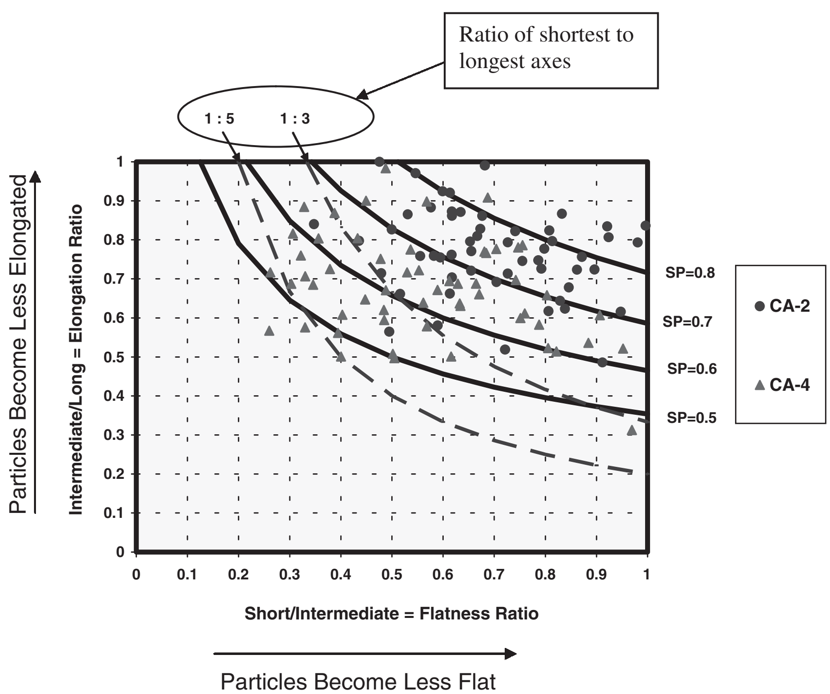

Figure 20. Chart for identifying flat, elongated, or flat and elongated aggregates.

the 5:1 requirement (both had less than 10 percent particles with dimensional ratio of 5:1), but have distinct distributions in terms of flat and elongated particles. Such analysis reveals valuable information about the distribution that would not have been obtained if aggregates were classified based on the ratio of 5:1 only. This information will help to understand the influence of aggregate characteristics on asphalt and concrete mix properties.

CHAPTER 3

Interpretation, Appraisal, and Applications

Aggregate characteristics influence the structural and functional properties of pavement materials. Aggregate shape specifications have generally developed based on the correlation between an indirect measure of aggregate shape and laboratory measurements of the physical and mechanical properties of pavement layers (*26–31*). These indirect aggregate tests have limited ability to identify and separate the fundamental characteristics (shape, angularity, and texture) (*31*). These limitations have led to discrepancies in terms of the extent of the influence of aggregate characteristics on performance. Consequently, specifications developed based on these tests may stipulate the need for superior aggregate characteristics, or otherwise allow for the use of marginal shape properties (*26–31*). Developing accurate methods for measuring and classifying aggregate characteristics is needed to specify the appropriate aggregate characteristics for each specific pavement application.

Test Methods

The test methods that were evaluated in this study exhibit significant differences in their operations, the characteristics being measured, and the analysis methods. Based on the evaluation of test methods, the following conclusions were reached:

- The Aggregate Imaging System (AIMS) is suited for use as a unified system for measuring the characteristics of both coarse and fine aggregates. It is capable of analyzing particles passing sieve 37.5 mm (1½ in.) and retained on sieve 25.0-mm (1.0 in.) and as small as particles retained on sieve #100 (0.15 mm). By capturing images of aggregates at specified resolutions, AIMS minimizes the influence of particle size on shape results. The results are presented in terms of cumulative distribution function rather than an average value only. The system has been used in the field and in a number of research studies. The system is equipped with an automated control of the top lighting for texture analysis, that significantly improved repeatability and reproducibility.
- The University of Illinois Aggregate Image Analyzer (UIAIA) has been shown to be accurate in measuring the characteristics of coarse aggregates; results are presented in terms of the distribution of aggregate characteristics in an aggregate sample. The system has already been used in a number of studies. Researchers at the University of Illinois are pursuing further improvement of the system to allow analysis of aggregates irrespective of their color.
- The Multiple Ratio Shape Analysis (MRA) is desirable for measuring the shape of coarse aggregates. It is inexpensive and provides the distribution of shape in an aggregate sample making it very desirable if the shape of coarse aggregate is the only property being sought. This test has already been used in a number of research studies.

These test methods appear to be appropriate for central laboratories. During the course of this study, members of the research team visited field laboratories of aggregate production companies to investigate the feasibility of using these test methods in field laboratories. They concluded that the space and facilities available can easily accommodate these test methods. In fact, the technicians and managers in some of these field laboratories have indicated that they already operate systems that include electronics similar to those used in the imaging systems, suggesting that the recommended test methods can easily be used in central and field laboratories.

Use of Aggregate Acceptance Tests in Specifications

The literature search has shown that state highway agencies vary significantly in the extent of their using tests for measuring aggregate characteristics and incorporating criteria based on these tests in specifications. These variations are caused by the laborious and subjective nature of the aggregate tests and the lack of clear evidence of strong correlations with the performance of pavement layers. The proposed test methods are rapid and accurate, making them well suited for use and specifications:

- Test methods currently used in practice that summarize the results in terms of average indices are of limited value. Such average indices do not reflect the changes in aggregate characteristics during production due to natural variation in aggregate composition or the processes used to produce these aggregates. Also, an average value alone does not indicate the likely performance of the pavement layer. The aggregate shape classification presented in this report is based on the distributions of aggregate characteristics in an aggregate sample, and yields the percentages of aggregate particles that belong to certain shape categories. Standard statistics can be employed to quantify the changes in these percentages, and consequently, develop specifications for the optimum percentages and allowable variations in these percentages in pavement layers.
- The recommended test methods include procedures for measuring texture and the loss of texture due to polishing. This feature can be used as an indicator of pavement friction characteristics.
- The distribution of aggregate characteristics can be measured rapidly and accurately as part of the quality control and quality assurance programs to detect changes in production and allow adjustment when needed.
- The recommended tests and classification methodology can be used to develop specifications for the combinations of aggregate characteristics needed to achieve the specific levels of pavement performance.

CHAPTER 4

Conclusions and Suggested Research

General Conclusions

The literature review conducted in this study revealed that the shape properties of coarse and fine aggregates used in hot-mix asphalt, hydraulic cement concrete, and unbound base and subbase layers influence the performance of the pavement system in which they are used. Aggregate characteristics can be decomposed to three independent scales: shape, angularity, and texture. Methods currently used for measuring these characteristics have several limitations: they are laborious, subjective, lack direct relation with performance parameters, and have limited ability to separate the influence of angularity from that of texture. A number of research studies have shown that aggregates, especially coarse aggregates that exhibit high texture, do not necessarily have high angularity. Consequently, it is important to develop methods that are capable of quantifying each of the aggregate characteristics rather than a manifestation of their interactions.

Test methods used for measuring aggregate shape properties were evaluated in this study. The evaluation considered accuracy, repeatability, reproducibility, cost, ease of use, ease of interpretation of the results, readiness of the test for implementation, portability, and applicability for the analysis of different sizes and types of aggregates. Thirteen different coarse aggregate types and five different fine aggregate types were used in this evaluation.

Analyses of repeatability and reproducibility results were conducted under the guidelines of ASTM standards E 177, C 802, and C 670. Accuracy of the analysis methods used in the imaging systems was assessed by analyzing some particle projections that have been used by geologists for visual evaluation of particles' shape. Also, all analysis methods were used to analyze images of aggregate particles in order to identify the ability of these methods to accurately rank aggregates and capture unique characteristics of aggregates. The analysis results revealed that some of the available analysis methods are influenced by both angularity and shape changes and, therefore, are not suitable to distinguish between these two characteristics. Also, some of the analysis methods do not distinguish between changes in texture and angularity. The following analysis methods are recommended:

- Texture: Wavelet analysis of gray images of particle surface (Implemented in AIMS software).
- Angularity: The gradient method (implemented in AIMS software) and the changes in the slope of a particle outline (implemented in the UIAIA software).
- Shape: Sphericity or the proportions of the three particle dimensions (implemented in MRA, AIMS, and UIAIA).

Accuracy of test methods was assessed through statistical analysis of the correlations between the results from test methods and measurements of shape using a digital caliper and visual rankings of surface irregularity and texture by experienced individuals.

The Analytical Hierarchy Process (AHP) was implemented in a program to rank the test methods. This process provided flexibility to examine the influence of changes in the importance of the characteristics on the ranking of test methods, and also provided extensive information on the relationship between test methods and desirable characteristics.

The Aggregate Imaging System (AIMS) is recommended for measuring the characteristics of both coarse and fine aggregates. It employs methods based on sound scientific concepts for the analysis of shape, angularity, and texture and provides the distribution of each of the characteristics in an aggregate sample. It has very good control of lighting and provides repeatable and reproducible results. The University of Illinois Aggregate Image Analyzer (UIAIA) can also be used for measuring the shape, angularity, and texture of coarse aggregates. For measuring the coarse aggregate shape only, the Multiple Ratio Shape Analysis method (MRA) is most desirable, and is much cheaper than all the other test methods. The MRA provides the distribution of shape in an aggregate sample, but it cannot be used for measuring angularity or texture.

A methodology that uses direct measurements of shape (three dimensions), angularity, and texture was developed to classify aggregates based on the distribution of their characteristics. It unifies the methods used to measure the characteristics of fine and coarse aggregates. The analysis methods are simple, and the results have physical meanings that can be interpreted easily. The classification ranges were found to be similar for the different aggregate sizes. This finding simplified the methodology, as one set of ranges is needed irrespective of aggregate sizes. This classification methodology is valuable for the interpretation of the results and in order to facilitate implementation.

The classification results are presented in terms of the distribution of shape properties within an aggregate sample. This feature gives capabilities to (1) explore the influence of different processes such as crushing and blending on aggregate shape, (2) conduct quality control activities to detect changes in the distribution of any of the aggregate characteristics, (3) relate the distribution of different characteristics to performance, and (4) develop specifications based on the distribution of aggregate characteristics rather than average indices.

Applicability and Suggested Research

This study provides the pavement community with practical, reliable, and accurate methods for rapidly measuring aggregate characteristics. The recommended methods can be used in the design of pavement layers, in Quality Control (QC) and Quality Assurance (QA) programs, and for problem diagnosis based on understanding of the effects of aggregates on performance of pavement structures. In addition, these methods will help the industry set criteria for providing aggregates with the desired characteristics.

The recommended methods can be implemented in the following aspects of pavement engineering:

- QA and QC procedures during aggregate production: statistical parameters based on the distribution of aggregate characteristics can be used to detect changes in these characteristics and make appropriate adjustments. This will ensure the supply of aggregates with the desired characteristics, thus leading to good performance and cost savings.
- Evaluation of crushing methods: crushing methods can be evaluated by measuring aggregate shape characteristics produced using these methods. This evaluation will help identify crushing methods that could produce aggregates with the desirable characteristics.
- Evaluation of changes in aggregate texture: the proposed imaging systems can be used to measure the aggregate texture and its change due to polishing which can be indicative of change in frictional characteristics.

The following research projects are recommended to enhance the study findings and their implementation:

1. Research to further evaluate the ruggedness of the recommended test methods. This work is essential to evaluate the ability of each test method to provide repeatable and reproducible results.
2. Research to develop methods for incorporating aggregate physical properties in the design of pavement materials. Generally, each of the paving mixtures (unbound aggregate layers and layers bound and/or stabilized with asphalt, hydraulic cement or other stabilizing material) does not consider aggregate characteristics, making it difficult to relate aggregate characteristics on performance. Although several studies have evaluated the relationship between physical characteristics and mixture performance, these studies have not developed adaptable specifications that accommodate variations in aggregate characteristics.
3. Research to develop methods for optimizing the design of paving mixtures based on the physical properties of aggregates. This study did not specify performance-based limits for shape, angularity, and texture that should be used in the mixtures of the different pavement layers. Such research will provide means to allow highway agencies and the industry to efficiently utilize the available sources of aggregates and reduce construction costs.

References

1. Janoo, V. C., and Korhonen, C. (1999). "Performance Testing of Hot-Mix Asphalt Aggregates." *U.S. Army Corps of Engineers Special Report 99-20,* Cold Regions Research & Engineering Laboratory, Hanover, NH.
2. Saeed, A., Hall, J., and Barker, W. (2001). "Performance-Related Tests of Aggregates for Use in Unbound Pavement Layers." *National Cooperative Highway Research Program Report 453,* Transportation Research Board, National Research Council, Washington, D.C.
3. Chowdhury, A., and Button, J. W. (2001). "Fine Aggregate Angularity: Conventional and Unconventional Approach, Aggregate Contribution to Hot-Mix Asphalt HMA Performance." *American Society for Testing and Materials (ASTM) Special Technical Publication, No. 1412,* 144–159.
4. Rao, C., and Tutumluer, E. (2000). "A New Image Analysis Approach for Determination of Volume of Aggregates." *Transportation Research Record 1721,* Transportation Research Board, National Research Council, Washington, D.C., 73–80.
5. Meininger, R. C. (1998). "Aggregate Tests Related to Performance of Portland Cement Concrete Pavements." *National Cooperative Highway Research Program Project 4-20A Final Report.* Transportation Research Board, National Research Council, Washington, D.C.
6. Yeggoni, M., Button, J. W., and Zollinger, D. G. (1996). "Fractals of Aggregates Correlated With Creep in Asphalt Concrete." *Journal of Transportation Engineering (ASCE),* 122 (1), 22–28.
7. Fowler, D. W., Zollinger, D. G., Carrasquillo, R. L., and Constantino, C. A. (1996). *Aggregate Tests Related to Performance of Portland Cement Concrete,* Phase 1 Unpublished Interim Report, National Cooperative Highway Research Program (NCHRP) Project 4-20, Lincoln, NE.
8. Weingart, R. L., and Prowell, B. D. (1999). "Specification Development Using the VDG-40 Videograder for Shape Classification of Aggregates." *Proceedings of the 7th Annual Symposium of the International Center for Aggregate Research (ICAR),* University of Texas, Austin, TX.
9. Tutumluer, E., Rao, C., and Stefanski, J. (2000). "Video Image Analysis of Aggregates." *Final Project Report, FHWA-IL-UI-278, Civil Engineering Studies UILU-ENG-2000-2015,* University of Illinois Urbana-Champaign, Urbana, IL.
10. Maerz, N. H., and Lusher, M. (2001). "Measurement of Flat and Elongation of Coarse Aggregate Using Digital Image Processing." *Transportation Research Board Proceedings, 80th Annual Meeting,* Washington D.C., Paper No. 01-0177.
11. Maerz, N. H., and Zhou, W. (2001). "Flat and Elongated: Advances Using Digital Image Analysis." *Proceedings of the 9th Annual Symposium of the International Center for Aggregates Research (ICAR),* Austin, TX.
12. Browne, C., Rauch, F. A., Haas, T. C., and Kim, H. (2001). "Comparison Tests of Automated Equipment for Analyzing Aggregate Gradation." *Proceedings of the 9th Annual Symposium of the International Center for Aggregates Research (ICAR),* Austin, TX.
13. Rittenhouse, G. (1943). "A Visual Method of Estimating Two Dimensional Sphericity." *Journal of Sedimentary Petrology,* 13(2), 79–81.
14. Wadell, H. (1932). "Volume, Shape, and Roundness of Rock Particles." *Journal of Geology,* 40, 443–451.
15. Wadell, H. (1935). "Volume, Shape, and Roundness of Quartz Particles." *Journal of Geology,* 43, 450–480.
16. Riley, N. A. (1941). "Projection Sphericity." *Journal of Sedimentary Petrology,* 11 (2), 94–97.
17. Powers, M. C. (1953). "A New Roundness Scale for Sedimentary Particles." *Journal of Sedimentary Petrology,* 23(2), 117–119.
18. Krumbein, W. C. (1941). "Measurement and Geological Significance of Shape and Roundness of Sedimentary Particles." *Journal of Sedimentary Petrology,* 11(2), 64–72.
19. Johnson, R. A., and Wichern, D. W. (2002). *Applied Multivariate Statistical Analysis.* Prentice Hall, Englewood Cliffs, NJ.
20. Morrison, D. (2004). *Multivariate Statistical Methods.* Brooks/Cole Thomson Learning, Stamford, CT.
21. Saaty, T. L. (1980). *The Analytic Hierarchy Process: Planning, Priority Setting, Resource Allocation,* McGraw-Hill Inc., New York, NY.
22. Garboczi, E. (2002). "Three-Dimensional Mathematical Analysis of Particle Shape Using X-Ray Tomography and Spherical Harmonics: Application to Aggregates Used in Concrete." *Cement and Concrete Research 32,* 1621–1638.
23. Garboczi, E., Marty, N., Saleh, H., and Livingston, R. (2001). "Acquiring, Analyzing, and Using Complete Three-Dimensional Aggregate Shape Information." *Proceedings of International Center of Aggregate Research 2001 Annual Symposium.* (CD-ROM) Publication.
24. Masad, E., Olcott, D., White, T., and Tashman, L. (2001). "Correlation of Fine Aggregate Imaging Shape Indices with Asphalt Mixture Performance." *Transportation Research Record 1757.* Transportation Research Board, The National Academies, Washington, D.C., 148–156.
25. Fletcher, T., Chandan, C., Masad, E., and Sivakumar, K. (2003). "Aggregate Imaging System (AIMS) for characterizing the shape of

fine and coarse aggregates." *Transportation Research Record 1832,* Transportation Research Board of the National Academies, Washington, D.C., 67–77.

26. Wedding, P. A., and Gaynor, R. D. (1961). "The Effect of Using Crushed Gravel as the Coarse and Fine Aggregate in Dense-Graded Bituminous Mixtures." *Association of Asphalt Paving Technologists Proceedings,* 30, 469–492.
27. Li, M. C., and Kett, I. (1967). "Influence of Coarse Aggregate Shape on the Strength of Asphalt Concrete Mixtures." *Highway Research Record 178,* Transportation Research Board, National Research Council, Washington, D.C., 93–106.
28. Parker, F., and Brown, R. E. "Effects of aggregate properties on flexible pavement rutting in Alabama." *ASTM Special Technical Publication, No. 1147,* ASTM, Philadelphia, PA, 1994, pp.68–89.
29. Kandhal, P. S., and Parker, F., Jr. (1998). "Aggregate tests related to asphalt concrete performance in pavements." *National Cooperative Highway Research Program Report 405,* Transportation Research Board, National Research Council, Washington, D.C.
30. Chowdhury, A., Button, J. W., Kohale, V., and Jahn, D. (2001). "Evaluation of Superpave Fine Aggregate Angularity Specification." *International Center for Aggregates Research (ICAR) Report 201-1,* Texas Transportation Institute, Texas A&M University, College Station, TX.
31. Masad, E. (2003). "The Development of a Computer Controlled Image Analysis System for Measuring Aggregate Shape Properties." *National Cooperative Highway Research Program NCHRP-IDEA Project 77 Final Report,* Transportation Research Board of the National Academies, Washington, D.C.

APPENDIX A

Proposed Test Methods

Disclaimer

"The proposed test methods are recommendations of the NCHRP Project 4-30A staff at Texas Transportation Institute. These methods have not been approved by NCHRP or by any AASHTO Committee or formally accepted for the AASHTO specifications."

Proposed Standard Method of Test for

Shape, Angularity, and Texture of Aggregate Particles Using the Aggregate Imaging System (AIMS)

1. Scope

1.1 This method quantifies three-dimensional shape, angularity, and texture of coarse aggregate particles as well as angularity of fine aggregate particles. Testing and analyses are accomplished using the integrated Aggregate Imaging System (AIMS).

1.2 Analysis of Coarse Aggregates (Method A)—This method uses aggregates that are retained on a 4.75-mm (No. 4) sieve.

1.3 Analysis of Fine Aggregates (Method B)—This method uses aggregates that pass through a 4.75-mm (No. 4) sieve.

1.4 Aggregates scanned using this process should be washed to remove clay, dust, and other foreign materials and separated into the appropriate sizes before being analyzed.

1.5 *This standard does not purport to address all of the safety problems, if any, associated with its use. It is the responsibility of the user of this standard to establish appropriate safety and health practices and determine the applicability of regulatory limitations prior to use.*

2. Referenced Documents

2.1 *ASTM Standards*:

D 75 Practice for Sampling Aggregates

C 136 Test Method for Sieve Analysis of Fine and Coarse Aggregates

C 702 Practice for Reducing Samples of Aggregate to Testing Size

E 11 Specification for Wire-Cloth Sieves for Testing Purposes

3. Terminology

3.1 *Definitions:*

3.1.1 *Shape*—describes the overall 3-dimensional shape of aggregate particles, e.g., round, elliptical, flat. The AIMS software sorts the three dimensions based on length and calculates the sphericity index as shown in Equation (1):

$$\text{Sphericity} = \sqrt[3]{\frac{d_s \cdot d_I}{d_L^2}} \tag{A-1}$$

where d_L is the longest dimension, d_I is the intermediate dimension, and d_s is the shortest dimension. A sphericity value of one indicates that a particle has equal dimensions.

3.1.2 *Angularity*—is related to the sharpness of the corners of 2-dimensional images of aggregate particles. The angularity is analyzed using the gradient method. This method quantifies the change in the gradient on a particle boundary. The gradient method starts by calculating the inclination of gradient vectors on particle boundary points from the x-axis (horizontal axis in an image). The average change in the inclination of the gradient vectors is taken as an indication of angularity as follows:

$$\textit{Angularity}\ (\text{Gradient Method}) = \frac{1}{\frac{N}{3}-1}\sum_{i=1}^{N-3}\left|\theta_i - \theta_{i+3}\right| \qquad \text{(A-2)}$$

where the subscript i denotes the ith point on the boundary of a particle, and N is the total number of points on the boundary.

3.1.3 *Texture*—describes the relative smoothness or roughness of aggregate particles surfaces. The wavelet method is used to quantify texture. The wavelet analysis gives the texture details in the horizontal, vertical, and diagonal directions in three separate images. The texture index is taken at a given decomposition level as the arithmetic mean of the squared values of the wavelet coefficients for all three directions. The texture index is expressed mathematically as follows:

$$\textit{Texture Index}_n = \frac{1}{3N}\sum_{i=1}^{3}\sum_{j=1}^{N}\left(D_{i,j}(x,y)\right)^2 \qquad \text{(A-3)}$$

where n denotes the level of decomposition and i takes a value 1, 2 or 3, for the three directions of texture, and j is the wavelet coefficient index.

4. Summary of Methods

4.1. *Method A*—Analysis of coarse aggregates includes 3-dimensional shape, angularity, and texture. The analysis starts by placing 56 aggregates particles on the aggregate tray at the specified locations. A 0.25X objective lens and camera acquire images of coarse aggregate particles. The maximum field of view achieved in the coarse aggregate module is 52.8×70.4 mm. The camera and video microscope assembly move incrementally in the x direction at a specified interval, acquiring an image of one particle at each increment. Once the x-axis range is complete, the aggregate tray moves in the y-direction for a specified distance, and the x-axis motion and image acquisition process is repeated. This process continues until all 56 aggregates are scanned. Two separate scans are conducted using backlighting and top lighting, respectively. Backlighting is used to acquire two-dimensional images for the analysis of angularity, while top lighting is used for acquiring images for surface texture analysis. These two types of scans are necessary for complete analysis of coarse aggregates shape.

4.2. *Method B*—Analysis of fine aggregate angularity. The 0.5X objective lens is used for acquiring images. The analysis starts by uniformly spreading a few grams of fine aggregate particles on the aggregate tray. Backlighting is used to acquire all images in this analysis. The camera and video microscope assembly move automatically over the aggregate tray until the entire area is scanned. In each x-y scan, the z-location of the camera is stipulated to meet specified resolution criteria. Aggregates that are not within the size range for which the scan is conducted are removed from the image.

5. Significance and Use

5.1. Shape, angularity, and surface texture of aggregates have been shown to directly affect the engineering properties of highway construction materials such as hot mix asphalt concrete, Portland cement concrete, and unbound aggregate layers. Most methods currently in use for measuring these properties of aggregate particles are indirect measurements of the desired properties. This test method provides direct measurement of aggregate shape, angularity, and texture and thus provides consistent values that are comparatively more beneficial for use in software designed to predict performance of highway pavements and structures.

6. Apparatus

6.1. The AIMS is an integrated system composed of a camera, video microscope, aggregate tray, backlighting and top-lighting systems, and associated software.

7. Sampling

7.1. Obtain aggregate specimens in accordance with Practice D 75, and reduce the specimen to an adequate sample size in accordance with Practice C 702.

8. Preparation of Test Samples

8.1. Wash and oven dry the reduced sample at 110 ± 5°C (230 ± 9°F) to substantially constant mass. The coarse aggregate sample should contain at least 56 particles. The fine aggregate sample should be about 50 gm.

9. Procedure

9.1. Analysis of Coarse Aggregate Angularity, Texture, and Shape

9.1.1. The user must ensure that the objective lens used is 0.25X and that the microscope is placed in the coarse position on the dovetail slide. The objective lens can be replaced by removing the fiber-optic ring light by unscrewing the three screws on the ring. Then unscrew the ring light holder from the lower end of the microscope. The user will be required to install the lens (0.25X in this case), return back the ring holder, and fix the top lighting ring back.

9.1.2. Position the microscope on the dovetail slide by releasing the knob of the retaining pin on the left side and sliding the microscope assembly upward or downward until the "coarse" labels on the left-hand side of the two pieces line up. The user needs to ensure that the retaining pin is engaged to secure the microscope. Then tighten the thumbscrew on the right-hand side of the microscope assembly.

9.1.3. On the integrated computer desktop, double click on the "AIMS" icon. The program interface will display a window along with a real time image (Figure A-1-1). On the program interface window, there are several active buttons with labels that indicate the process they perform.

9.1.4. Start the analysis by clicking on the "Project Settings" button. The user must select a name for the project so the analysis results for the aggregate sample will be saved in a file name under the specified directory. This step will allow the user to specify type and size of aggregates to be analyzed. The user is required to click on the "Modify Parameters" button that is available in the "Analysis Parameters" window (Figure A-1-2).

9.1.5. At the "Project Parameters" window (Figure A-1-3), enter the drive and directory path desired for the project. Then enter a project name for the aggregates to be analyzed. Then from the "Aggregate Range" drop-list, the user can select the type of aggregate to be evaluated. For Method A, the user must select "Coarse." Then click "OK."

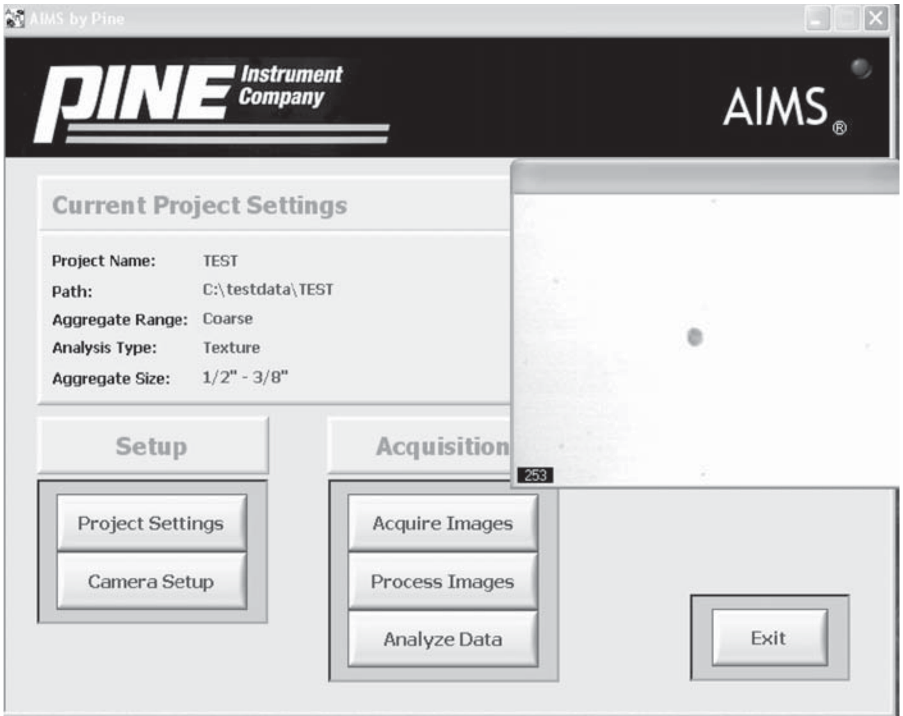

Figure A-1-1. Computer screen for setting up an AIMS test.

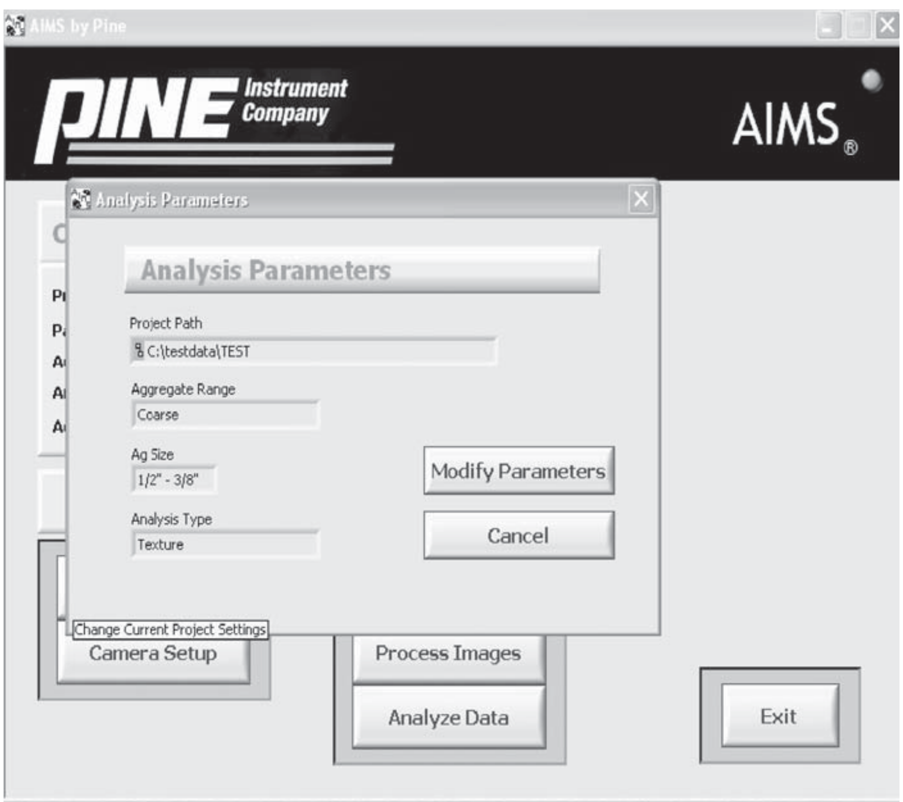

Figure A-1-2. "Analysis Parameters" window for AIMS test setup.

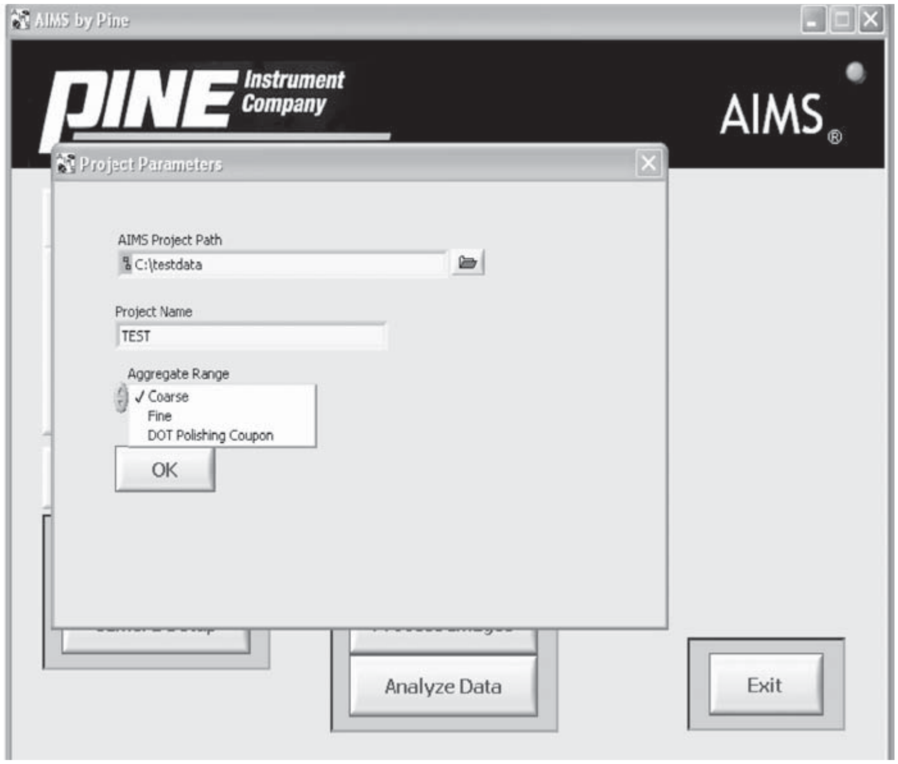

Figure A-1-3. "Project Parameters" window for AIMS test setup.

9.1.6. Clicking the "OK" button on the "Project Parameters" window will display the "Coarse Aggregate Parameters" window (Figure A-1-4). From the "Analysis Type" drop-list, the user must select the type of analysis to be performed (i.e., Angularity, in this case), and click the "OK" button. A "Coarse Aggregate Parameters" window will appear, and the user must select from the drop-list the aggregate size to be analyzed (Figure A-1-5) and click the "OK" button. The first program interface window will appear, showing the information previously entered for current project settings.

9.1.7. Turn on the light beneath the aggregate tray, and allow it to warm up for a minimum of two minutes.

9.1.8. To calibrate the camera and microscope, click on the "Camera Setup" button. An "AIMS Camera Setup" window will appear, showing a real-time image (Figure A-1-6). Now, the user must focus the camera and microscope on the calibration point marked on the aggregate tray. This point will be used as a reference point for the scan where (x, y, z) coordinates are set to (0, 0, and 0). The user must ensure that the target point is in the center of the image by moving the aggregate tray in x and y direction using the joystick on the controller box. This process is easier if the magnification is at the lowest level (M = 1.0). A magnification of 1.0 is achieved by rotating the dial on top of the controller box while the switch button on the front of the controller is at zoom position. The magnification (M-value) appears on the digital screen on the controller box; this value will change when rotating the dial. The minimum value is 1.0 and the maximum value is 16, where maximum magnification is achieved.

9.1.9. After centering the calibration point in the image window, the user must click on the "16X" button. Clicking this button will cause the microscope to zoom in and achieve maximum magnification. If the point is not clear or not viewable

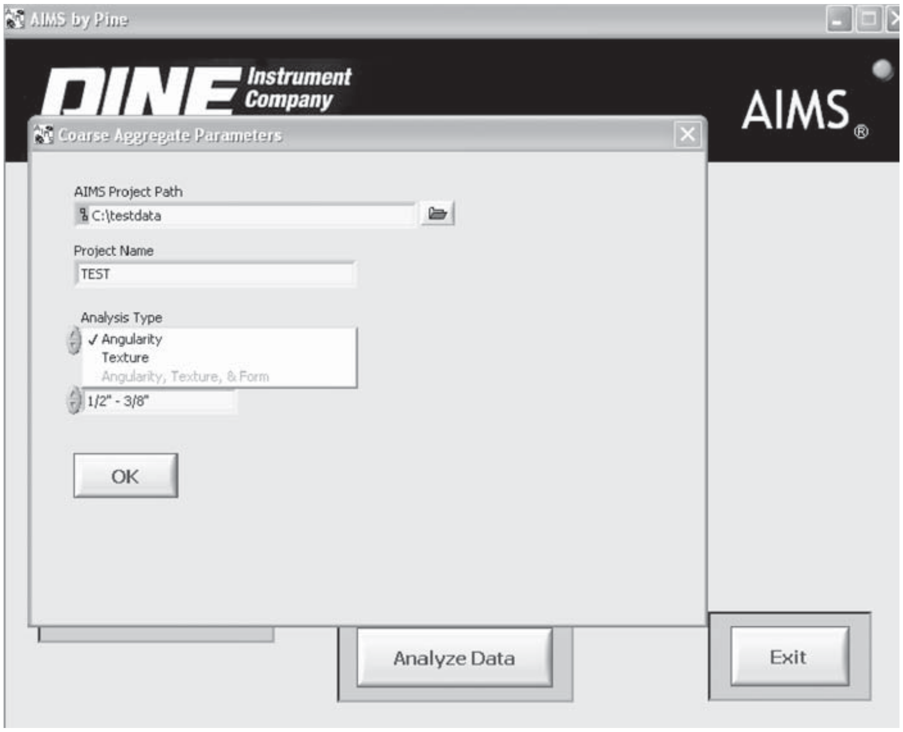

Figure A-1-4. "Coarse Aggregate Parameters" window for AIMS test setup.

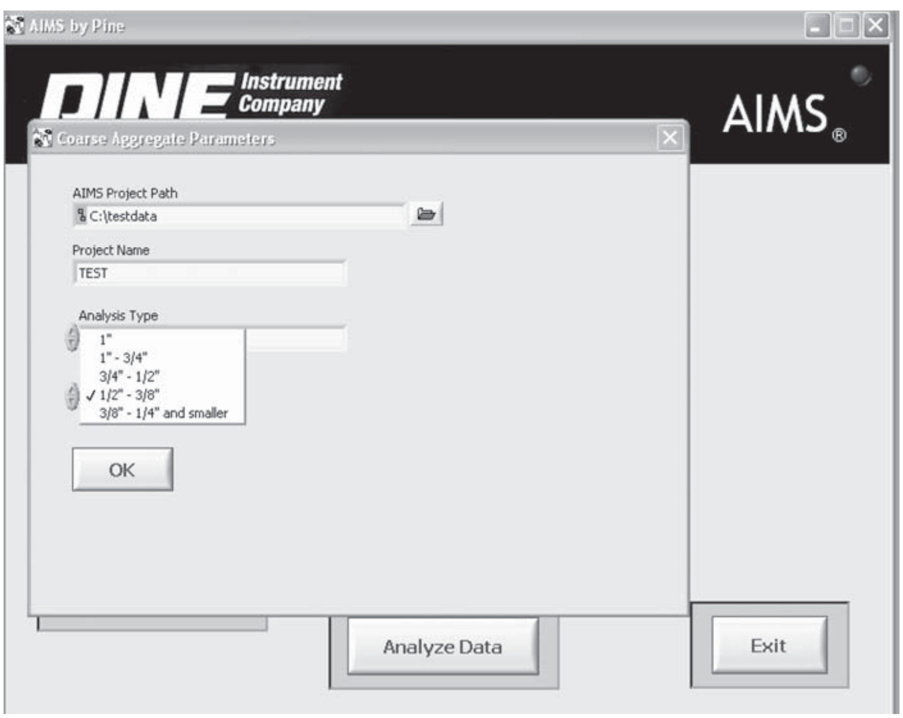

Figure A-1-5. "Coarse Aggregate Parameters" window for AIMS test setup.

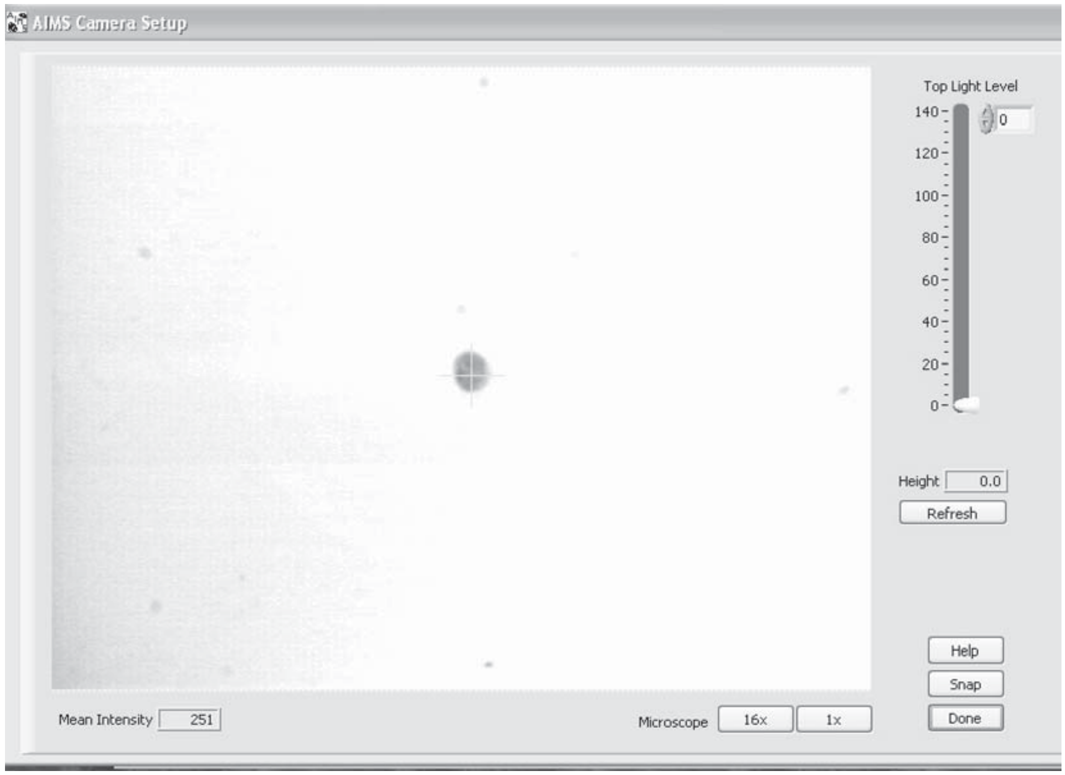

Figure A-1-6. "AIMS Camera Setup" window.

in the image, move the switch at the front of the controller box to the "Focus" position. Then rotate the dial on top of the controller box to move the microscope up or down until the image becomes clear. If the calibration point does not appear in the image window, move the joystick in x and/or y direction until the calibration point appears in the center of the image (Figure A-1-8).

Put the switch in the focus position, and use the dial to focus the image at the maximum magnification (M = 16). This approach is illustrated in Figures A-1-6, A-1-7, and A-1-8.

9.1.10. Once the calibration point is centered and well focused in the image, tap the "@" on the controller. This button will cause the microscope to perform autofocusing and achieve the best image. Then, tap the "Zero" button on the controller box. Then tap "Home." The "Zero" button will set the x, y, and z coordinates to 0, 0, and 0, respectively. The "Home" button will cause the camera and microscope to return to the start point after finishing the scan. Then, click the "Done" button on the "AIMS Camera Setup" window; this window will close, and the program interface window will appear again.

9.1.11. Image acquisition begins by clicking on the "Acquire Images" button on the computer screen. A new message window will appear giving the option for performing camera setup. If camera setup was not performed in the previous step, it can be done here; otherwise, select "No," if already performed (Figure A-1-9). When omitting the camera setup option, a new message window appears with instructions (Figure A-1-10).

9.1.12. The term "camera origin," on the screen, signifies camera setup may be performed at this time; however, that is normally performed in the previous step. If so, click cancel, and place aggregate particles on the tray at the indicated locations. Placement of aggregates can be performed at the beginning, but in that case, the user

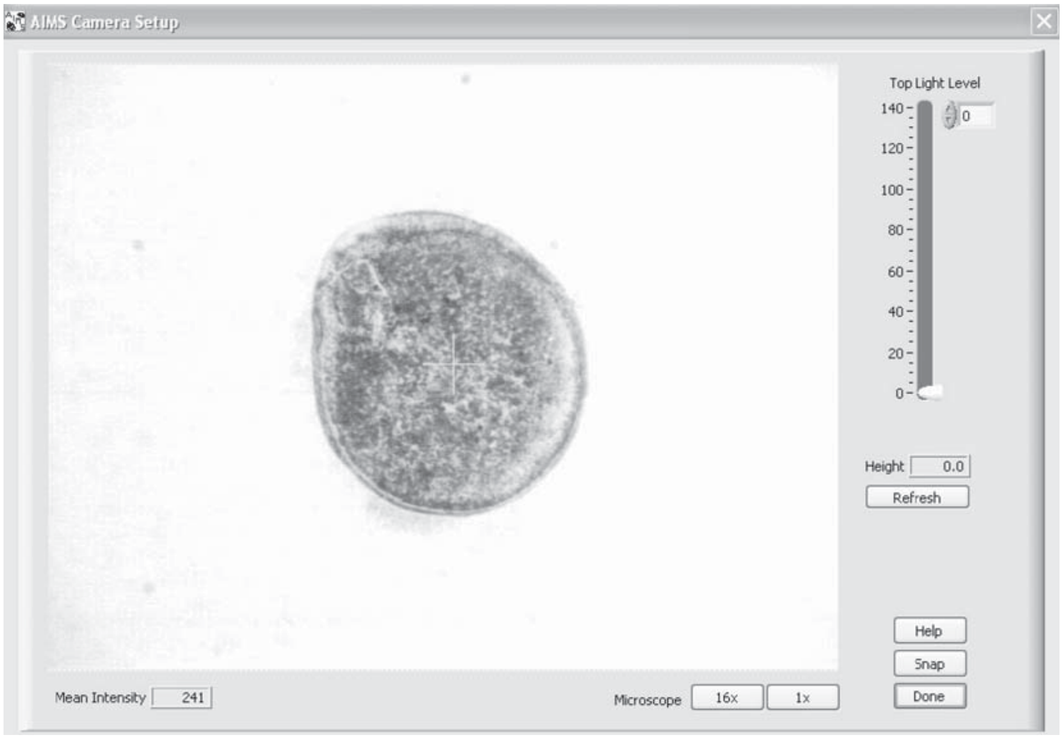

Figure A-1-7. Calibration point centered at an intermediate magnification.

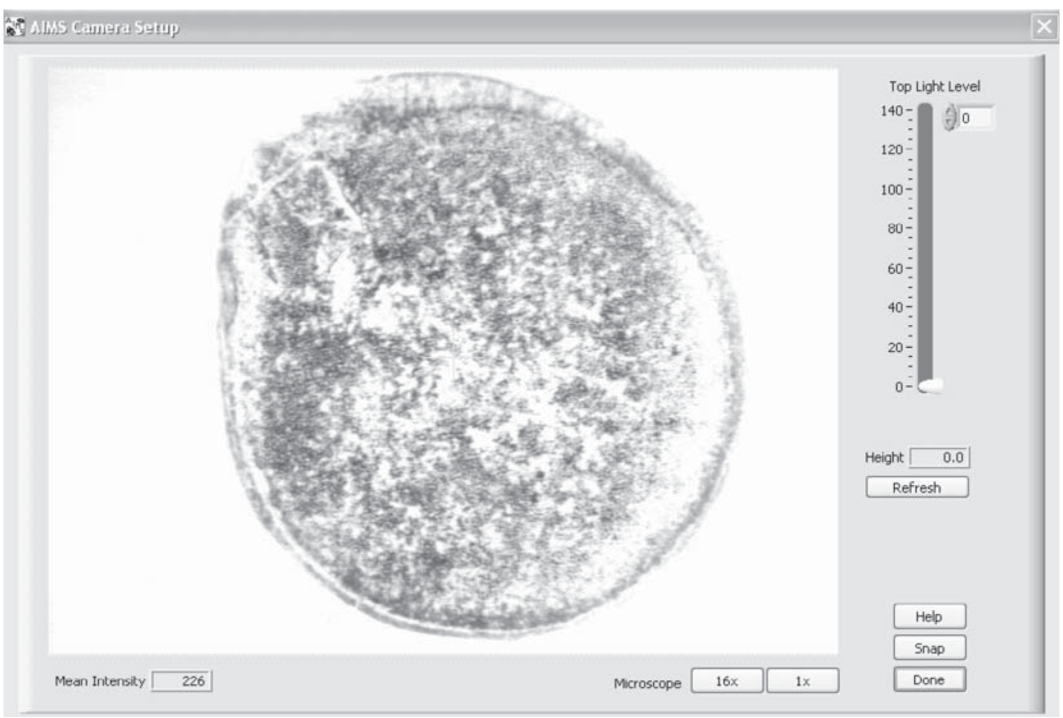

Figure A-1-8. Calibration point centered, focused, and at maximum magnification.

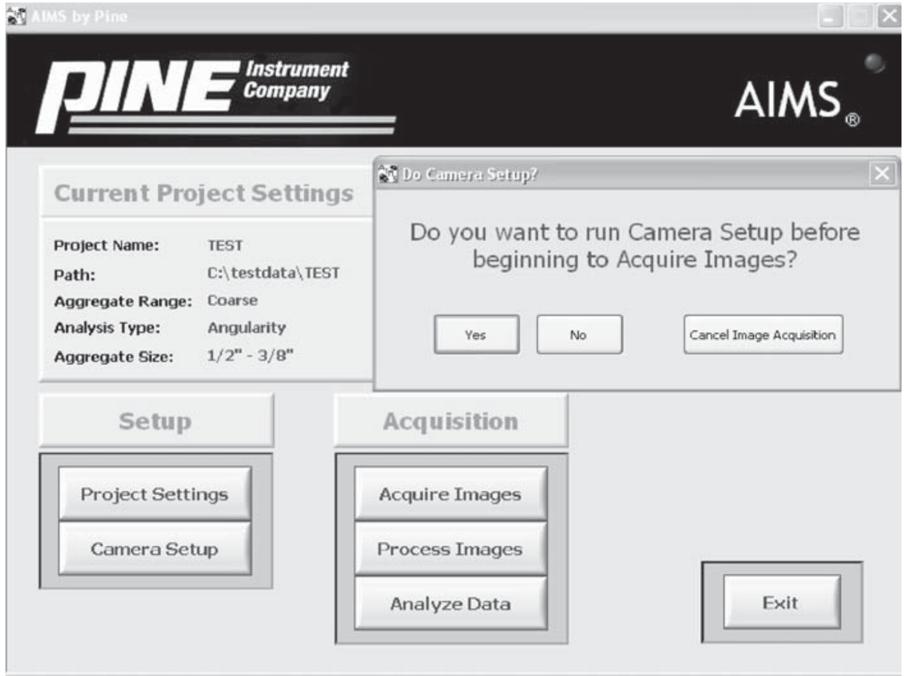

Figure A-1-9. Window providing second opportunity for camera setup.

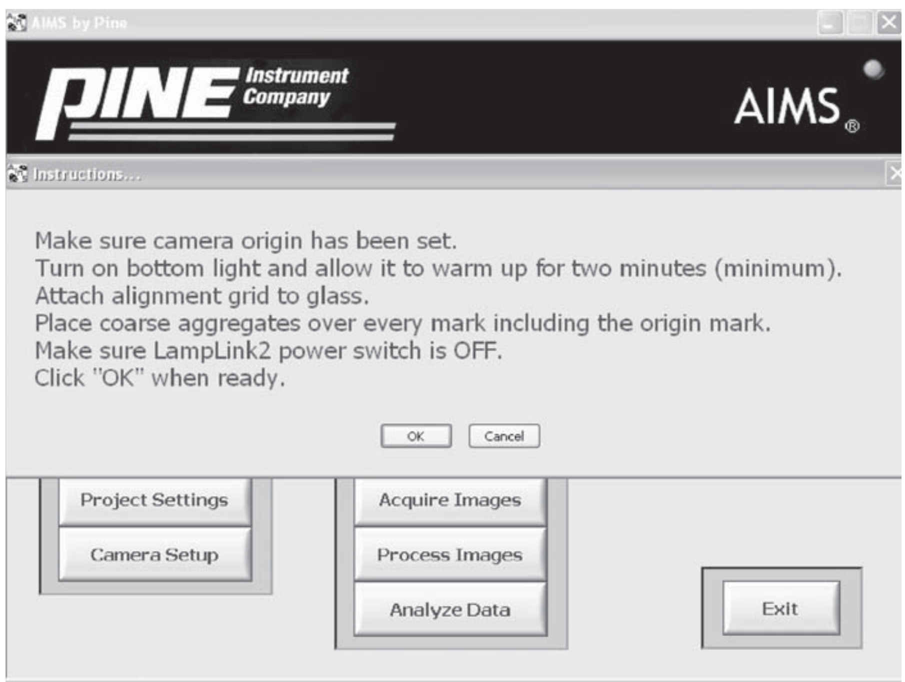

Figure A-1-10. Window providing options for AIMS test setup.

must ensure that the calibration mark is exposed so the camera setup can be performed. If calibration has been performed, one can place aggregates on every marking including the calibration mark. Placement of the aggregates begins by placing a translucent sheet (Mylar film) between the aggregate tray and the lighting table, which has an alignment grid indicating the position for 56 particles

(Figure A-1-11). The Mylar sheet is prepared such that the spacing between the center of the particles is approximately 50 mm in the x-direction and 40 mm in the y-direction. To ensure that the aggregates are properly aligned, the two markings on the right side of the glass aggregate tray should align with the corresponding markings on the Mylar grid sheet (Figure A-1-12). Remove grid sheet after all the particles are positioned. Figure A-1-13 shows the coarse aggregates properly positioned on the glass tray.

9.1.13. After all instructions have been followed, click "OK," and AIMS will start scanning. Upon scanning all aggregate particles on the aggregate tray, the camera will return to the starting point. Figure A-1-14 shows an example of an image from the scanning process.

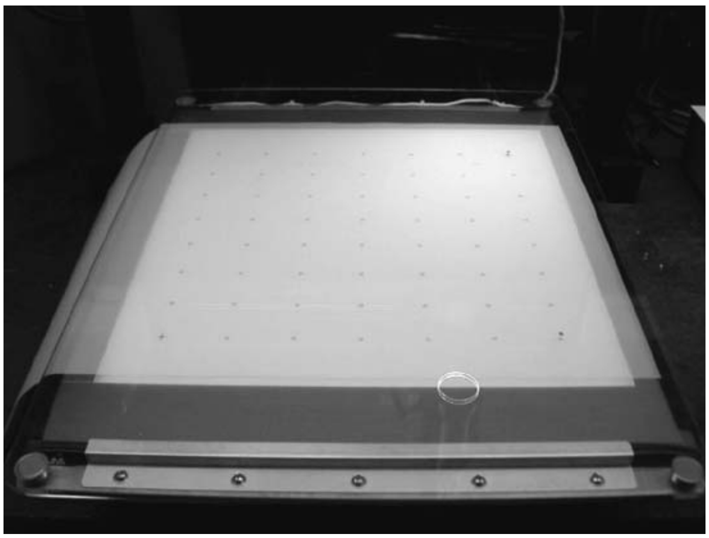

Figure A-1-11. Aggregate tray with Mylar grid sheet showing proper positions of aggregate particles.

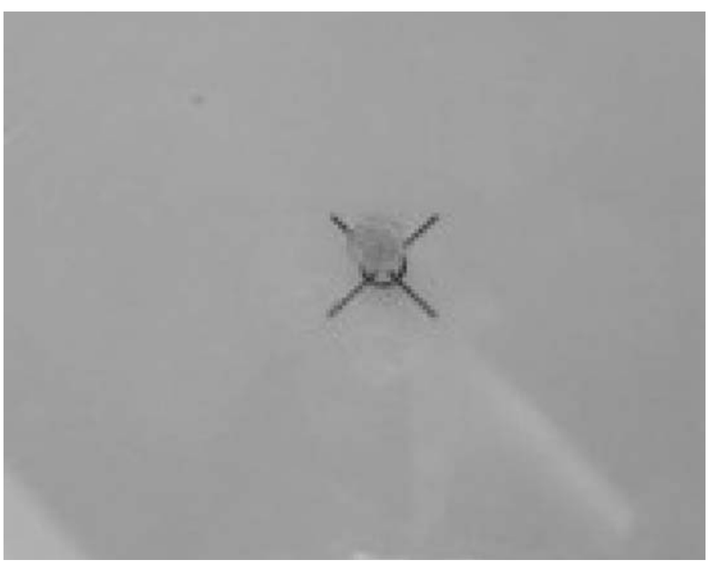

Figure A-1-12. Close-up view of Mylar sheet over light table. (Note: objects in photo appear misaligned due to parallax error. Look straight down on light table to achieve the optimum alignment.)

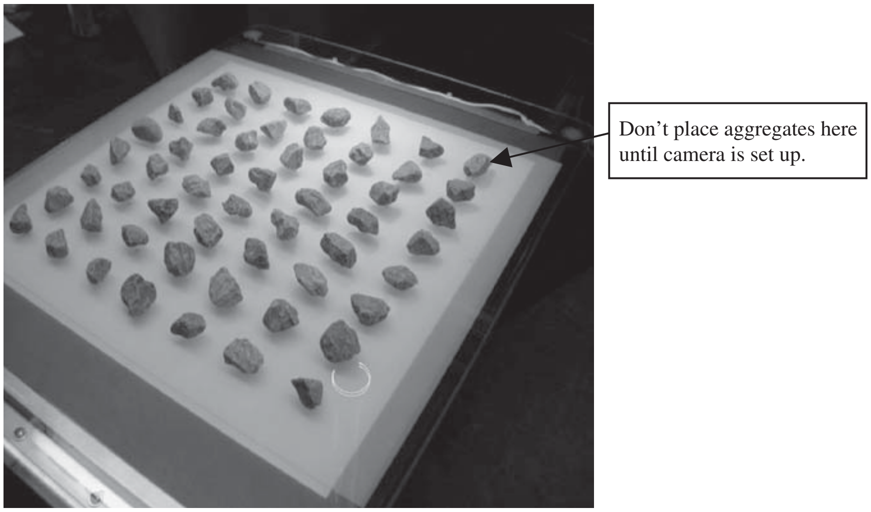

Figure A-1-13. Coarse aggregates properly positioned on glass tray.

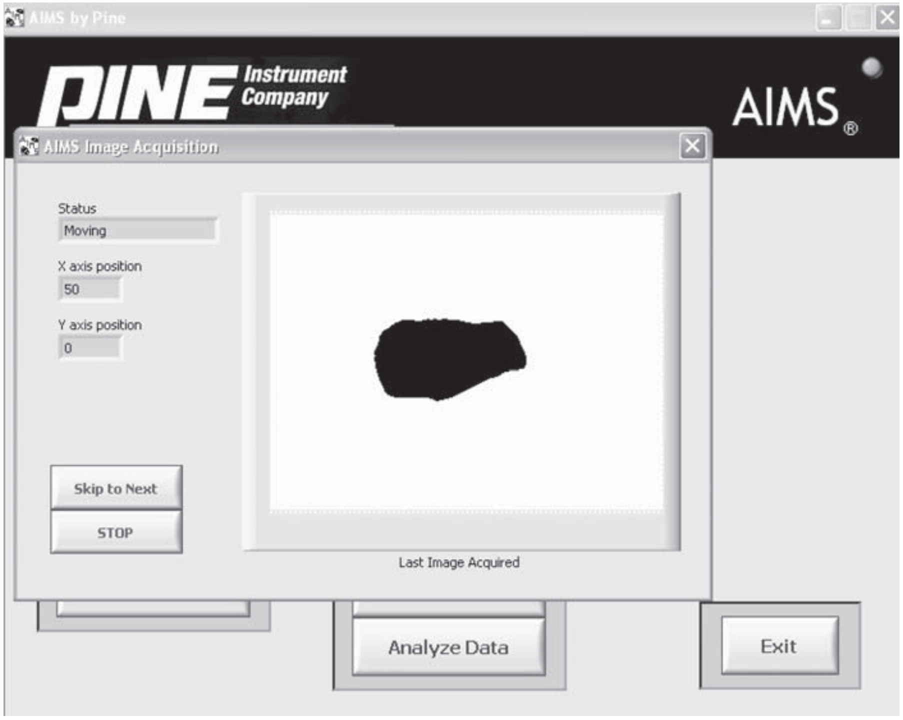

Figure A-1-14. Example of a 2-dimensional image of an aggregate particle.

9.1.14. For analysis of coarse aggregate texture, the same steps are followed as in the angularity measurement, except in Step 9.1.6 for analysis type, select "Texture."

9.1.15. Click on the "Acquire Images" button, and a message window appears, as shown in Figure A-1-15. Follow the instructions and turn off the bottom lighting, and turn on top lighting.

9.1.16. Once the "OK" button is pressed, the system starts scanning the aggregates and acquiring grayscale images for each particle. The system will automatically focus on the top of each aggregate particle and adjust the top lighting. The camera and

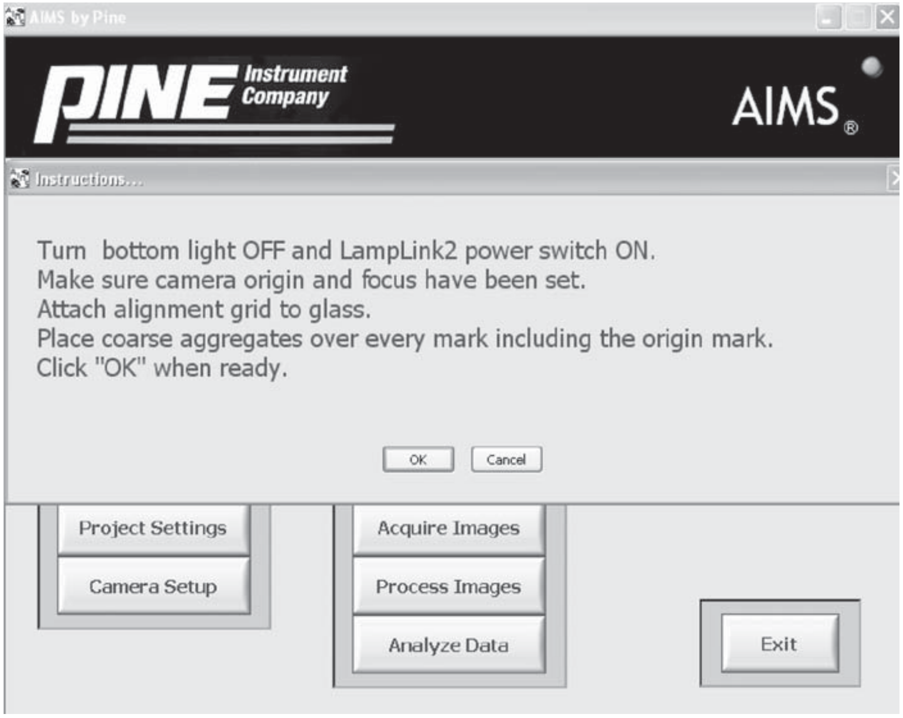

Figure A-1-15. Message screen when entering the texture measurement mode.

the microscope will return to the starting point when the scan is completed. Figure A-1-16 shows an example of the scanning process. The system records the vertical location of the microscope while it is in focus at the top of each particle. The difference between the location of the microscope while it is in focus at the top of a particle and its initial location when it is focused on the lighting table (see step 9.1.10) is recorded in a text file as the depth of the particle.

9.1.17 Once the images are collected, they are saved under the directory path specified in Step 9.1.5. Click on the "Process Images" button to process the images using the analysis software. In the new window that appears, specify the project name or the path of the directory in which the images are to be saved. If the analysis was conducted for different aggregate sizes under the same project name, the user has the option to run the analysis for one single size or for all sizes available in that directory (Figure A-1-17).

9.1.18 Select "OK," and a new window will appear showing that the analysis process is being performed (Figure A-1-18). As soon as the analysis is completed, the window will close.

9.1.19. Click on the "Analyze Data" button to analyze and obtain the desired data. The new window displayed will allow the user to select the analysis for a single particle size or for all sizes in the directory (Figure A-1-19). Then another window appears (Figure A-1-20), allowing the user to select from a drop-list the directory that contains the processed images and the type of analysis desired (Figure A-1-21). Select the analysis type and the directory, and click on the "Analyze" button. The results will be plotted in cumulative distribution formats (Figures A-1-22 and A-1-23). This process can be repeated sequentially for different analysis types.

9.1.20. Results for each analysis type are saved in an Excel spreadsheet in a folder named "Analysis" that has been created in the directory where the images are saved.

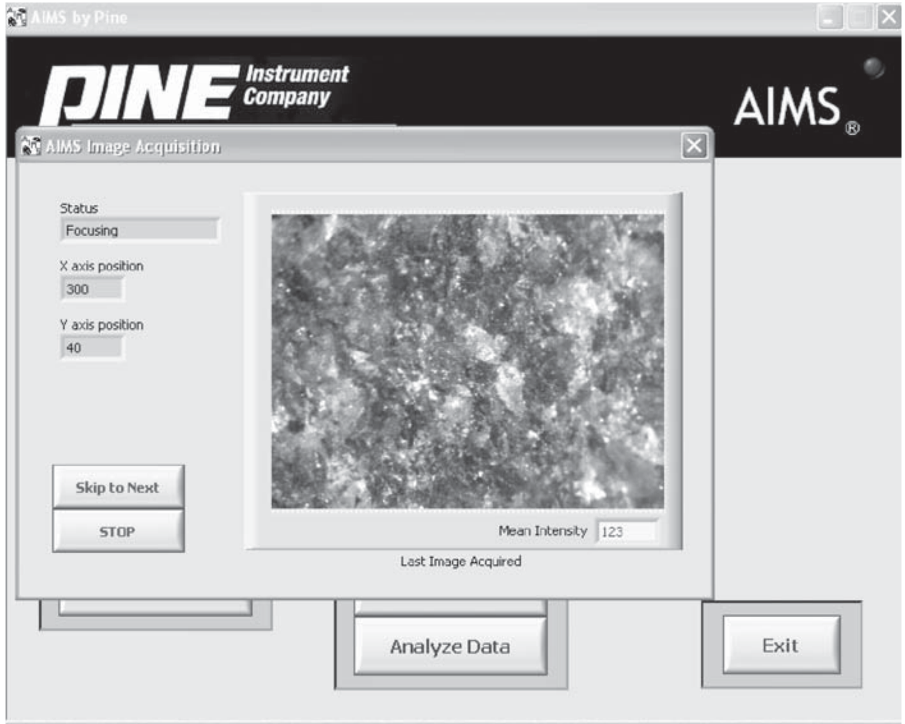

Figure A-1-16. An example of the texture scanning process.

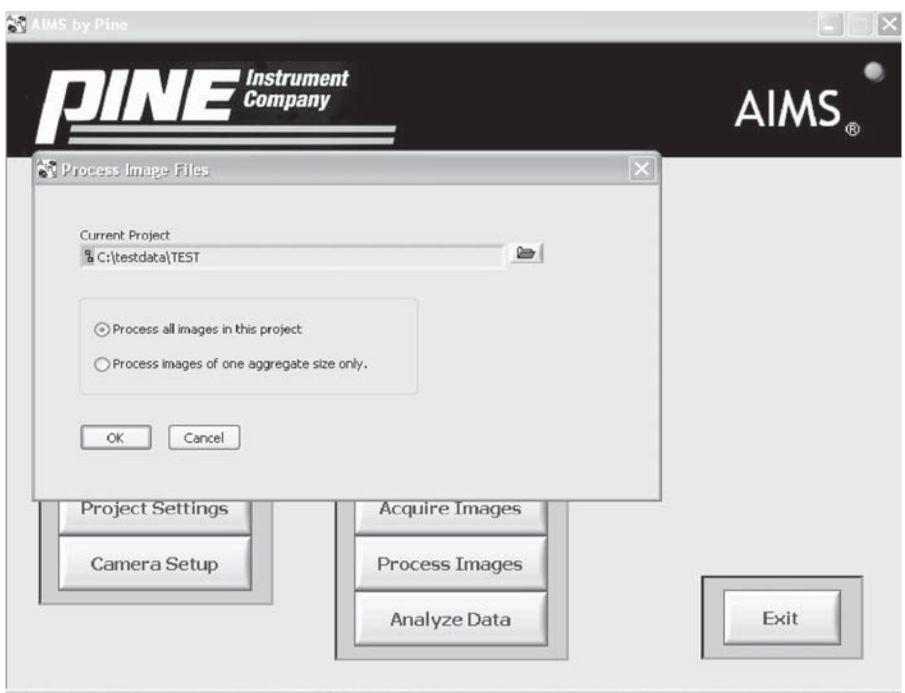

Figure A-1-17. AIMS permits processing of all images or only those of a given size.

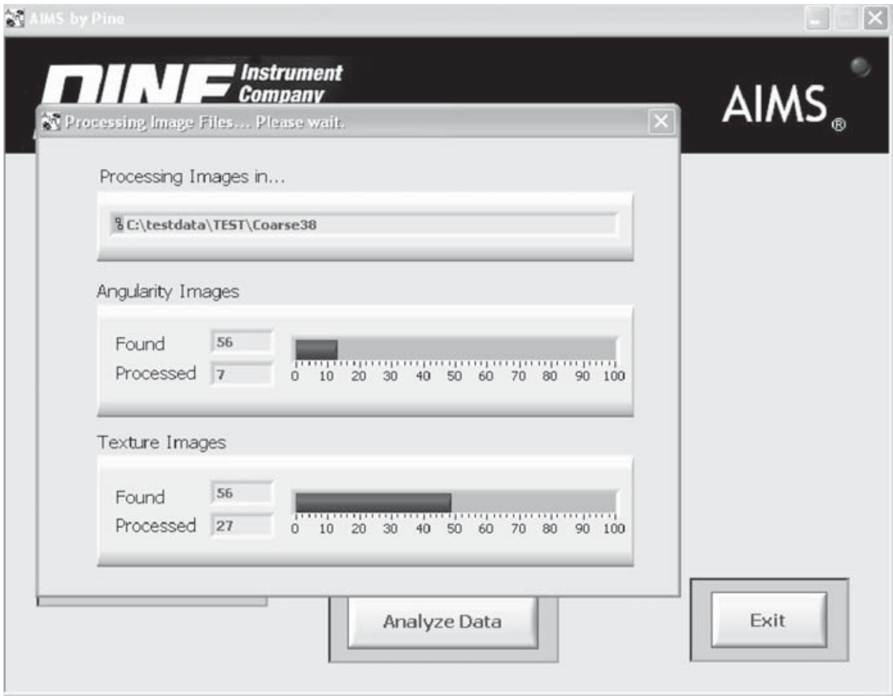

Figure A-1-18. Window showing that angularity and texture analyses are being performed.

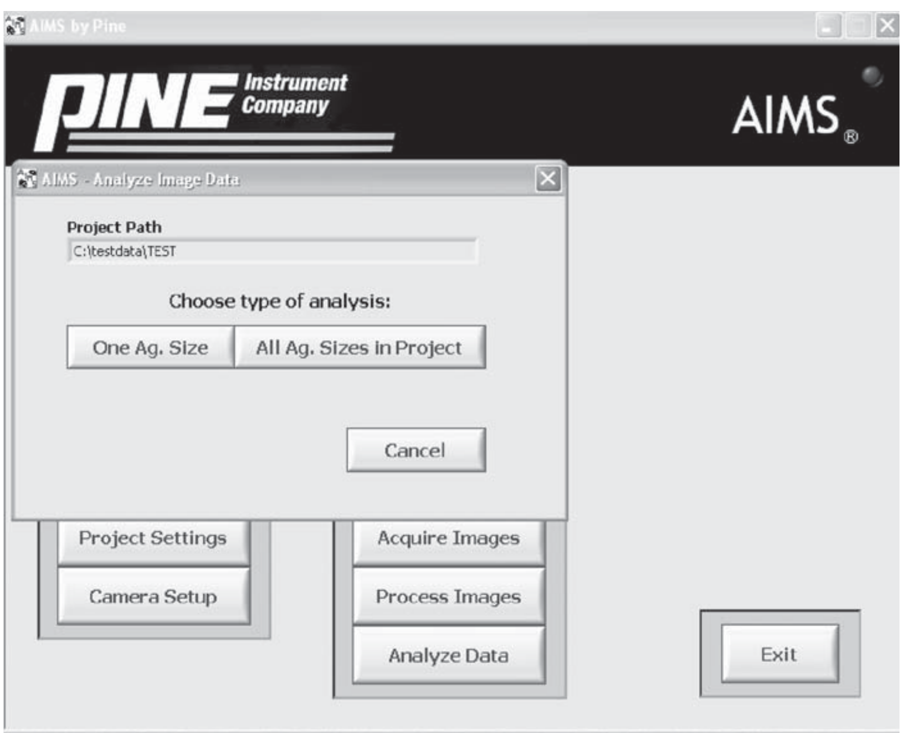

Figure A-1-19. Window for selecting one or all aggregate sizes for analysis.

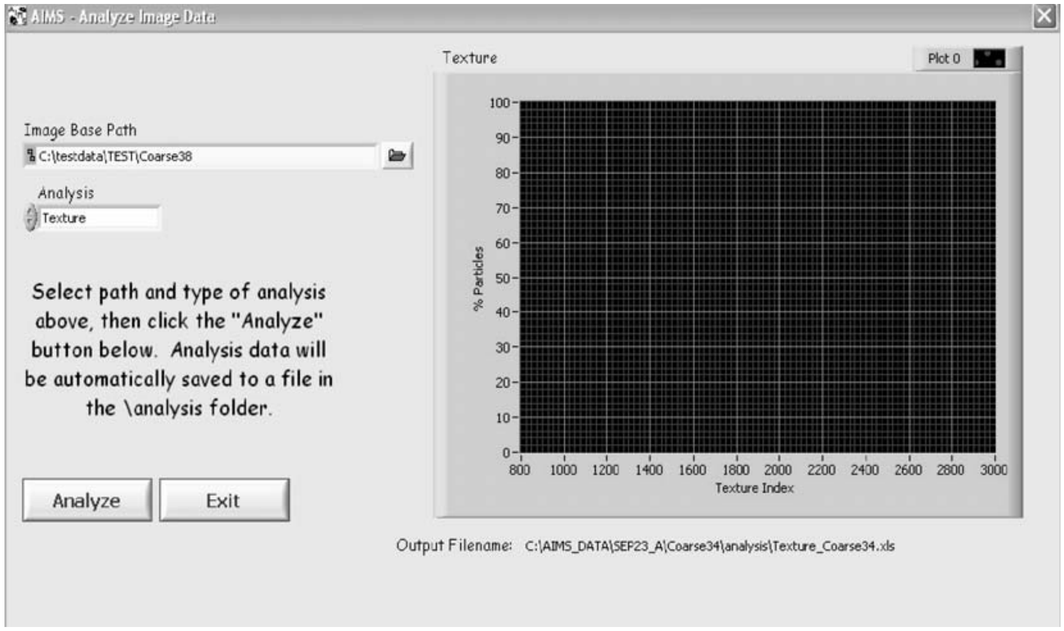

Figure A-1-20. Window for selecting directory type of analysis desired.

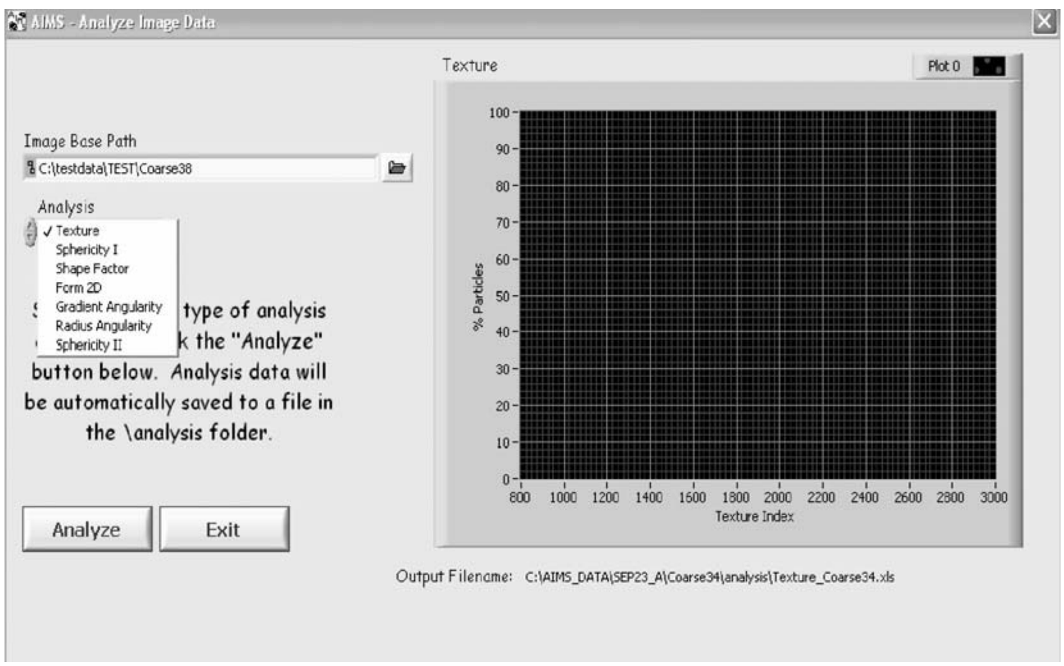

Figure A-1-21. Drop-list for selecting type of analysis.

9.2. The "AIMS Analysis Workbook" is another program that can be used to obtain statistics from the data analysis, provide percent of particles in each shape property category, and plot analysis results on Excel charts. The program is self-guided and very easy to use.

9.3. *Method B*—Fine Aggregate Angularity Analysis Procedure: Analysis of fine aggregates is similar to that for coarse aggregate, except the fine aggregates are uniformly spread on the aggregate table.

9.3.1 Analysis of fine aggregates starts by uniformly spreading a few grams of fine aggregate particles on the aggregate tray such that individual particles are not

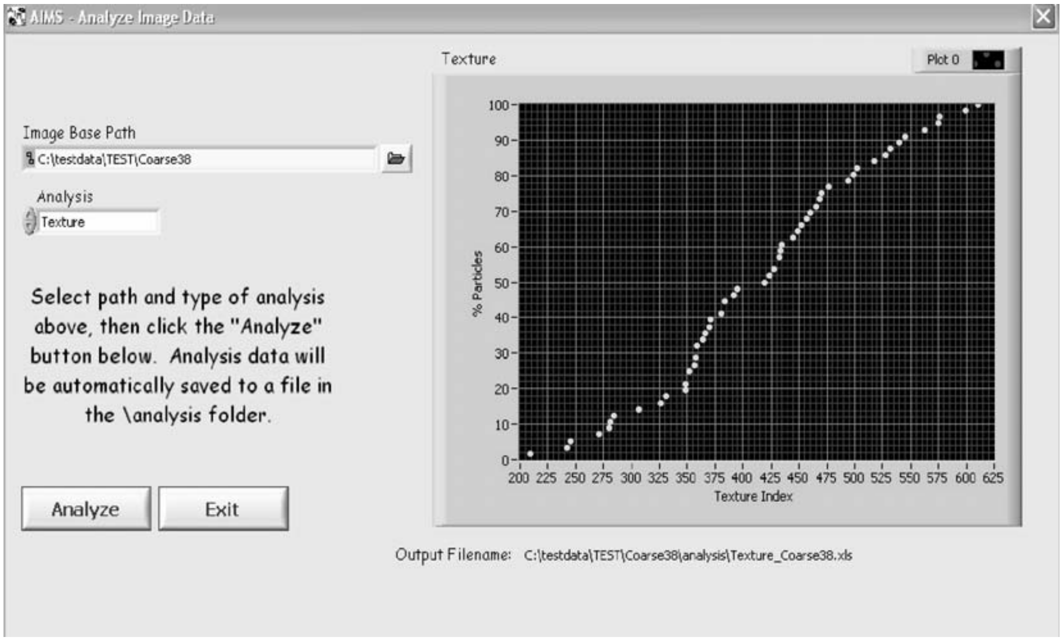

Figure A-1-22. Example of cumulative distribution for surface texture index.

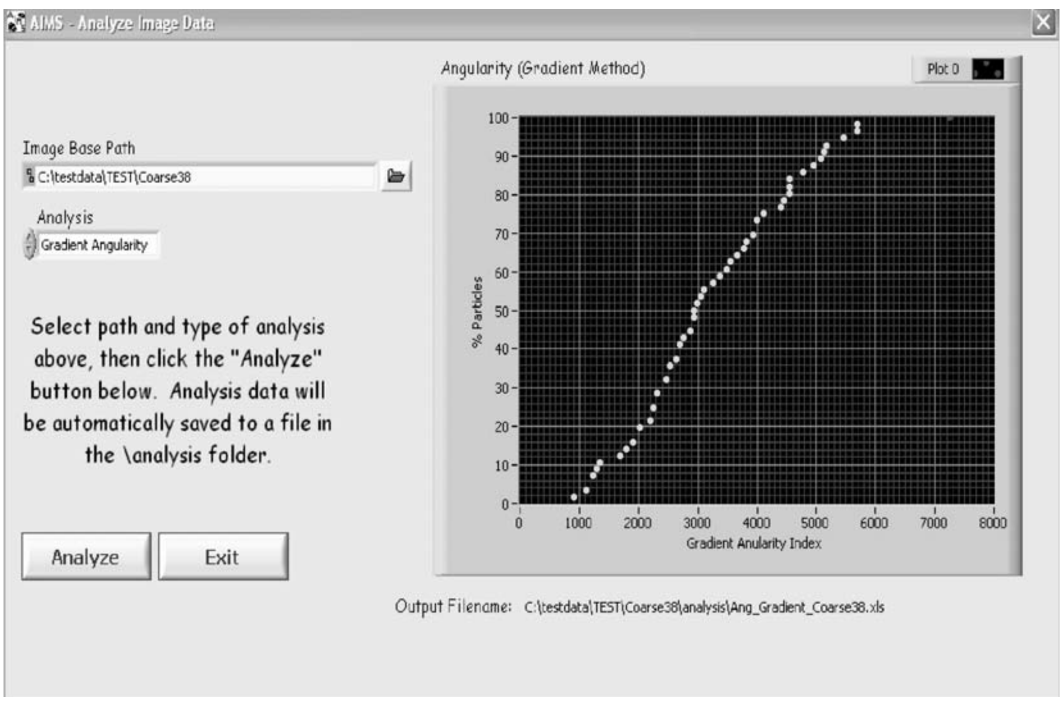

Figure A-1-23. Example of cumulative distribution for gradient angularity index.

touching each other. The 0.5X objective lens is used for acquiring images of fine aggregates. The maximum field of view achieved in the fine aggregate module is 26.4 mm × 35.2 mm. Backlighting is used to acquire all images in this analysis. The camera and video microscope assembly move incrementally in the x direction at a specified interval and acquire an image at each increment. Once the x-axis range is complete, the aggregate tray moves in the y-direction for a specified distance and the x-axis motion is repeated. This stepwise process continues until the entire area is scanned. In each x-y scan, the z-location of the camera is stipulated to meet some specified resolution criteria. Aggregates that are not within the size range for which the scan is conducted are consequently removed from the image automatically by the system.

9.3.2 Ensure the objective lens is 0.5X and the microscope is placed in the fine position on the dovetail slide. The objective lens is interchanged by removing the fiber-optic ring light and the ring light holder from the lower end of the microscope. Then the required objective lens can be installed on the microscope. The microscope can be easily positioned on the dovetail slide by releasing the knob of the retaining pin on the left side and sliding the microscope assembly upward or downward until the "Fine" labels on the left-hand side of the two pieces are aligned. Ensure that the retaining pin is engaged so the microscope cannot fall. Then tighten the thumb-screw on the right-hand side of the microscope assembly.

9.3.3 Specify the drive and directory path for the project. Enter a project name for the aggregates to be analyzed. From the "Project Parameters" drop-list, select "Fine," then select "OK" (Figure A-1-24).

9.3.4 Selecting "OK" on "Project Parameters" will display the "Fine Aggregate Parameters" window (Figure A-1-25). From the drop-list, select the desired aggregate size, then select "OK," and the first program interface window will display showing the new entered information for the current project.

9.3.5 Turn on the bottom light and allow it to warm up for minimum of two minutes.

9.3.6 Adjust the camera settings following the same procedures used for coarse aggregates (Subsection 9.1.8).

9.3.7 Initiate image acquisition selecting "Acquire Images." A new message window will appear giving the option to perform camera setup. If not accomplished in the previous step, camera setup can be performed here; otherwise, select "No." When omitting the camera setup option, a new message window displays with instructions that must be followed (Figure A-1-26).

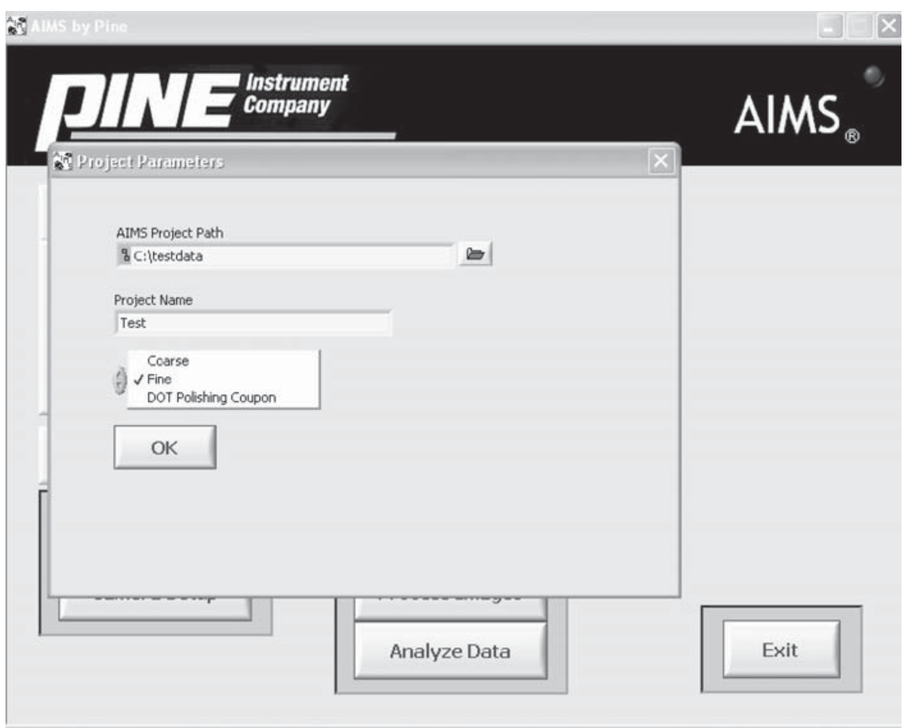

Figure A-1-24. Aggregate range drop-list for fine aggregate.

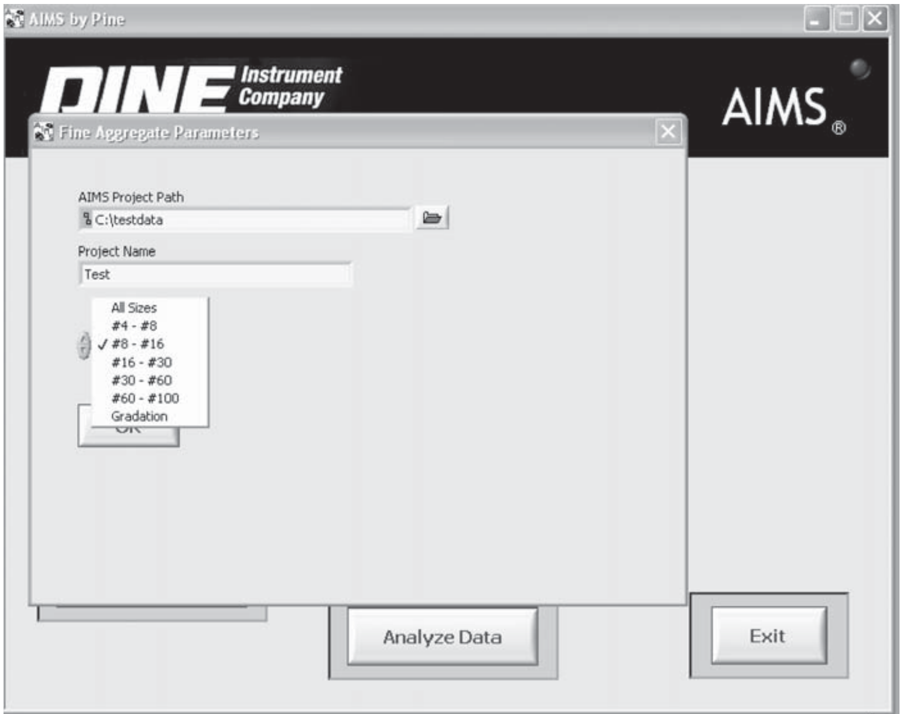

Figure A-1-25. Drop-list for fine aggregate parameters.

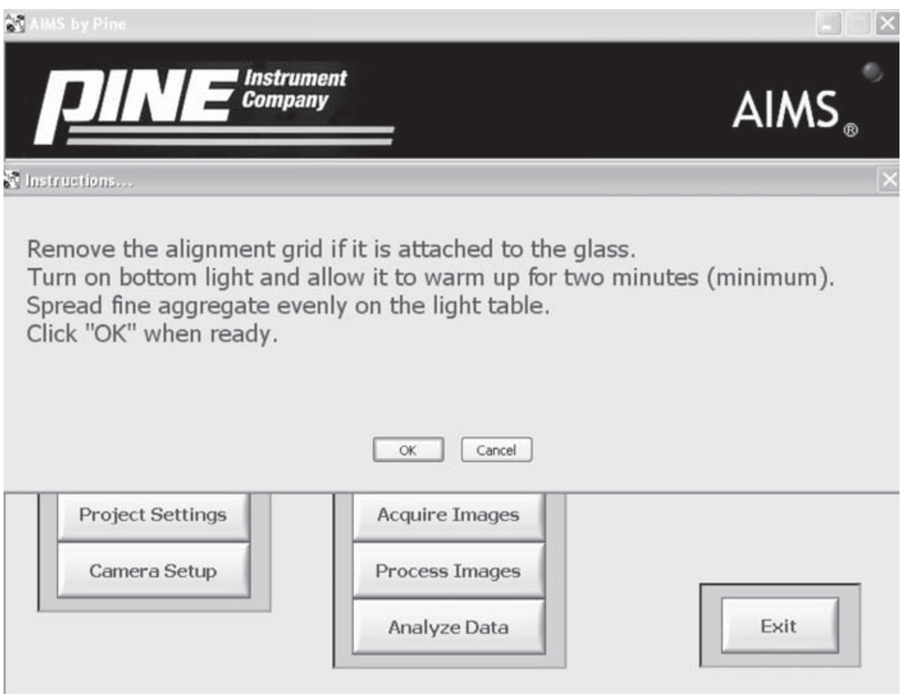

Figure A-1-26. Specific instructions for fine aggregate analysis.

9.3.8 Spread fine aggregate uniformly on aggregate tray (translucent Mylar alignment grid is not used in this segment), and click the "OK" button. The AIMS system will scan the entire tray and return to the starting point.

9.3.9. Fine aggregate image processing is identical to that for coarse aggregates, except no texture images are acquired.

9.3.10. Data analysis for fine aggregate is similar to that for coarse aggregate, except the number of analysis parameters (gradient angularity, radius angularity, and 2-D form) are fewer (Figures A-1-27 and A-1-28).

9.3.11. Results for each analysis type are automatically saved in an Excel spreadsheet in a folder named "Analysis" that is created in the directory selected in Step 9.3.3.

10. AIMS Analysis Workbook

10.1 The AIMS Analysis Workbook contains additional software that can be used to generate statistics from the analysis data, provide percent of particles in each shape category, and plot analysis results on Excel charts. The program is self-guided and very easy to use.

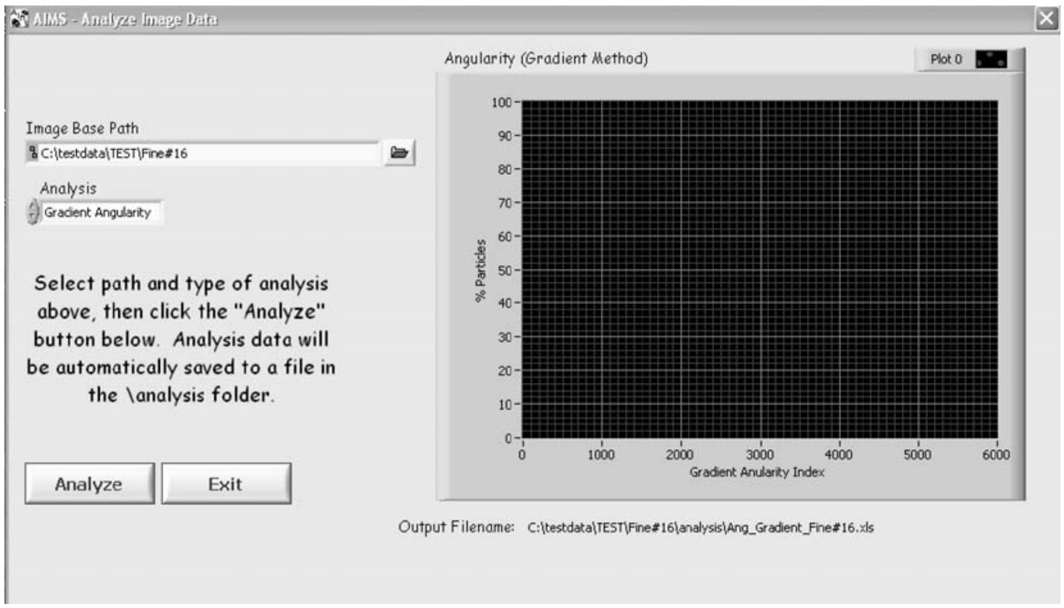

Figure A-1-27. Gradient angularity screen for AIMS fine aggregate analysis.

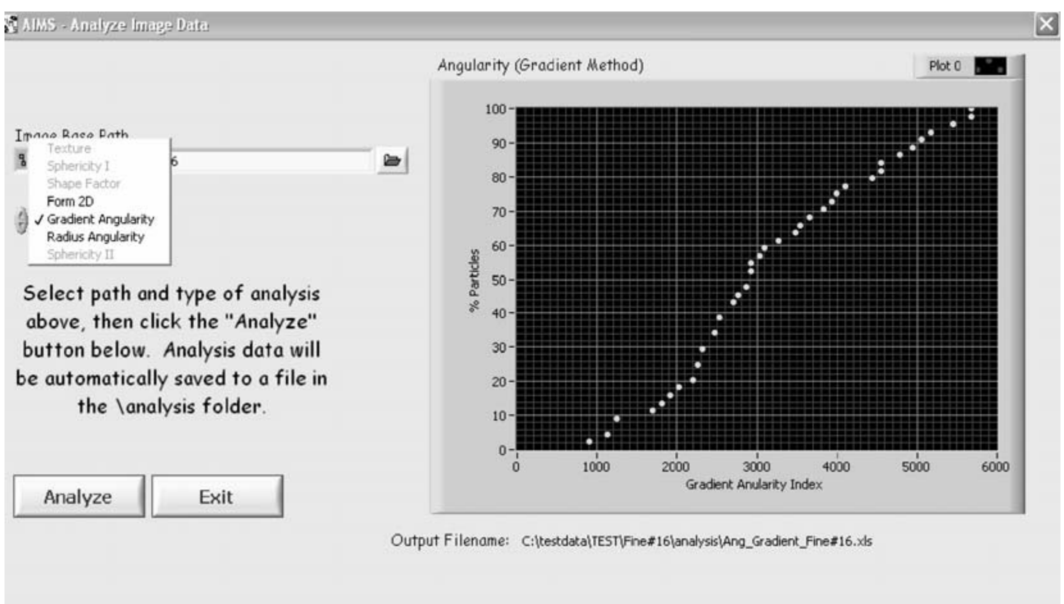

Figure A-1-28. Gradient angularity screen for showing analysis type drop-list.

Proposed Standard Method of Test for

Aggregate Particle Shape Using Multiple Ratio Analysis

1. Scope

1.1. Multiple Ratio Analysis (MRA) quantifies and categorizes the overall shape of coarse aggregate particles. Testing and analyses are typically performed using a digital flat and elongated (F&E) measuring device, however, testing and analyses can be performed using a proportional caliper with multiple posts.

1.2. *This standard does not purport to address all of the safety problems, if any, associated with its use. It is the responsibility of the user of this standard to establish appropriate safety and health practices and determine the applicability of regulatory limitations prior to use.*

2. Referenced Documents

2.1. *AASHTO Standards:*

T 2	Sampling of Aggregates
T 248	Reducing Samples of Aggregate to Testing Size
T 27	Sieve Analysis of Fine and Coarse Aggregates

2.2. *ASTM Standards*:

D 75	Practice for Sampling Aggregates
D 4791	Test Method for Flat or Elongated Particles in Coarse Aggregate
C 136	Test Method for Sieve Analysis of Fine and Coarse Aggregates
C 702	Practice for Reducing Samples of Aggregate to Testing Size
E 11	Specification for Wire-Cloth Sieves for Testing Purposes

3. Terminology

3.1. *Definitions:*

3.1.1. *Shape*—describes the maximum and minimum dimensions of coarse aggregate particles.

3.1.2. *Coarse Aggregate*—aggregates that are retained on a 4.75-mm or No. 4 sieve.

3.1.3. *Multiple Ratio Analysis*—a method for quantifying and categorizing the overall shape of coarse aggregate particles into five different F&E ratios, i.e., <2:1, 2:1 to 3:1, 3:1 to 4:1, 4:1 to 5:1, >5:1.

4. Summary of Method

4.1. MRA is an improved method for categorizing the various particle shapes found in a sample of aggregate. The ability to define the various particle shapes found within the coarse aggregate particles will lead to improved hot mix asphalt mix design procedures for performance optimized combined gradations based around particle shapes. MRA analysis may be used in the aggregate production process to optimize crusher performance and evaluate product consistency. This method features a new digital flat and elongated measuring device that easily and accurately determines the various coarse aggregate particle shapes found in an aggregate sample.

5. Significance and Use

5.1. Shape of aggregate particles has been shown to directly affect the engineering properties of highway construction materials such as hot mix asphalt concrete, Portland cement concrete, and unbound aggregate layers. Most methods currently in use for measuring these properties of aggregate particles are indirect measurements of the desired properties. This test method provides direct measurement of aggregate particle shape and thus provides consistent values that are beneficial for use in software designed to predict performance of highway pavements and structures.

5.2. MRA is typically performed on an aggregate sample from a given stockpile. MRA gives an accurate representation of the particle shapes within an aggregate sample by evaluating the sample based on five different F&E ratios (<2:1, 2:1 to 3:1, 3:1 to 4:1, 4:1 to 5:1, >5:1) instead of one (as with ASTM D 4791). The caliper device measures the different F&E ratios found within a sample at the same time. Particles can easily be sorted into the various ratios without having to change the pivot point and re-measure the particles for each separate ratio. With the single ratio caliper device, a sample would need to be measured five separate times.

5.3. Important information can be obtained by examining the MRA of the various size fractions in the aggregate blend for the job mix formula of a paving mix. An example showing the percentages of various sizes of materials in each of five flat and elongated categories is shown in Figure A-2-1.

5.4. This procedure is useful for evaluating aggregates used in paving mixtures and for evaluating aggregates from different phases of the aggregate production process.

6. Apparatus

6.1. The MRA apparatus (Figures A-2-1 and A-2-2) is an integrated system composed of a device for measuring minimum and maximum aggregate dimensions and a computer with associated software to store data, categorize particle shapes, and produce tables and graphs to illustrate the findings.

7. Sampling

7.1. Obtain aggregate specimens in accordance with Practice D 75, and reduce the specimen to an adequate sample size in accordance with Practice C 702.

8. Preparation of Test Samples

8.1. A suitable reduced coarse aggregate sample should contain at least 100 particles.

8.2. Normally, coarse aggregate samples are suitable for testing without any processing. If aggregates are dirty, wash and air dry or oven dry the reduced sample at 110 ± 5°C (230 ± 9°F) to substantially constant mass.

9. Procedure

9.1. Validate the accuracy of the MRA caliper by sequentially placing three flat-faced steel blocks of known lengths (from about 2.54 mm to 25.4 mm or 0.1 to 2 inches) in the caliper, and ensure the measurements match the known lengths of the cylinders within ±0.0254 mm (±0.001 inch). (Note: These quantities and tolerances are merely a suggestion for this draft standard and are based on no analyses). If the readings are not accurate within the specified limits, the device must be calibrated following the manufacturer's instructions. Validate caliper at the beginning of each day of testing.

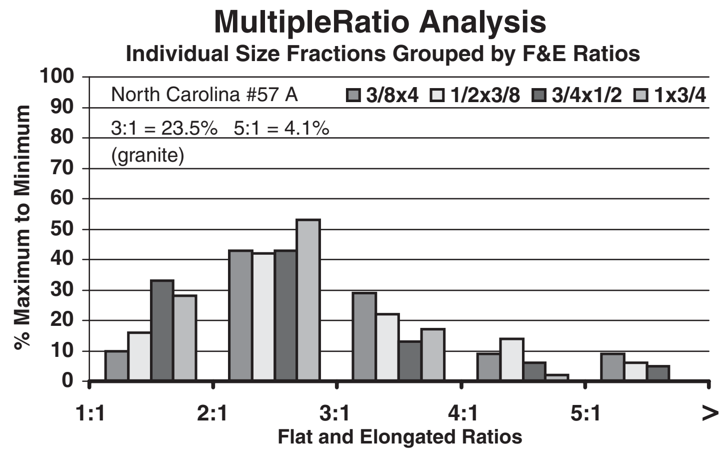

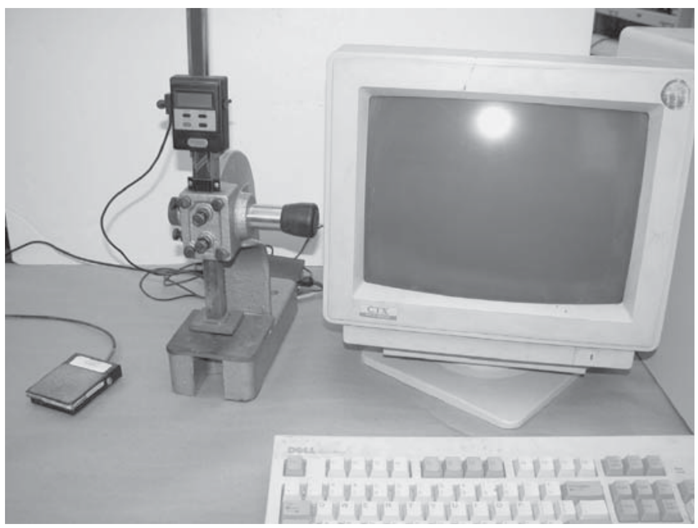

Figure A-2-1. View of the original prototype multiple ratio analysis system.

Figure A-2-2. View of a commercially-available multiple ratio analysis system.

9.2. The MRA system uses five different colors to represent five different flat and elongated ratios (<2:1, 2:1 to 3:1, 3:1 to 4:1, 4:1 to 5:1, >5:1). Therefore, prepare five empty bowls with the same color indicators to receive the aggregates as they are categorized by the MRA system. Place the bowls near the caliper.

9.3. Select a single aggregate particle from the sample and place it in the caliper with the maximum dimension in the vertical orientation. Slowly lower caliper head until it contacts the particle. Press the foot pedal to record the maximum dimension of the particle on the computer.

9.4. Place the same particle under the caliper with the minimum dimension in the vertical orientation. Slowly lower caliper head until it contacts the particle. Press the foot pedal to prompt the computer to record the minimum dimension of the particle and calculate the flat and elongated ratio category of the aggregate particle.

9.5. When the color code appears on the screen, place the aggregate particle in the appropriate color-coded bowl.

9.6. Select another aggregate particle and repeat Steps 9.3 through 9.5. Repeat these steps with all aggregate particles in the sample.

9.7. Weigh and determine the mass of the aggregate particles in each bowl. Sum the masses of the aggregate particles in all five bowls. Determine the percentage of aggregate particles in each flat and elongated category by dividing the mass of particles in each bowl by the total mass of all particles.

9.8. Alternatively, count the number of aggregate particles in each bowl. Sum the number of aggregate particles in all five bowls. Determine the percentage of aggregate particles in each flat and elongated category by dividing the number of particles in each bowl by the total count of all particles.

Proposed Standard Test Method for

Volume, Flat and Elongated Ratio, Angularity, and Surface Texture of Coarse Aggregate Particles Using the University of Illinois Aggregate Image Analyzer (UIAIA)

1. Scope

1.1. This method is intended for simple three-dimensional (3-D) reconstruction of individual coarse aggregate particles for volume, flat and elongated ratio, angularity, and surface texture of coarse aggregate particles. Testing and analyses are performed using the integrated University of Illinois Aggregate Image Analyzer (UIAIA).

1.2. Analysis of Coarse Aggregates—This method uses aggregates that are retained on a 4.75-mm (No. 4) sieve.

1.3. Coarse aggregates scanned using this process should be washed to remove clay, dust, and other foreign and deleterious materials and separated into the appropriate sizes before being analyzed.

1.4. *This standard does not purport to address all of the safety problems, if any, associated with its use. It is the responsibility of the user of this standard to establish appropriate safety and health practices and determine the applicability of regulatory limitations prior to use.*

2. Referenced Documents

2.1. *ASTM Standards*:

D 75 Practice for Sampling Aggregates
C 136 Test Method for Sieve Analysis of Fine and Coarse Aggregates
C 702 Practice for Reducing Samples of Aggregate to Testing Size
E 11 Specification for Wire-Cloth Sieves for Testing Purposes

3. Terminology

3.1. *Definitions:*

3.1.1. *Volume*—with three orthogonally positioned digital cameras, the UIAIA aggregate image analysis system has the ability to perform *volume* computation for an aggregate particle. An estimate of its weight can then be determined using the known bulk specific gravity. The imaging based volume computation is achieved by combining the information in the three 2-D binary images as shown in Figure A-3-1. The 3-D space is meshed into a 3-D array of pixel cuboids or voxels. It is then simply required to count the number of voxels corresponding to the particle contained in the rectangular box in Figure A-3-1. Any voxel belonging to the particle has the corresponding three projection pixels in the x-y, y-z, and z-x planes. The number of voxels that satisfies this condition finally gives the volume of the particle in units of pixel length cube. The *volume* computation program used in the UIAIA scans over the entire 3-D space and examines if each voxel belongs to the particle.

3.1.2. *Flat and Elongated Ratio (F&E Ratio)*—describes the overall 3-dimensional shape of aggregate particles. The UIAIA software sorts the evaluated aggregate particles into three categories: *F&E Ratio* <3:1, 3:1 < *F&E Ratio* < 5:1 and *F&E Ratio* > 5:1, based on *F&E Ratio* calculated using Equation 1:

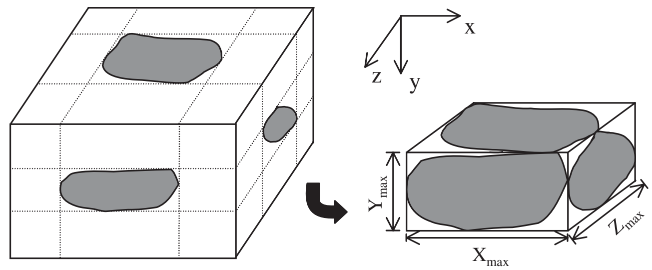

Figure A-3-1. The smallest rectangular box encompassing a particle.

$$F\&E\ Ratio = \frac{Longest\ Dimension}{Shortest\ Perpendicular\ Dimension} \qquad \text{(A-1-1)}$$

where *Longest Dimension* is the longest dimension measured by UIAIA software from the three orthogonally positioned camera images, i.e., the top, side and front images. *Shortest Perpendicular Dimension* is the shortest dimension from the three images, which is perpendicular to the *Longest Dimension* as shown in Figure A-3-2.

3.1.3. *Angularity Index (AI)*—is related to the corner sharpness of 2-D images of aggregate particles. The angularity index (*AI*) is defined based on tracing the changes in slope of the particle image outline obtained from each of the top, side and front images. The outline of each image is extracted and approximated by an n-sided (n is taken as 24 in the *AI* definition) polygon as shown in Figure A-3-3. The frequency distribution of the changes in the vertex angles is established in 10-degree class intervals. The number of occurrences in a certain interval and the magnitude are then related to the angularity of the particle profile. Accordingly, the *AI* procedure first determines an angularity index value for each 2-D image as shown in Equation A-1-2:

$$Angularity,\ A = \sum_{e=0}^{170} e \times P(e) \qquad \text{(A-1-2)}$$

where e is the starting angle value for each 10-degree class interval and $P(e)$ is the probability of each angle change in the range e to $(e+10)$.

Then, a final *AI* is established for the particle according to Equation A-1-3, by taking a weighted average of its angularity determined for all three views. The *AI* has the same degree unit as an angle does.

$$AI = \frac{\sum_{i=1}^{3} (Angularity_i \times Area_i)}{\sum_{i=1}^{3} Area_i} \qquad \text{(A-1-3)}$$

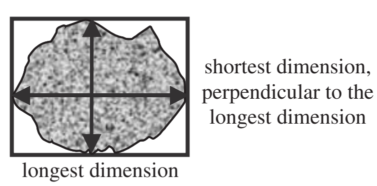

Figure A-3-2. The longest and shortest dimensions of a coarse aggregate particle.

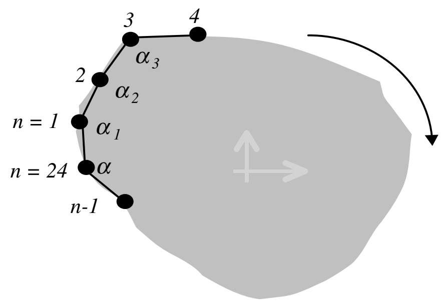

Figure A-3-3. An n-sided polygon approximating the outline of an aggregate particle.

3.1.4. Surface Texture (*ST*)—describes the surface irregularities of aggregate particles. The surface texture of an aggregate particle is defined using an image analysis technique known as Erosion and Dilation. Erosion cycles followed by the same number of dilation cycles tend to smooth the surface of a particle by losing shape peaks and patching sharp dents on the boundary. The image area difference before and after erosion and dilation of the same number of cycles leads to the definition of the *ST* for one of the three particle projection images as shown in Equation A-1-4:

$$ST = \frac{A_1 - A_2}{A_1} \times 100 \qquad \text{(A-1-4)}$$

where
ST = Surface texture parameter for each 2-D image;
A_1 = Area (in pixels) of the 2-D projection of the particle in the image;
A_2 = Area (in pixels) of the particle after performing a sequence of "n" cycles of erosion followed by "*n*" cycles of dilation.
Then, an ST index, denoted as $ST_{particle}$, is established for the particle by taking a weighted average of each *ST* determined from all three views, which measures the overall surface irregularities of a particle. $ST_{particle}$, is computed as according to Equation (A-1-5). The ST is a dimensionless quantity, as it measures the ratio of the areas before and after erosion and dilation.

$$ST_{particle} = \frac{\sum_{i=1}^{3}\left(ST_i \times Area_i\right)}{\sum_{i=1}^{3} Area_i} \qquad \text{(A-1-5)}$$

where i takes values from 1 to 3 for top, front, and side orthogonal views. ST_i is the surface texture parameter for each 2-D image, and $Area_i$ is the correspon-ding area of each 2-D image.

4. Summary of Method

4.1. Analysis of coarse aggregate particles includes determining volume, flat and elongated ratio, angularity, and surface texture. The UIAIA features a moving conveyor belt that carries the individual aggregate particle into the view of a sensor, which detects the particle and immediately triggers the cameras. Once triggered, the three synchronized cameras capture in one-tenth of a second the images of the front, top, and side views of the particle. The captured images are then processed for size and shape properties and indices using software developed specifically for this application.

5. Significance and Use

5.1. Volume, shape, angularity, and surface texture of coarse aggregates have been shown to directly affect the engineering properties of highway construction materials such as hot mix asphalt concrete, Portland cement concrete, and unbound aggregate layers. Most methods currently in use for measuring these properties of aggregate particles are indirect measurements of the desired properties. This test method provides objective and direct measurements of aggregate volume, shape (flatness and elongation), angularity, and texture to quantify these properties and provide repeatable results that are comparatively more beneficial for use in performance prediction of highway pavements and structures.

6. Apparatus

6.1. The UIAIA is an integrated system with a fixture framework for mounting and positioning the cameras, sensor, and other components. Three progressive scan CCD cameras are adopted to capture the images of moving particles, which are commonly used in motion control applications. The mechanical details of the UIAIA include a working conveyor belt operated using a variable speed AC motor, which provides smooth and steady operation at speeds as low as 3 inches/sec. Three fluorescent lights were used behind the cameras to provide adequate brightness. A black background was provided for all three views in order to provide a contrast and collect sharp images.

7. Sampling

7.1. Obtain aggregate specimens in accordance with Practice D 75, and reduce the specimen to an adequate sample size in accordance with Practice C 702.

8. Preparation of Test Samples

8.1. Wash and oven dry the reduced sample at 110 ± 5°C (230 ± 9°F) to substantially constant mass, typically 1 or 2 kilograms of aggregates depending on the average particle sizes.

9. Procedure

9.1. UIAIA System Setup—the UIAIA system is shown in Figure A-3-4 with an operator. Turn on the AC motor and warm up the system by keeping the AC motor running for ten minutes, so that the conveyor can move smoothly and steadily. Turn on the cameras and the sensor, and adjust the lens of the cameras until images of particles with sharp boundaries are obtained. Before image acquisition starts, take the images of a dummy calibration specimen to make sure the cameras and sensors work properly.

9.2. UIAIA System Calibration—calibration is a process by which measurements made in pixels from digitized images can be converted to equivalent engineering units through proportionality or equivalency factors. The calibration factors are determined from images of standard objects with known dimensions. Such calibration factors are of the form "X pixels = Y length units". Once the calibration procedure is completed and calibration factors are established, the original configuration of the test setup including the camera focus, image resolution, light conditions, and so on, should not be altered.

Figure A-3-4. Photo of the UIAIA system with operator passing aggregate particles.

Commercially manufactured white colored, precision spheres of diameter 0.5-inch, 0.625-inch, 0.75-inch, and 1-inch were used as standard specimens to establish calibration factors in the UIAIA system. The relative sizes of the spheres are shown in Figure A-3-5. The sizes of the standard specimens chosen are representative of typical coarse aggregate particle sizes encountered in paving applications. Furthermore, the choice of a regular shaped object such as a sphere was made to expedite the calibration process by making it easier to detect and correct measurement irregularities between the different views. To establish calibration factors, images of the spheres need to be captured while the belt is moving. The diameters of the spheres are measured in pixel units from each of the three views. Calibration can then be accomplished by taking an average of the sphere diameter (in pixels) measured from the front, top, and side images for each trial and for each sphere size. The calibration factor for each size is obtained by comparing the diameters of the spheres in real dimensions in the form of "X pixels = Y length units". To acquire images for the calibration process, please refer to Step 9.2 in this protocol.
Image Acquisition—to start the image acquisition of the aggregate sample, first go to the software package of UIAIA, click on the LABVIEW file titled "triggered_capture" that has an extension of ".vi". A window is opened as shown in Figure A-3-6.
Operators can decide whether to display images, use trigger, or save gray scale and/or binary images during the image acquisition. Also, operators can specify the starting number of images and path of the saved images. The time delays for the three cameras indicate the time interval between the triggering of the sensor and the front camera, and the time interval between the front camera and the top camera and the side one. These three time delays have been calibrated, therefore should not be changed dramatically.

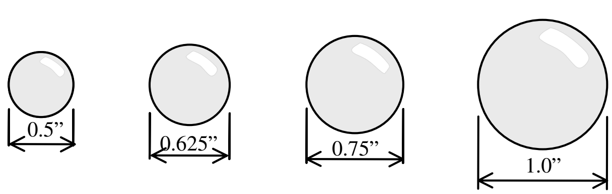

Figure A-3-5. Perfect spheres used for the calibration of UIAIA system.

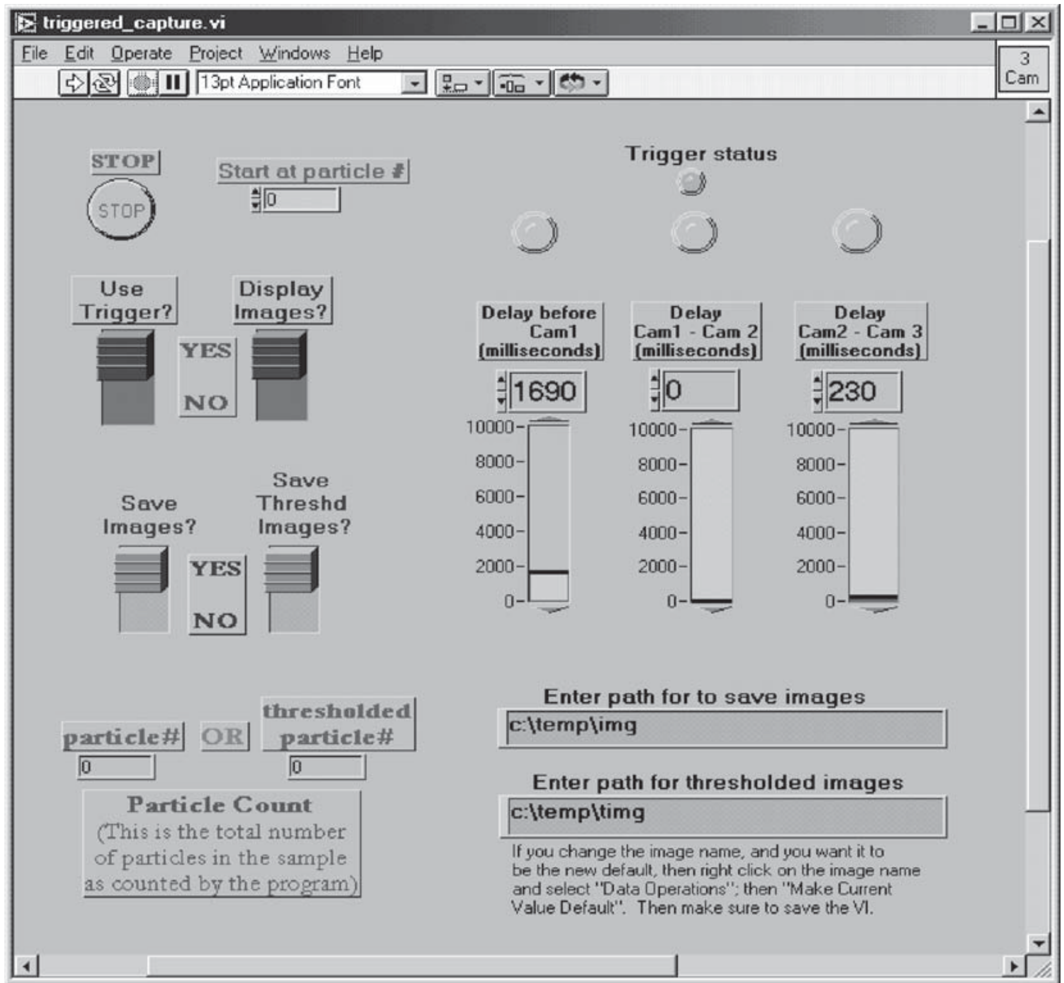

Figure A-3-6. UIAIA user interface (virtual instrument [VI]) for image acquisition.

The image acquisition can be started for a washed and oven dried aggregate sample by clicking on the arrow icon in the Tools bar of the user interface. An operator is needed to drop the individual particles one by one onto the moving conveyor belt (see Figure A-3-4). During the image acquisition process, captured images can be monitored by both the audio signal and the acquired three images shown on the computer screen. All images captured are automatically saved in a temporary folder in the computer.

9.3. Calculation of Coarse Aggregate Size and Shape Properties—the size and shape indices from the three-camera based aggregate particle reconstruction, i.e., the volume, gradation, flat and elongated ratio, angularity, and surface texture are computed using the algorithms or the virtual instruments (VIs) processing the acquired images for each sample. Each program to calculate each of these quantities is an individual VI file in UIAIA system.

9.3.1. Coarse Aggregate Volume

The imaging based volume computation is achieved by combining the information in the three 2-D binary images as shown in Figure A-3-1. The 3-D space is meshed into a 3-D array of pixel cuboids or voxels. It is then simply required to count the number of voxels corresponding to the particle contained in the rectangular box in Figure A-3-1. Any voxel belonging to the particle has the corresponding three projection pixels in the x-y, y-z, and z-x planes. The number of voxels that satisfies this condition finally gives the volume of the particle in units of pixel length cube. The volume computation program used in the UIAIA scans over the entire 3-D space and examines if each voxel belongs to the particle.

The volume computation algorithm can be viewed during operation as the three front, top, and side images of an aggregate particle are switched one by one on the screen. A screenshot of this process is shown in Figure A-3-7.

9.3.2. Coarse Aggregate F&E Ratio

Go to the software package of UIAIA, click on the LABVIEW file titled "fe_sieve_maxinter" with the extension of .vi. The window as shown in Figure A-3-8 will be opened. Set up the parameters as shown in Figure A-3-8 by entering the drive and directory path desired for the project, and specifying a project name for the aggregates to be analyzed. The F&E Ratios are computed for each particle in the aggregate sample by clicking on the arrow icon in the Tools bar of the user interface. The F&E Ratios of all the particles are automatically saved in an Excel file, *feratio.xse* in the Results folder under C:\, which needs to be established beforehand. Three other Excel files will also be generated that measure the sieve dimension, the maximum dimension and the minimum dimension of the individual particles respectively. The sieve dimension will be used to plot the ***gradation*** of the evaluated aggregate sample. The maximum dimension and the minimum dimension report the length and width of the individual particles.

9.3.3. Coarse Aggregate Angularity

Go to the software package of UIAIA, click on the LABVIEW file titled "angularity" with the extension of .vi. A window as shown in Figure A-3-9 will be opened. Set up the parameters as shown in Figure A-3-9 and the angularity index (AI) is calculated for each particle in the aggregate sample by clicking on the arrow icon

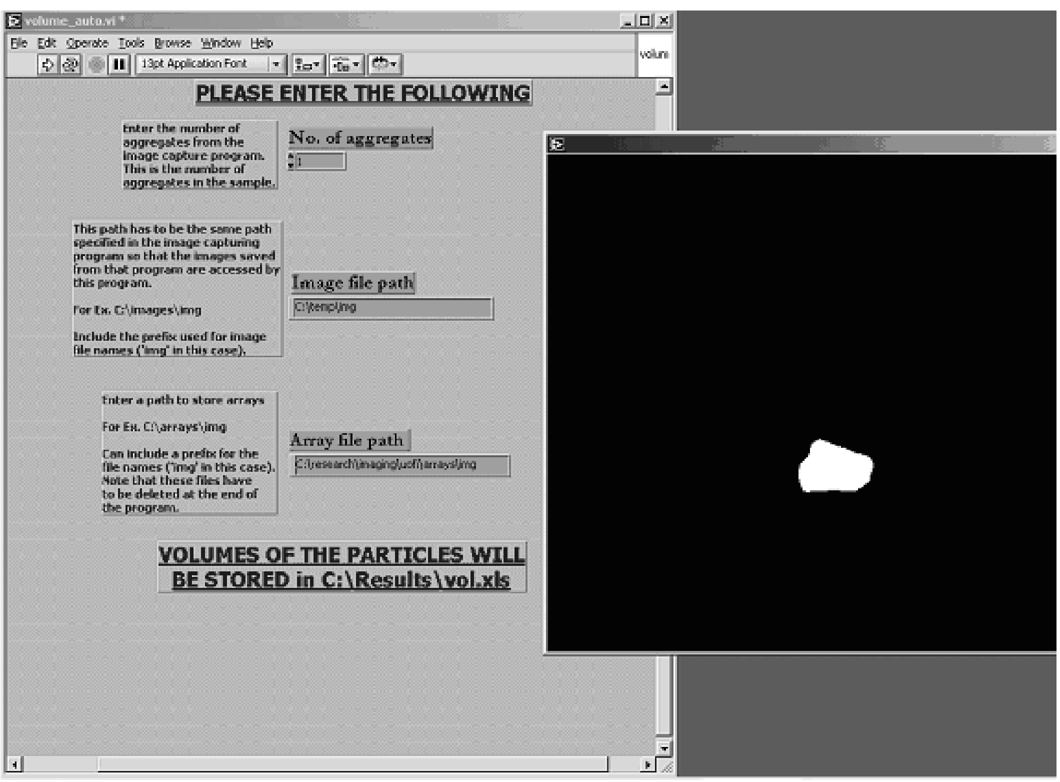

Figure A-3-7. Screenshot showing operation of volume computation user interface or VI.

Figure A-3-8. Screenshot of user interface or VI for coarse aggregate F&E Ratio.

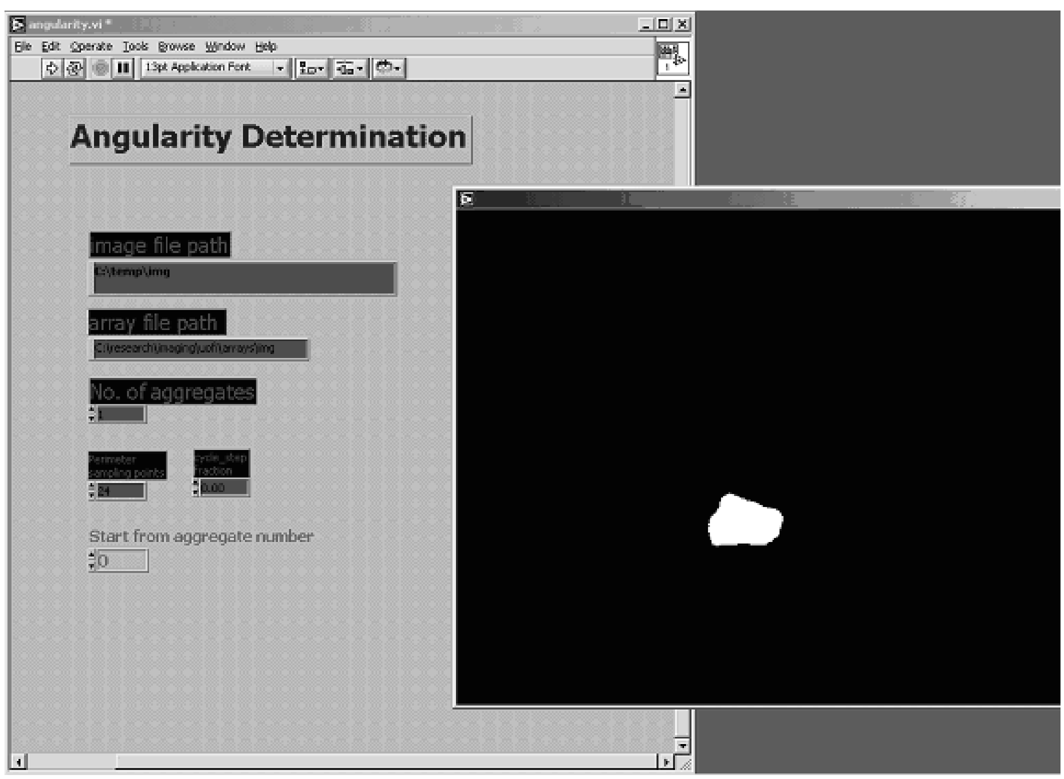

Figure A-3-9. Screenshot of user interface or VI for coarse aggregate angularity.

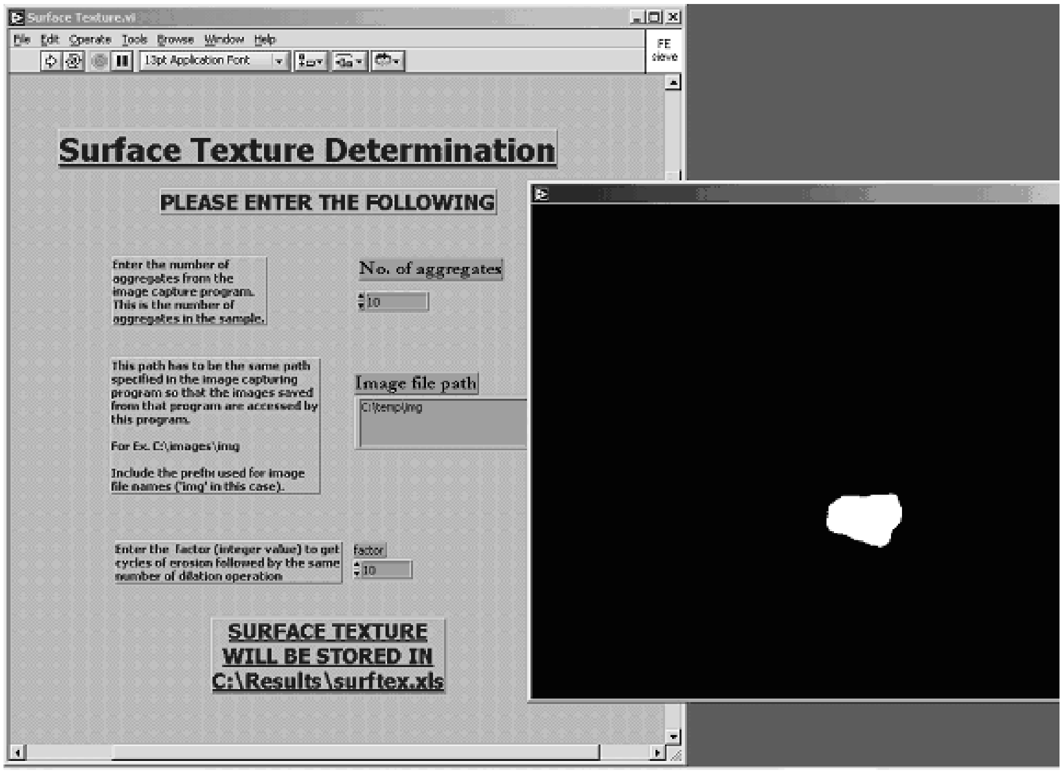

Figure A-3-10. Screenshot of user interface or VI for coarse aggregate surface texture.

in the Tools bar of the user interface. Angularity of all the particles will be automatically saved in an Excel file, *ang.xse* in the Results folder under C:\.

9.3.4. Coarse Aggregate Surface Texture
Go to the software package of UIAIA, click on the LABVIEW file titled "surftex" with the extension of .vi. The window as shown in Figure A-3-10 will be opened. Set up the parameters as shown in Figure A-3-10; the surface texture (ST) index is computed for each particle in the aggregate sample by clicking on the arrow icon in the Tools bar of the user interface. Surface texture of all the particles will be automatically saved in an Excel file, *surftex.xls* in the Results folder under C:\.

When the size and shape properties and indices, i.e., maximum, minimum, intermediate dimensions, gradation curve, flat and elongated ratio, angularity, and surface texture, are calculated for all the individual aggregate particles in a sample, the average flat and elongated ratio, angularity, and surface texture can be calculated to evaluate the size and shape property of the aggregate sample.

10. UIAIA Analysis Workbook

10.1. The UIAIA Analysis Workbook contains additional software that can be used to plot the gradation of the evaluated aggregate sample. The program is self-guided and easy to use.

APPENDIXES
B, C, D, AND E

UNPUBLISHED MATERIAL

Appendixes B through E contained in the research agency's final report are not published herein. These appendixes are accessible on the web as *NCHRP Web-Only Document 80* at http://www4.trb.org/trb/onlinepubs.nsf. These appendixes are titled as follows:

Appendix B: Review of Aggregate Characteristics Affecting Pavement Performance

Appendix C: Image Analysis Methods for Characterizing Aggregate Shape Properties

Appendix D: Test Methods for Measuring Aggregate Characteristics

Appendix E: Photographs of Aggregate Samples

Abbreviations and acronyms used without definitions in TRB publications:

AASHO	American Association of State Highway Officials
AASHTO	American Association of State Highway and Transportation Officials
ACRP	Airport Cooperative Research Program
ADA	Americans with Disabilities Act
APTA	American Public Transportation Association
ASCE	American Society of Civil Engineers
ASME	American Society of Mechanical Engineers
ASTM	American Society for Testing and Materials
ATA	American Trucking Associations
CTAA	Community Transportation Association of America
CTBSSP	Commercial Truck and Bus Safety Synthesis Program
DHS	Department of Homeland Security
DOE	Department of Energy
EPA	Environmental Protection Agency
FAA	Federal Aviation Administration
FHWA	Federal Highway Administration
FMCSA	Federal Motor Carrier Safety Administration
FRA	Federal Railroad Administration
FTA	Federal Transit Administration
IEEE	Institute of Electrical and Electronics Engineers
ISTEA	Intermodal Surface Transportation Efficiency Act of 1991
ITE	Institute of Transportation Engineers
NASA	National Aeronautics and Space Administration
NCFRP	National Cooperative Freight Research Program
NCHRP	National Cooperative Highway Research Program
NHTSA	National Highway Traffic Safety Administration
NTSB	National Transportation Safety Board
SAE	Society of Automotive Engineers
SAFETEA-LU	Safe, Accountable, Flexible, Efficient Transportation Equity Act: A Legacy for Users (2005)
TCRP	Transit Cooperative Research Program
TEA-21	Transportation Equity Act for the 21st Century (1998)
TRB	Transportation Research Board
TSA	Transportation Security Administration
U.S.DOT	United States Department of Transportation